RECOMBINANT EQUINE INTERLEUKIN-1 INDUCED MODELS OF EQUINE JOINT DISEASE

by

Vivian Ann Takafuji

Dissertation submitted to the faculty of Virginia Polytechnic Institute and State University for the degree of

Doctor of Philosophy

In

Veterinary Medical Sciences

Committee

Rick D. Howard, chair
Mark V. Crisman, co-chair
Xiang-Jin Meng, member
William R. Huckle, member
Kimberly F. Williams, member
Robert S. Pleasant, member
Anthony Blikslager, external examiner

November 2003

Blacksburg, VA

Keywords: equine interleukin-1, osteoarthritis, gene expression

RECOMBINANT EQUINE INTERLEUKIN-1 INDUCED MODELS OF EQUINE JOINT DISEASE

Vivian Ann Takafuji

(ABSTRACT)

Osteoarthritis (OA) is a debilitating disease of joints that afflicts horses of all ages and breeds and can result in lameness, suboptimal performance, and decreased quality of life. The pro-inflammatory cytokine interleukin-1 (IL-1) has been associated with the initiation and pathogenesis of joint disease. In part, this occurs by induction of proteases and oxidative pathways that contribute to the degradation of structural components of the articular cartilage extracellular matrix. Elucidating the complex macromolecular and molecular effects of IL-1 on articular tissues may further our understanding of the roles of IL-1 and inflammation in OA pathobiology. Full-length gene sequences encoding three recombinant equine interleukin-1 proteins (EqIL-1α, EqIL-1β, and EqIL-1 receptor antagonist), were previously cloned and expressed *in-vitro*. The objectives of this dissertation were to 1) establish EqIL-1 induced experimental models of equine OA, and 2) to investigate specific IL-1-induced immuno-inflammatory responses.

Effects of EqIL-1 on articular cartilage explant proteoglycan metabolism and synthesis of a downstream inflammatory product, prostaglandin E_2, established culturing conditions and furthered the rationale to use EqIL-1 in the *in-vitro* modeling of early joint disease. A customized cDNA array was used to profile changes in mRNA levels resulting from EqIL-1 treatments of cultured articular cartilage chondrocytes. EqIL-1α induced elevated mRNA levels corresponding to six genes after 1 hour relative to media control chondrocytes ($p<0.05$). EqIL-1β increased transcript levels of seven genes after 6 hours ($p<0.0004$); 102 additional transcripts were elevated > 2-fold over controls. A subset of the array-generated data was verified using optimized reverse transcriptase-PCR amplification. Results of principal component analysis indicate co-regulation of EqIL-1

induced transcript levels to relate to chondrocyte differentiation and cell-cycle processes. Subtractive hybridization-PCR identified 148 differentially expressed cDNAs in synovium resulting from a 6-hour intra-articular EqIL-1β injection.

Combined results demonstrate the potent bioactivity of our equine IL-1 proteins and support the argument for crucial roles of IL-1 in pro-inflammatory processes and cytokine imbalances underlying early OA pathogenesis. These results add to the current knowledge of IL-1 modulated transcription that may precede ECM catabolic processes characteristic of OA. The culture systems, assays, and techniques for gene expression analysis may be useful for future studies attempting to elucidate macromolecular and transcriptional events underlying inflammatory-associated joint disease processes in horses. Reported information may further efforts toward improved diagnostic and preventive strategies and development of anti-IL-1 directed therapies.

DEDICATION

This dissertation is dedicated to my grandmother, Akiko Tasaki Takafuji.

In loving memory

ACKNOWLEDGEMENTS

I thank my family and all of my friends who helped me through this experience, who shared with me the good as well as the trying moments. Thank you, Tyler, for being my constant and loving support (even through the phone line) and for your unquestioning help with the many software, graph, and chart problems I threw at you. I thank my graduate student advisor and committee members who were invaluable to my progress, were always willing to help me when I hit blocks in the road, and were incredibly flexible when scheduling our many committee meetings. Thank you to the technicians, Kristi Seat and Shannon Woody, for your special friendships and your help to keep me relatively sane at times. Thank you to Dan Ward, for being such a good confidant, counselor, and an exceptional help with the monstrous statistics involved in my work. I thank the office of research and graduate studies for stipend support throughout my education. Finally, I thank my precious miniature dachshund, Mocha, for making me smile everyday, through it all!

DECLARATION OF WORK

This is to declare that I, Vivian Ann Takafuji, performed the work involved in this dissertation at the VA-MD Regional College of Veterinary Medicine, Virginia Polytechnic and State University, Blacksburg, VA.

TABLE OF CONTENTS

TABLE OF FIGURES

LIST OF TABLES

CHAPTER I: Introduction

1.A. Overview

This dissertation was designed to study the role of equine interleukin-1 (EqIL-1) in early stages of equine joint disease processes using two *in-vitro* models for osteoarthritis and one *in-vivo* model for an acute synovitis. Exogenous EqIL-1 exposures of articular cartilage, isolated chondrocytes, and synovium were hypothesized to result in: 1) increased proteoglycan degradation, 2) decreased proteoglycan synthesis, 3) increased prostaglandin E_2 synthesis, and 4) increased mRNA levels. The first chapter includes a description of the components of the hyaline joint, an introduction to the clinical problem, and pertinent literature in existence of the known roles of various cytokines, growth factors, and soluble mediators in propagated inflammation and imbalances in cartilage extracellular matrix repair mechanisms. The second chapter describes an evaluation of the effects of EqIL-1 alpha and EqIL-1 beta on proteoglycan metabolism and prostaglandin E_2 production in equine articular cartilage explants. The third and fourth chapters correspond to studies directed to identify proximal effects of EqIL-1 on mRNA levels in cultured equine articular cartilage chondrocytes using a customized complementary DNA array analysis. The fifth chapter includes a study of early changes in equine synovium mRNA levels induced by an intra-articular EqIL-1 injection using a suppression subtractive hybridization-PCR technique. The final chapter attempts to describe how the combined results of the previous four chapters may contribute to the current understanding of the complexity of IL-1 mediated inflammation and effects on cartilage breakdown in joint disease pathogenesis in horses.

1.B. The synovium

Diarthrodial joints consist of opposing articular cartilage surfaces within a fluid filled synovial cavity lined by a thin synovium (composed of intimal and subintimal layers), and enclosed by a fibrous joint capsule (Todhunter, 1996). The synovium is a

vascular organ that supplies fluid and nutrients to the avascular, alymphatic, and aneural articular cartilage. Hyaluronic acid and lubricin released to the synovial fluid contribute to the lubrication of cartilage and synovial surfaces for efficient low friction joint movement. Macrophage-like type A and fibroblast-like type B synoviocytes and infiltrating leukocytes populate the synovial lining, and are important sources and targets of chemokines, cytokines, soluble mediators, and growth factors (Platt, 1996; Todhunter, 1996).

1.C. Hyaline cartilage

Extracellular matrix (ECM) content and integrity are crucial to articular cartilage strength and capability to effectively distribute load and enable repetitive near frictionless articulation. The composition of normal equine articular cartilage has been described as 50% collagen, 35% proteoglycan, 10% glycoproteins, 3% mineral, and 1% lipid (by dry mass) (Todhunter, 1996). Articular cartilage lacks nerve endings and lymphatic supply; the microenvironment is largely anerobic, and nutrients and other materials are accessible to the chondrocyte by diffusion (< 69 kDa) (Todhunter, 1996). Proteoglycan content increases with increasing depth from the articulating surface conferring a corresponding increase in compressive strength, whereas collagen concentrations are greatest at the surface for increased resistance to tensile stress.

a. Collagens

Collagens are insoluble glycoproteins synthesized as procollagen monomeric units linked by disulfide bonds as they pass through the endoplasmic reticulum and Golgi, and are polymerized into mature triple helical fibrils once secreted outside the cell. A unique abundance of glycine and hydroxylated proline / lysine (X) residues (repeating Gly-Pro-X motifs) enable the formations of tight secondary helical structures. Hydrogen and peptide bonding and oxidation of distinct lysine residues further reinforce the interactions between collagen monomers. Procollagen globular propeptides are

enzymatically cleaved upon polymerization, and have been used as serum markers for collagen turnover (Malemud, 1993).

Type II collagen is the principal collagen synthesized in normal equine articular cartilage (~ 97%) (Todhunter, *et al.*, 1994). Type II collagen is structurally homotrimeric (300 nm in length, 67 nm in diameter), composed of three identical α1(II) chains, and regularly associates with type IX and XI collagens and small amounts of types VI, XII, and XIV collagens to form dense aggregated fibrillar network structures to which proteoglycans bind. The heterotrimeric type I collagen (300 nm in length, 67 nm in diameter) is comprised of two α1(I) chains and one α2(I) chain wound in a characteristic right-handed triple helix. Type I collagen is found primarily in tendon, bone, ligaments, and fibrocartilage; type I collagen is expressed in low levels in normal articular cartilage associated with types V and VI collagen microfibrils (Todhunter, *et al.*, 1994; Lodish, *et al.*, 1999). Type X collagen has also been localized to normal articular cartilage and hypertrophic chondrocyte clusters in osteoarthritic cartilage (Rucklidge, *et al.*, 1996).

Type II collagen monomers contain more internal glycosylated hydroxylysine amino acid residues than type I collagen, contributing to interfibril aldol cross-linking. This additional type II collagen bridging endows a greater three-dimensional compressional strength to articular cartilage relative to the elastic strength of type I collagen networks (Lodish, *et al.*, 1999). Unique type II collagen amino acid sequences allow for formation of smaller diameter fibrils believed to assist in the maximal spacing of collagen fiber aggregates and interspersed proteoglycans. Type II collagen (and cartilage-specific chondroitin sulfate proteoglycan, CSPG) are commonly used as signature markers for articular cartilage and differentiated chondrocytes, whereas type I collagen abundance is considered more characteristic of a de-differentiated chondrocyte phenotype resulting from adherent culturing conditions or disease (Lefebvre, *et al.*, 1990a, b). Increased type II collagen expression levels in terminal OA cartilage may indicate high matrix remodeling activity (Aigner, *et al.*, 2001).

b. Proteoglycans

Aggrecan (~ 5 x 10^8 Da) is the most abundant proteoglycan in hyaline cartilage by mass, comprised of monomers (~ 2 x 10^6 Da) of repeating sulfated disaccharide glycosaminoglycan (GAG) units attached to a core protein at 40 nm intervals (Hamerman, 1993) **(Figure 1.1, insert)**. Aggregates of up to 100 aggrecan monomers are non-covalently linked to a hyaluronan protein backbone and stabilized by glycoprotein link proteins (40-50 kDa). Glycosaminoglycans contain one uronic acid sugar (D-glucoronic acid or L-iduronic acid) and either N-acetylglucosamine (keratan sulfate) or N-acetylgalactosamine (chondroitin sulfate). The polar charges of sulfate groups enable aggrecan to closely associate with surrounding collagen fibril networks, draw in water molecules, and establish an osmotic pressure. Aggrecan core proteins (250 kDa) contain two N-terminal globular domains and extended domains to which GAGs bind; specific amino acid motifs of the interglobular domain (IGD), between the first hyaluronic acid binding region (G1) and second globular domain (G2), are targets for increased cleavage by activated proteinases during proteoglycan breakdown in disease (McIlwraith, 1996). Keratan sulfate size and chondroitin sulfate binding patterns are reported to be age related; sulfate esters bind more commonly to the sixth carbon of galactosamine (C-6-S) in adult cartilage and bind to the fourth carbon (C-4-S) in younger animals (Hamerman, 1993; Brown, *et al.*, 1998).

Smaller, non-aggregating proteoglycans in cartilage, including the leucine-rich and dermatan sulfate containing proteoglycans, decorin and biglycan, may play important roles in cell attachment to the collagen and proteoglycan components of the ECM, cellular differentiative processes, and growth factor balances in the joint (Platt, 1996). Biglycan (dermatan sulfate proteoglycan I, DSPGI) interacts with type VI collagen and hyaluronan in cartilage and may play roles in chondrocyte membrane interactions with the ECM. Decorin (or DSPGII) has been localized to articular cartilage superficial layers, cross links type II collagen networks, may be involved in mechanical function,

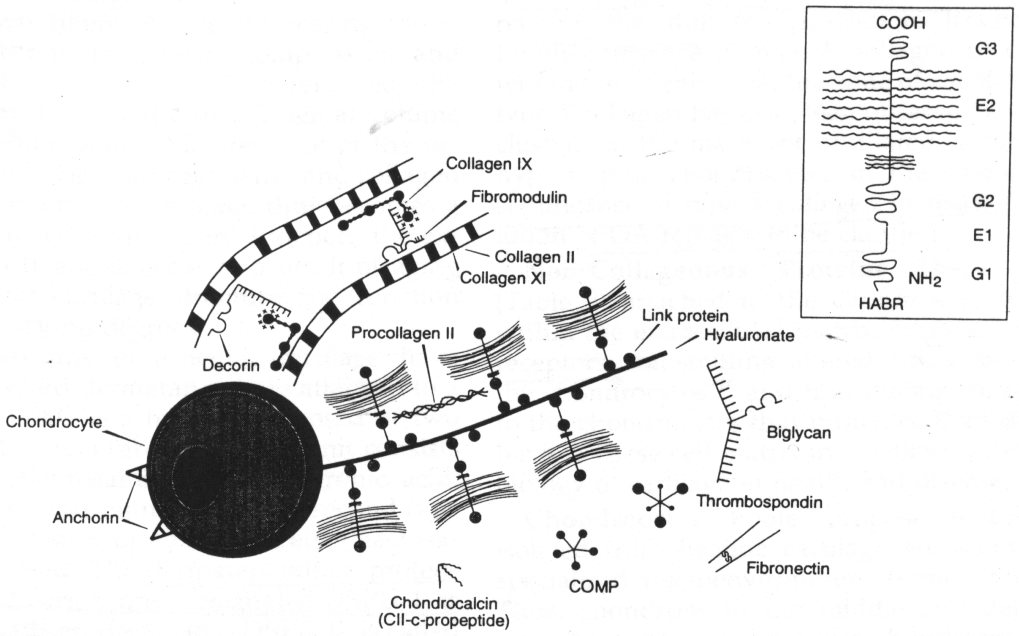

Figure 1.1 - Chondrocyte interactions with the cartilage extracellular matrix.

The insert is an enlarged schematic of aggrecan: HABR = hyaluronan binding region; G1, G2, G3 = globular domains; E1, E2 = extended domains. The shorter side chains represent keratan sulfate and the longer chains chondroitin sulfate.
Re-printed with permission from *JAGS*: Hamerman, D. Aging and osteoarthritis: basic mechanisms. *JAGS* 41:760-770, 1993.

and regulates transforming growth factor beta (TGFβ) activity. Heparan sulfate cell surface proteoglycans enable chondrocyte adhesion to the ECM and growth factors. Fibromodulin is involved in type II collagen fibrillogenesis. Versican (or CSII) directly or indirectly regulates cell adhesion and survival, proliferation, migration, phenotype, and extracellular matrix assembly. Lumican is a keratan sulphate proteoglycan most closely resembling fibromodulin that may participate in the regulation of collagen fibrillar networks.

c. Non-collagenous proteins

Additional glycoproteins arbitrate chondrocyte associations with the ECM and influence a range of biological processes (McIlwraith, 1996). Fibronectin is a cell surface-associated dimer (70 nm monomer peptides, 2-3 nm in diameter) that anchors cells to proteoglycans and collagens via integrins and cell surface associated proteoglycans. Fibronectin content is greater in OA cartilage than in normal cartilage; ECM degradation in diseased states may increase interactions of fibronectin to proteoglycans (Potts and Campbell, 1996; Aigner, *et al.*, 2001). Cartilage oligomeric matrix protein (COMP) is a high molecular-weight thrombospondin family with purported involvement in matrix repair (Recklies, *et al.*, 1998). Other described cartilage proteins include anchorin (a cell surface ECM binding protein of the calpactin/lipocortin/annexin family), tenascin (a component of embryonic cartilage), and chondroadherin (a cell associated protein shown to interact with collagen and influence collagen fibrillogenesis).

d. Chondrocytes

Chondrocytes are the sole cellular component of articular cartilage (4.7×10^4 cells/mg cartilage, 1-12% by volume), capable of producing a spectrum of pro-inflammatory mediators and responsible for regulating collagen and proteoglycan turnover (Todhunter, 1996; Kim, *et al.*, 1998). Chondrocytes are of mesenchymal origin, differentiating first as chondroblast progenitor cells. More basal chondrocytes are

rounded in shape, oriented perpendicularly to the articulating surface, and receive nutrients from the subchondral vascular channels. The chondrocytes in the superficial layer are flattened in shape, oriented parallel to the cartilage surface, and receive nutrients from the synovial fluid. Functional differences are indicated, with superficial chondrocytes demonstrated to be more receptive to cytokine stimulation, and basal chondrocytes suggested to be more involved in regulation of aggrecan synthesis (Fukuda, *et al.*, 1995). Integral cell membrane proteins (i.e. integrins), anchorins, discoidin-containing collagen receptors, and hylauronan binding receptors permit chondrocyte anchorage in the ECM and regulate cellular survival, differentiation, and matrix turnover by mechanisms still not completely understood (Hamerman, 1993; Svoboda, 1998; Lotz, 2001).

1.D. Equine osteoarthritis

Equine osteoarthritis (OA), formerly described by the term degenerative joint disease (DJD), is the most common cause of lameness in athletic horses of all breeds, characterized by complex morphological and biochemical changes in the articular cartilage, underlying subchondral bone, synovial fluid, synovium, and capsule of diarthrodial joints (McIlwraith, 1987). The result is progressive and irreversible deterioration of the structural and functional integrity of the afflicted joint articular cartilage. A survey of racing thoroughbreds revealed 53% to be affected with musculoskeletal conditions resulting in some degree of lameness; 20% were of a severity that prevented them from further racing (Jeffcott, *et al.*, 1982).

a. Diagnosis and treatment

Current methods for equine OA diagnosis are effective, but delayed from onset to when the animal displays symptoms of pain, at which time damage to joint tissues has already begun. Clearly, the need exists for improved diagnostic methods, and efforts have been made to identify serum / joint fluid markers for earlier detection, including glycosaminoglycans (keratan sulfate), proteoglycans (hyaluronan, decorin, biglycan),

collagens (chondrocalcin type II collagen propeptides), and matrix proteins (cartilage oligomeric matrix protein (COMP), link protein); however, no single marker has proven reliable in prediction of disease (Hamerman, 1993; Malemud, 1993). Suspect joints may be confirmed for disease using physical examination, gait evaluation, ultrasonography, thermography, scintigraphy, computerized tomography, magnetic resonance imaging, radiography, diagnostic anesthesia, and arthroscopy (McIlwraith, 1996). Irregularities of cartilage surface, decreased proteoglycan staining, abnormal clustering of basal chondrocytes, changes in size and ease of PG extractability, and increased water content are indicative of affected cartilage at the macromolecular level of evaluation. No cure exists for OA once it is established; many treatments for OA are currently used, but are directed toward reducing symptoms of pain and inflammation and improving joint function and athletic performance. Orthopedic surgery may be warranted in some cases to address structural pre-disposing conditions in the attempt to slow the OA progression.

b. Articular cartilage pathobiology

The pathogenesis of OA is characterized by disruption of the dynamic equilibrium between proteoglycan and collagen degradation and chondrocyte mediated repair mechanisms (McIlwraith, 1987). Severe cartilage ECM degradation can result in loss of joint mobility by soft tissue fibrosis and pain related to exposed nerves and changes in the subchondral bone and soft tissues. This imbalance towards ECM catabolism predominates since articular chondrocytes demonstrate a limited capacity for complete restoration of morphologic and biomechanical function of the ECM once it is destroyed. It is unclear whether collagen or proteoglycan breakdown is the primary event in ECM depletion associated with osteoarthritis (McIlwraith, 1996). Mechanical trauma resulting in cartilage damage may progress to OA; however, the primary etiology of the disease remains unclear (D'Lima, *et al.*, 2001). The initiation of OA may be influenced by a number of additional factors, including age, conformational abnormalities, previous injury, or chronic synovitis. Later stages of OA are characterized by inadequate

chondrocyte mediated ECM repair, loss of cartilage integrity, and chondrocyte apoptosis (Blanco, *et al.*, 1995; Blanco, *et al.*, 1998; D'Lima, *et al.*, 2001).

c. Synovitis

Inflammation of the synovium may occur as a result of repeated trauma to the joint and damage to the fibrous capsule. Clinical stages of OA and other joint diseases are associated with variable degrees of synovitis. Arthroscopically, synovitis is diagnosed by hyperemia and thickening of villi, and some degree of edema and fibrin formation. The synovium is an immunologically reactive tissue; infiltrating leukocytes are thought to be major contributors to antigen presentation and acquired immune responses. These cells, in addition to activated resident synoviocytes, may produce excessive levels of cytokines, zinc-dependent neutral matrix metalloproteinases (MMPs), lysosomal enzymes, and inflammatory factors (i.e free radicals, prostanoids, and kinins). These synovial secreted factors may influence articular cartilage biology; experimental models of synovitis have been developed to understand the role of the synovium in early pathological changes of cartilage breakdown associated with joint disease (Todhunter, *et al.*, 1996).

d. Proteinases in joint disease

Normal cartilage extracellular matrix turnover is closely regulated through balanced rates of degradation and synthesis. This regulation is largely mediated by the activity of MMPs and their specific inhibition by tissue inhibitors of matrix metalloproteinases (TIMPs). Elevated levels of MMPs and TIMPs have been detected in the articular tissues and synovial fluid of human osteoarthritic and rheumatoid arthritic joints (Pelletier, *et al.*, 1983; Dean, *et al.*, 1989; Martel-Pelletier, *et al.*, 1994; Reboul, *et al.*, 1996; Zafarullah, *et al.*, 1996). The MMPs are grouped based on their substrate activity: collagenases (MMP-1, -3, -8, -13), gelatinases (MMP-2, -9), stromelysins / proteoglycanases (MMP-3, -10), and membrane type MMPs (MT-MMPs). Interstitial collagenase-1 (MMP-1) is produced in most tissues, cleaves native triple-helical

structures of type II (Gly^{775}-Ile^{776}) and type X collagens, and may be involved in cartilage catabolism by superficial and upper layer chondrocytes in articular cartilage (Moldovan, *et al.*, 1997; Tardif, *et al.*, 1999). Interstitial collagenase-3 (MMP-13) is expressed almost exclusively by chondrocytes, is more active than MMP-1 at digesting type I and type II collagens, and has been proposed to function in remodeling processes in articular cartilage (Reboul, *et al.*, 1996; Moldovan, *et al.*, 1997; Tardif, *et al.*, 1999). Increased MMP-13 expression has also been detected in cartilage from late stage OA joints (Aigner, *et al.*, 2001; Aigner, *et al.*, 2003). Stromelysin-1 (MMP-3) cleaves link protein (His^{16}-Ile^{17}), fibronectin, the non-helical regions of types II, IV, IX, X, XI collagens, and the aggrecan core protein (Asn^{341}-Phe^{342}). High levels of baseline MMP-3 expression have been reported for normal and early OA cartilage, with lower levels of expression in tissues from late stage disease (Aigner, *et al.*, 2001; Aigner, *et al.*, 2003). The gelatinases have been detected in equine synovial fluid and late stage OA human cartilage, proposed to degrade minor collagens, aggrecan, and link protein (Clegg, *et al.*, 1997; Clegg and Carter, 1999; Aigner, *et al.*, 2001; Aigner, *et al.*, 2003). Members of the disintegrin and metalloproteinases (ADAMTS) family of proteases possess similar catalytic sites as MMPs, have been identified in human cartilage and chondrocytes, and are suggested to function in ECM metabolism, although their exact roles have not been defined (Flannery, *et al.*, 1999b).

Matrix metalloproteinase activity is controlled at the levels of transcription / protein synthesis, and extracellular activation and inhibition (Birkedal-Hansen, *et al.*, 1993). MMPs are secreted as inactive proenzymes with cysteine residues blocking amino terminal zinc binding catalytic sites. MMP activation is induced by dissociation and cleavage of inhibitory propeptide fragments by extracellular proteases, alkylating agents, organomercurials, or disulfide compounds. MMP-3 is capable of autoactivation and the activation of other MMPs; the MT1-MMP (MMP-14) is thought to activate MMP-2 and MMP-13, but not MMP-1 or MMP-8 (Richardson and Dodge, 1998; Tardif, *et al.*, 1999). Inhibited MMP and ADAMTS activities are mediated by specific and irreversible

associations of these enzymes with TIMPs. Matrix metalloproteinase / TIMP regulation is crucial to homeostatic connective tissue remodeling; disruptions in these systems at the levels of gene or protein expression are suggested to characterize joint destruction associated with osteoarthritis and other joint diseases (Dean, *et al.*, 1989; Martel-Pelletier, *et al.*, 1994).

Plasminogen activator / plasminogen activating inhibitor (PA/PAI) systems are purported to play a role in protease regulated ECM metabolism (Hamilton, *et al.*, 1991). Plasmin cleavage products are involved in fibrin degradation, thrombolysis, and pro-inflammatory responses; plasmin can activate latent pro-collagenase and pro-stromelysin, implicating a possible mechanism for PA-mediated ECM remodeling (McIlwraith, 1996). Elevated PA levels have been reported in the synovial fluid of patients with osteoarthritis (urokinase-PA, u-PA) and rheumatoid arthritis (tissue-PA, t-PA and u-PA) (Kikuchi, *et al.*, 1987). A colony stimulating growth factor network for PA activation, influenced by cytokine stimulation (IL-1 and TNFα), has been proposed in the joint (Hamilton, *et al.*, 1991). Plasminogen activator inhibitor-1 and PAI-2 levels have been evaluated in cartilage, chondrocytes, and synoviocytes in culture; further understanding of cytokine mediated PAI expression mechanisms may suggest possible modulations of PA activity in therapeutic approaches (Hamilton, *et al.*, 1991; DiBattista, *et al.*, 1994).

e. Cytokine mediation of disease

IL-1 and TNFa

A cytokine-driven chronic inflammation is thought to be responsible for the progressive and debilitating destruction of articular cartilage in OA. Key players in cytokine mediated extracellular matrix deterioration include interleukin-1 (IL-1) (*refer to 1.D.*) and tumor necrosis factor alpha (TNFα). IL-1 and TNFα are produced by activated chondrocytes, synoviocytes, and infiltrating inflammatory cells, and stimulate production of prostaglandin E_2 (PGE_2), nitric oxide (NO), matrix degrading proteases (e.g. MMPs), and other pro-inflammatory mediators and cytokines (e.g. IL-1, IL-6, and IL-8) (Lotz, *et*

al., 1995; Lotz, 2001; Fernandes, *et al.*, 2002). Secondary effects include increased risk for cell death by apoptosis (via NO pathways), inhibited proteoglycan synthesis in chondrocytes, and bone resorption by osteoclasts (Blanco, *et al.*, 1995; Lotz, 2001). The two cytokines mediate similar pro-inflammatory and ECM catabolic effects via distinctly different cell surface receptors and signal transduction pathways (Lotz, *et al.*, 1995; van den Berg, *et al.*, 1999). Increased cytokine receptor levels or increased auto-activation are possible mechanisms for enhanced sensitivity of chondrocytes and synoviocytes to the effects of the cytokines during inflammation and disease (Fernandes, *et al.*, 2002).

IL-6, IL-8, IL-17, IL-18, and LIF

Interleukin (IL-6) has well described roles in systemic acute phase responses and pro-inflammatory effects. However, the role of IL-6 in joint pathobiology remains incompletely understood; conflicting reports exist on its effect on proteoglycan synthesis and bone resorption / remodeling (Ishimi, *et al.*, 1990; Nietfeld, *et al.*, 1990; al-Humidan, *et al.*, 1991; Van de Loo, *et al.*, 1997). IL-6 was shown to induce tissue inhibitor of matrix metalloproteinase (TIMP) expression, suggesting a role for the cytokine in ECM homeostasis (Lotz and Guerne, 1991). Interleukin-8 (IL-8) is a potent chemotactic agent for polymorphonuclear cells, and enhances the production of reactive oxygen and 5-lipoxygenase metabolic products (Lotz, *et al.*, 1992b). Interleukin-17 (IL-17) has been shown to stimulate IL-1β, TNFα, IL-6, nitric oxide, and MMP synthesis in macrophages and chondrocytes (Attur, *et al.*, 1997; Jovanovic, *et al.*, 1998b; Fernandes, *et al.*, 2002). Interleukin-18 (IL-18) belongs to the IL-1 family and has been shown to induce nitric oxide production, inhibit TGFβ mediated proliferation, and glycosaminoglycan release in chondrocytes (Olee, *et al.*, 1999). Leukemia inducing factor (LIF), belonging to the IL-6 family of cyokines, induces IL-1β, IL-6, TNFα, and IL-8 expression in chondrocytes and fibroblasts, and suppresses proteoglycan synthesis in chondrocytes (Lotz, *et al.*, 1992a; Van de Loo, *et al.*, 1997).

IL-4, IL-10, and IL-13

The anti-inflammatory cytokines, interleukin-4 (IL-4), interleukin-10 (IL-10), and interleukin-13 (IL-13), suppress the effects of pro-inflammatory cytokines (e.g. IL-1 and TNFα) and have been found in increased concentrations in OA synovial fluid (Fernandes, 2002 #176). Interleukin-4 and IL-10 inhibit the production of IL-1β, TNFα, PGE_2, and MMP, and up-regulate TIMP and interleukin-1 receptor antagonist (IL-1ra). It was suggested that IL-4 and IL-10 suppressed TNFα activity by down-regulation of TNF receptor (Hart, *et al.*, 1995; Fernandes, *et al.*, 2002). Interleukin-13 has been shown to decrease IL-1β, TNFα, and MMP-3 production and increase production of IL-1ra in human OA synovium and synovial fibroblast cultures (Jovanovic, *et al.*, 1998a). Interleukin-4 and IL-13 may down-regulate MMP-13 synthesis; studies describing treatment of OA synovial tissue *in-vitro* suggest these cytokines may have potential in treatment in clinical OA (Bendrups, *et al.*, 1993; Jovanovic, *et al.*, 1998a; Tardif, *et al.*, 1999). Interleukin-10 is currently being tested as a therapeutic agent in clinical trials for rheumatoid arthritis in human patients (Fernandes, *et al.*, 2002).

f. Growth factors in joint biology

TGFb and BMP

Members of the transforming growth factor family (TGFβ) play important roles in ECM anabolism by inducing hyaluronan, aggrecan, and collagen synthesis while reducing ECM degradation, presumably by decreasing MMP production and increasing protease inhibitor levels (TIMPs and PAIs) (Hamerman, 1993; Lotz, *et al.*, 1995). Other effects of TGFβ include increased fibroblast and monocyte chemotaxis, fibroblast proliferation, cartilage calcification, and bone formation (Lotz, *et al.*, 1995). The TGFβ1-3 isoforms induced dose-dependent proliferation in differentiated chondrocytes (Villiger and Lotz, 1992; Guerne, *et al.*, 1994). Inactive TGFβs are ECM sequestered by binding to decorin core protein; activation occurs *in-vivo* following proteolytic cleavage of an inhibitory binding protein. Interestingly, TGFβ has a role in the control of decorin

synthesis, suggesting a check-and-balance system for active levels of this growth factor in cartilage (Hamerman, 1993). IL-1 has been shown to inhibit the growth promoting effects of TGFβ, possibly via induction of PGE_2 and nitric oxide (Guerne, *et al.*, 1994; Rediske, *et al.*, 1994). Conversely, TGFβ was shown to inhibit IL-1 induced MMP mediated cartilage catabolism; this direct antagonism between TGFβ and IL-1 in the regulation of chondrocyte function is of particular interest regarding development of anti-IL-1 therapeutic strategies (van Beuningen, *et al.*, 1993; Lotz, *et al.*, 1995). The bone morphogenetic proteins (BMPs) are members of the TGFβ family, reported to stimulate growth plate chondrocyte growth and differentiation, increase expression of type II collagen and aggrecan in chondrocytes, independently induce endochondral ossification, and play critical roles in bone development (Hiraki, *et al.*, 1991; Luyten, *et al.*, 1994).

IGFs

The insulin-like growth factors (IGF-I and -II) were demonstrated to be mediators of growth, differentiation, and survival in cultured chondrocytes (Bhaumick and Bala, 1991; Loeser and Shanker, 2000). Different regulatory roles for IGF-1 and IGF-II have been proposed in differentiating chondrocytes: IGF-I has been associated with growth and differentiation and IGF-II with glucose metabolism (Bhaumick and Bala, 1991). It has been suggested that chondrocyte compromised sensitivity to IGF-1, an important stimulator of aggrecan and type II collagen production, may correlate with active arthritis or severity of disease (Platt, 1996; Davies, *et al.*, 1997). To date, eight known binding carrier proteins (IGFBPs) and their associated degradative proteinases assist in regulating IGF biology (Heemskerk, *et al.*, 1999). Interleukin-1 (IL-1α and IL-1β) induced chondrocyte IGFBP3 and IGFBP5 synthesis and suppressed IGF-1 mediated proteoglycan synthesis, representing a possible mechanism for dysregulation of cartilage remodeling (Olney, *et al.*, 1995; Sunic, *et al.*, 1998). Circulating IGF-1 and growth hormone (GH) are potent mitogens for growth plate chondrocytes; locally synthesized IGF-1 and IGF-II stimulate osteoblast and chondrocyte proliferation and are implicated in

chondrocyte survival and pro-differentiation (McCarthy, *et al.*, 1989; Guerne, *et al.*, 1994; Loeser and Shanker, 2000).

PDGF and FGF

Other growth factors with reported involvement in joint pathobiology include the platelet derived growth factors (PDGFA, PDGFB) and the acidic and basic fibroblast growth factors (aFGF, bFGF). Platelet derived growth factor exhibits chemotactic properties for monocytes, stimulates osteoblast, chondrocyte, and fibroblast proliferation, and up-regulates IL-1 receptors in fibroblasts (Hamerman, 1993; Guerne, *et al.*, 1994). Basic FGF associates with ECM proteoglycans and chondrocyte surface membrane syndecan in articular cartilage; the growth properties of FGFs synergize with IGF-1, TGFβ, and epidermal growth factor (EGF) effects in chondrocytes (Osborn, *et al.*, 1989; Crabb, *et al.*, 1990; Hamerman, 1993). Basic FGF also increases collagen and proteoglycan synthesis in growth plate chondrocytes, in synergy with TGFβ effects (Hill, 1992). Exogenous bFGF enhances fibroblast proliferation, increases IL-1 receptors, and assists in IL-1-induced proteinase levels (Chin, *et al.*, 1991; Guerne, *et al.*, 1994). FGF released from diseased chondrocytes may also induce angiogenesis, and stimulate osteoclastic precursor cells and bone formation (Canalis, *et al.*, 1988).

g. Prostaglandins in joint disease

Prostaglandins are short-lived pro-inflammatory mediators derived from cell membrane phospholipid 20-carbon unsaturated fatty acids (i.e. arachidonic acid) by way of the cyclooxygenase pathway. Phospholipase A2 (PLA2) levels are thought to originate from articular chondrocytes in high-pressure articulating cartilage surfaces of the joint; PLA2 activity has been shown to increase downstream production of prostaglandins, platelet activating factor, and lysophospholipids (Pruzanski, *et al.*, 1991). Prostaglandin E_2 (PGE_2), in particular, has been attributed to imbalances in cartilage extracellular matrix metabolism possibly associated with joint disease pathogenesis. PGE_2 is present in normal equine joint synovium and synovial fluid (12-940 pg/ml) and

relative PGE_2 levels may be correlated with arthritis conditions and degree of lameness (McIlwraith, 1996). Interleukin-1 and lipopolyssacharide (LPS) have been shown to stimulate PGE_2 production in cultured equine chondrocytes and synovial cells (May, *et al.*, 1989, 1992a, c; MacDonald, *et al.*, 1994). PGE_2 is thought to contribute to vasodilation, enhancement of pain perception, increased PA production, and bone demineralization. Additionally, PGE_2 increases adenyl cyclase activity, resulting in elevated intracellular cyclic AMP levels and subsequent increased protein synthesis that may contribute to proteoglycan degradation by induced release of latent MMPs (Drezner, *et al.*, 1976; Malemud and Sokoloff, 1977).

Current clinical therapies are directed at lowering elevated prostanoid levels in inflamed joints. Corticosteroids have been used for their inhibitory effects on PLA2 activity and production of pro-inflammatory products of both the cyclooxygenase (COX) and lipoxygenase pathways; decreased PGE_2 levels and clinical improvement of joint function have resulted from corticosteroid treatments (McIlwraith, 1996). Non-steroidal drugs (NSAIDS) are often used for targeted inhibition of cyclooxygenase-mediated inflammatory cascades that convert arachidonic acid to prostaglandins and thromboxanes. Inhibitors of COX-2 are of current interest for joint disease treatment since they confer anti-inflammatory effects without inhibiting COX-1 derived prostaglandins important for normal function of platelets and the gastrointestinal tract. Side effects of prolonged use of NSAIDS include edema and hematopoietic problems, as well as stomach (COX-1 inhibitors), renal, and heart (COX-2 inhibitors) complications, and as such, may be a concern for some patients.

h. Chondrocyte phenotype in OA

Osteoarthritis, aging, and *in-vitro* subculture have been associated with articular cartilage chondrocyte de-differentiation to a fibroblastic phenotype with associated changes in cellular morphology and biochemical characteristics (Chrisman, 1969; Hamerman, 1993). Chondrocytes in monolayer culture are decreased in cellular density,

acquire elongated shapes, produce a predominance of type I and III collagens (instead of type II collagen), and demonstrate decreased synthesis of the aggrecan cartilage-specific proteoglycan relative to primary cultures (Lefebvre, *et al.*, 1990a, b). Altered collagen composition in subcultured chondrocytes has been reported as 41% type I, 25% type V, 20% type I trimer, 13% type III, and less than 1% type II (Benya, *et al.*, 1978). Chondrocyte differentiative modulation can be distinguished in two processes: the first is a suppression of the differentiated phenotype, and the second is the induction of the de-differentiated phenotype, which may be species-specific and dependent on cartilage location (Benya, *et al.*, 1978). Cell adhesion, growth, and actin-mediated changes in morphology following removal of chondrocytes from existing ECM structures of cartilage are potential causes of modulated chondrocyte phenotype, presumably mediated by changes in gene expression (Mallein-Gerin, *et al.*, 1991). These changes in phenotype, cell shape, and expression patterns are apparently reversible by three-dimensional culturing or dihydrocytochalasin B or staurosporine treatments (Benya and Shaffer, 1982; Reginato, *et al.*, 1994).

Interleukin-1 strongly inhibits the differentiated chondrocyte phenotype, possibly through depressed expression of transcription factors and chondrocyte-specific genes (Goldring, *et al.*, 1988; Murakami, *et al.*, 2000). Dedifferentiated chondrocytes in subculture exhibit reduced extracellular matrix collagen incorporation, increased basal TIMP levels, and increased procollagenase in response to IL-1 and TNFα (Lefebvre, *et al.*, 1990a, b). Interleukin-1 inhibits proliferation of chondrocytes grown in explant culture and primary monolayers, but induces growth in de-differentiated and diseased chondrocytes (Guerne, *et al.*, 1994; Lotz, *et al.*, 1995). Increased sensitivity of de-differentiated chondrocytes to IL-1 and TNFα may contribute to chondrocyte mediated cartilage destruction during states of disease.

1.E. Interleukin-1

The interleukin-1 (IL-1) polypeptides are potent stimulators of a variety of physiologic, hematopoietic, metabolic, and immunologic responses occurring at femtomolar concentrations and in response to binding a small fraction of available cell surface receptors (Dinarello, 1994a; Lotz, 2001). The IL-1 family has been distinguished as important pro-inflammatory cytokines inducing the translation of a variety of proteins leading to inflammation and the cascade of events progressing to a variety of diseases (Dinarello, 1996). IL-1 has been described to mediate both general and local inflammatory responses in specialized epithelial, endothelial, keratinocyte, fibroblast, and dendritic cells (Dinarello, 1994b). These effects are mediated in conjunction with TNFα and IL-6 in the generation and release of the hepatic acute-phase proteins, a critical response to bacterial infection or other inflammatory agents. IL-1 activates specific phospholipase pathways that generate arachidonic acid metabolites that contribute to the pyrogenic response to infection and fever. IL-1 also plays critical roles in immunological responses, including T-cell activation, B-cell proliferation / maturation, macrophage antigen presentation, and the induction of IL-2, IL-2 receptors, IL-3, IL-4, IL-5, and IL-6.

Interleukin-1 beta (IL-1β) is synthesized as an inactive precursor cleaved by the interleukin-1 converting enzyme (ICE) to its secreted and biologically active form. IL-1β is implicated with paracrine, autocrine, and endocrine stimulatory effects (17 kDa mature protein). IL-1 alpha (IL-1α) is cleaved by other intracellular proteases and remains primarily cytosolic, usually not found in the circulation or inflammatory effusions (17 kDa mature protein) (Dinarello, 1994a). IL-1 receptor antagonist (IL-1ra) is the naturally occurring inhibitor of IL-1 activity that binds to the same IL-1 receptors without inducing signal transduction. Three IL-1ra proteins have been identified: one soluble (IL-1sRa) and two intracellular (icIL-1RaI and icIL-1RaII) forms. Two IL-1 receptors have been identified in cell membrane-associated and soluble forms: IL-1RI is constitutively expressed on the cell surface of a variety of cell types and involved in signal transduction, whereas IL-1RII is thought to act as a decoy receptor and a natural

modulator of IL-1β effects (Dinarello, 1994a; Attur, *et al.*, 2000). Binding to IL-1RII, in its membrane-bound or soluble forms, does not activate signaling cascade events and instead serves in the competitive binding of IL-1 for the IL-1RI receptor. A strong affinity of IL-1ra for soluble IL-1RI, and IL-1β for soluble IL-1RII, has been described. Subtle changes at any point of these tightly regulated and interactive mechanisms could result in imbalances in IL-1 effects that contribute to disease processes (Fernandes, *et al.*, 2002).

a. Interleukin-1 in joint disease

Results of *in-vitro* studies convincingly support the notion that IL-1 may play an important role in the pathogenesis of the cartilage destruction associated with equine OA (MacDonald, *et al.*, 1992; Morris and Treadwell, 1994; Platt and Bayliss, 1994). Elevated synovial fluid IL-1 activity has been significantly associated with naturally occurring equine OA (Morris, *et al.*, 1990; Alwan, *et al.*, 1991). The initiators of IL-1 production in a naturally occurring joint disease have not been identified, but may involve mechanical stress or degraded components of the ECM, such as fibronectin and cartilage fragments (Homandberg, 1999; Lotz, 2001). Injection of IL-1 into joints of animals resulted in synovial fluid leukocytosis, proteoglycan (PG) and chondrocyte loss, fibroplasia, and subchondral bone resorption (Pettipher, *et al.*, 1986; Chandrasekhar, *et al.*, 1992). Previous studies have demonstrated IL-1 to increase PG degradation and to inhibit PG synthesis in articular cartilage explant cultures in equine and non-equine models (Tyler, 1985; Pettipher, *et al.*, 1986; MacDonald, *et al.*, 1992; Arner, 1994; Morris and Treadwell, 1994; Platt and Bayliss, 1994; Frisbie and Nixon, 1997). This imbalance in PG metabolism may occur via IL-1 stimulated MMP-1, MMP-2, MMP-3, MMP-9, MMP-13, MT1-MMP, metalloelastase, and TIMP-1 synthesis in chondrocytes and fibroblasts (Gowen, *et al.*, 1984; May, *et al.*, 1992a; Morris and Treadwell, 1994; DiBattista, *et al.*, 1995a; Caron, *et al.*, 1996; Imai, *et al.*, 1997; Clegg and Carter, 1999; Richardson and Dodge, 2000).

Other effects of IL-1 in chondrocytes include the induction of IL-1, IL-6, decreased expression of hyaline cartilage specific collagens types II, IX, and XI, link protein, aggrecan, biglycan, and decorin, and apoptosis via nitric oxide pathways (Tyler, *et al.*, 1990; Taskiran, *et al.*, 1994; Blanco, *et al.*, 1995; Hardy, *et al.*, 1998b; Richardson and Dodge, 2000). Protective anti-apoptotic mechanisms induced by IL-1 have also been described via transcription factor NFkB / tyrosine kinase activation (Kuhn, *et al.*, 2000). In chondrocytes, IL-1 increases levels of urokinase-type PA (u-PA) and tissue-type PA (t-PA) serine proteases associated with cartilage matrix resorption (Campbell, *et al.*, 1988). In synoviocytes, IL-1 induces cyclooxygenase dependent synoviocyte u-PA secretion (Hamilton, *et al.*, 1991). IL-1 also induces chondrocyte production of phospholipase A2, and cyclooxygenase, resulting in increased levels of PGE_2 (Chang, *et al.*, 1986; Campbell, *et al.*, 1990).

Interleukin-1 is a key mediator of inflammatory and immunological activity in osteoclasts (Tani-Ishii, *et al.*, 1999; Suda, *et al.*, 2001). IL-1 has been suggested to regulate mature osteoclast survival by decreased caspase-3 activity and reduced spontaneous apoptosis (Lee, *et al.*, 2002). In conjunction with TNFα, IL-1 stimulates production of osteoblast-like multinucleated cells and local bone resorption (Tani-Ishii, *et al.*, 1999). IL-1 also stimulates peripheral mononuclear blood cell mobilization and osteoblast differentiation (Suda, *et al.*, 2001; Tokukoda, *et al.*, 2001).

b. IL-1 signaling

Interleukin-1 signal transduction may vary depending on cell type, cellular phenotype or physiology, and the particular biological response of interest (Dinarello, 1994b; O'Neill, 1995). IL-1 can bind to specific transmembrane IL-1 receptors (IL-1RI) and initiate recruitment of an extracellular receptor accessory protein (IL-1RacP) to the receptor complex. The IL-1RI cytoplasmic domain (213 amino acids) is involved in binding to the cytosolic proteins MyD88 and Tollip (Li, *et al.*, 2001). The IL-1 receptor associated serine-threonine kinases (IRAK-1 and IRAK-2) are recruited to the complex to

associate with TRAF6, which itself is complexed to TAK1 and TAB1, by TAK2 translocated from the cell-surface membrane. Activated TAK1 in turn phosphorylates IkB kinases via NFkB inducing kinase activation. The IkB kinases phosphorylate NFkBs and mediate translocation to the cell nucleus for transcriptional regulation. IL-1 up-regulated NFkB (relB, p100/p52, p105/p50, IkB-e, c-rel, p65), AP-1 (fra-1 and junB), and ETS (ets-1) transcription in a chondrocyte cell line; competitive binding of multiple transcription factors for DNA binding sites was suggested (Vincenti and Brinckerhoff, 2001).

IL-1 induced cAMP levels (via phospholipase C), ceramide pathways via sphingomyelinase activation, and tyrosine kinase activity have also been demonstrated in chondrocytes **(Figure 1.2)** (Kolesnick, *et al.*, 1994; Lotz, *et al.*, 1995). It is suggested that IL-1 signaling also involves mitogen activated protein kinase (MAPK) pathways leading to c-jun N-terminal kinase (JNK), ATF, and AP1 transcription factor activation. In chondrocytes, IL-1 was shown to activate early response kinase (ERK) and p38 at a 1.0 ng/ml concentration, and JNK at 10 ng/ml; maximal activation occurred within 15 minutes and baseline levels were restored by 1 hour (Scherle, *et al.*, 1997). IL-1 was shown to increase transcription of G-proteins (e.g. rho6, Gem) and to decrease others (e.g. rho7, RAD1, and p160ROCK), further highlighting the complexity of IL-1 signal transduction in chondrocytes (Vincenti and Brinckerhoff, 2001). Inhibition of SMAD4, one of the essential signaling mediators of TGFβ stimulation, was suggested to mediate IL-1 antagonism of TGFβ effects in chondrocytes (Vincenti and Brinckerhoff, 2001).

Interleukin-1 signaling is complex and may involve distinct cis regulatory elements and nuclear trans acting factors in the transcriptional activation of different genes responsible for altered ECM remodeling associated with joint disease. IL-1 induced MMP-13 transcription in chondrocytes via MAPK mediators (p38, Runx-2, AP1, JNK) and NFkB activation (Mengshol, *et al.*, 2001). However, in a separate study, IL-1 induced MMP-1 transcription was not affected by inhibition of MEK (a MAPK kinase),

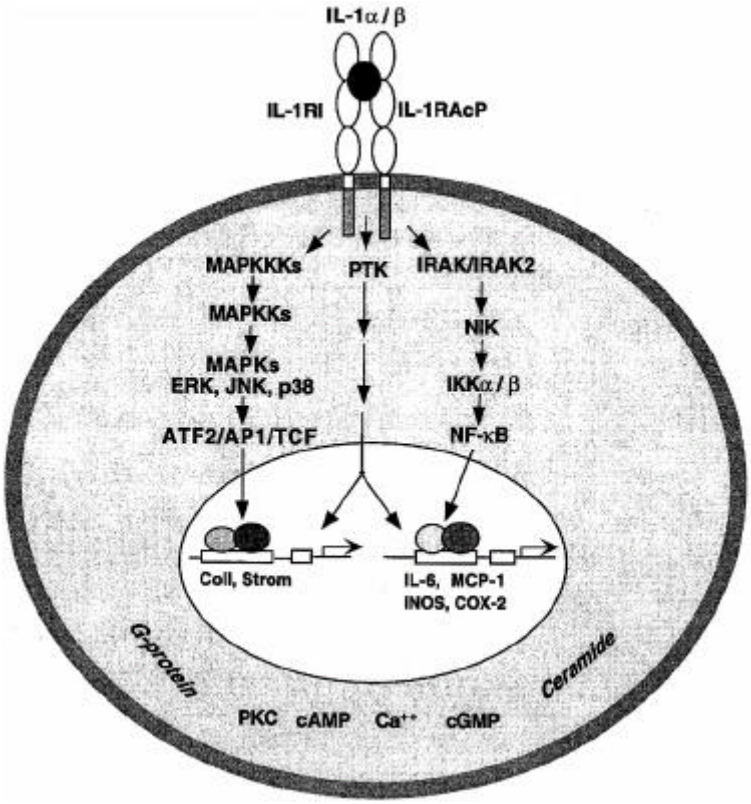

Figure 1.2 - Intracellular signaling events activated by IL-1 in chondrocytes.

Interleukin-1 alpha / IL-1 beta binding to the IL-1 receptor (IL-1R) recruits the IL-1R accessory protein (IL-1RAcP). The three major signaling pathways are: (1) mitogen activated protein kinase (MAPK), leading to the activation of the transcription factors ATF1/AP1/TCF; (2) protein tyrosine; and (3) NF-kB. Interleukin-1 also activates intracellular G-proteins, protein kinase C (PKC), cAMP, intracellular calcium, cGMP, and ceramide. These signals may modulate expression of subsets of IL-1 responsive genes.

Re-printed with permission from *Lippincott Williams & Wilkins* (www.lww.com): Lotz, M. Cytokines in cartilage injury and repair: *Clin Orthop* 1(391) SUPPLEMENT: S108-S115, 2001.

and inhibition of p38 kinase yielded variable effects (Mengshol, *et al.*, 2001). Another study indicated IL-1 to activate the signal transducer and activator of transcription (STAT-3) in interstitial collagenase transcription, although no specific binding of STAT-3 to the promoter was described (Catterall, *et al.*, 2001). A study using an immortalized costal chondrocyte cell-line described up-regulation of c-fos, c-jun, egr-1, and jun-B intermediate signaling genes to occur within 1 hour of IL-1β stimulation prior to MMP-1 and MMP-3 induced expression at 6 hours (Goldring, *et al.*, 1994). Another report suggested similar signaling mechanisms were involved in the IL-1β dose-dependent and protein kinase C mediated MMP-1, MMP-3, and TIMP-1 transcriptional activation in fibroblasts (DiBattista, *et al.*, 1995b).

1.F. Complementary DNA array hybridization

Microarray technology is a sophisticated molecular-based tool used to compare differential transcript levels present in one cell / tissue type relative to another (Schena, 1999; Schena, 2003). Preparation of microarrays, or 'biochips', involve the fixation of cDNA 'targets' onto non-porous surfaces (e.g. glass slides) using piezoelectric / microspotting robotics or photolithographic solid phase 3'-5' oligonucleotide synthesis. Expression levels of up to thousands of cDNAs corresponding to known (or unknown) identity and function can be simultaneously measured by hybridizing the array with the fluorescently labeled cDNA populations of interest. Two cDNA populations are enzymatically tagged with separate florescent markers (e.g. cy3 and cy5) and hybridized to the same microarrays. Fluorescence signals are detected using confocal scanning coupled with laser excitation.

The more traditional cDNA hybridization technology uses the incorporation of a radioactively labeled dNTP during cDNA synthesis and the hybridization of separate membrane-based arrays with two cDNA populations being compared, similar to a large-scale Southern blotting analysis. Positive signals are identified by exposure of the

hybridized arrays to radiographic film or a phosphorimaging screen and analyzed using a densitometer or a phosphorimager **(Figure 1.3)**.

Applications of array technology

Microarray / gene array applications are quickly growing in present day biomedical approaches to the study of diseases in man and animals. Recent microarray studies have been helpful in the profiling gene expression patterns and identifying transcripts unique to diseased tissues or disease states for further investigation into possible points of disease intervention or therapy (Nguyen, *et al.*, 1995; Schena, *et al.*, 1996; Wodicka, *et al.*, 1997; Schena, *et al.*, 1998; van Hal, *et al.*, 2000). Possible applications of these data may assist in the understanding and diagnosis of progressive disease pathogenesis, as in the case of cancer or chronic inflammatory-mediated disorders, in which complex pathways and cell-signaling cascades are involved (DeRisi, *et al.*, 1996; Heller, *et al.*, 1997). Other applications of microarrays include mutation mapping, pathogen identification, polymorphism analysis, and evolutionary-based investigations (Schena, 1999). Microarrays may also have applications to pharmacogenetic research, drug screening, and drug discovery.

1.G. Array data mining and modeling

a. Array data analysis

A major obstacle to cDNA array expression analysis is managing large volumes of data from which confident and clear interpretations must be made. The statistical measures employed must be carefully chosen, tested, and tailored for each data set / experiment studied. Statistical approaches for microarray data include on the most basic level, the retrieval of raw image data and simple comparisons of signal intensities within a studied cDNA ('hypothesis testing'). Visualization tools, such as scatter plots, are often used to graphically represent microarray data in two-dimensions for intuitive diagnostic evaluation of data quality and assistance in ratio calculations. More complex analyses are involved when attempting to identify effects at a higher level of organization, including

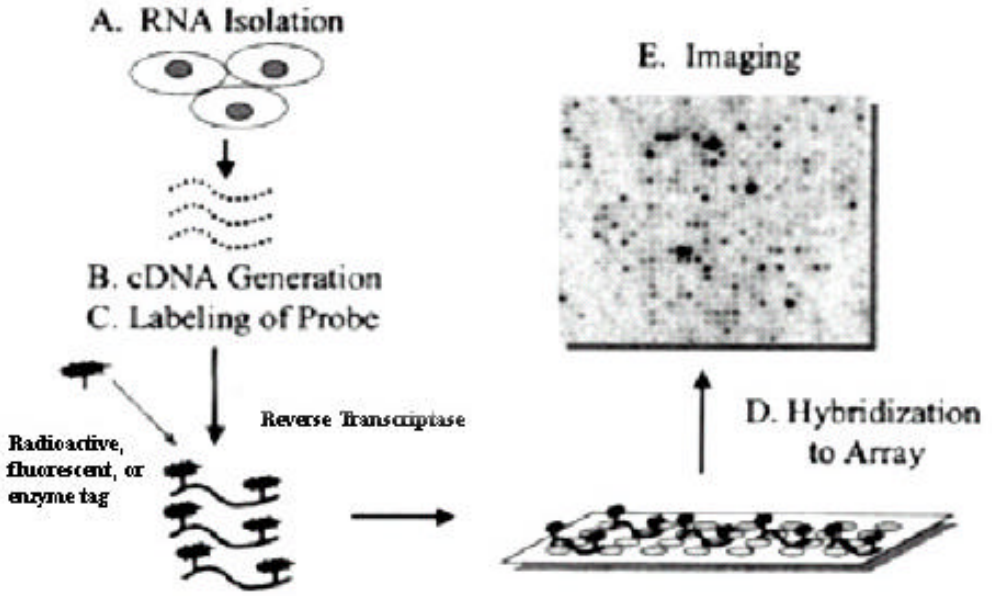

Figure 1.3 - Schematic illustration of the steps involved in cDNA macroarray analysis.

Re-printed with permission from *AJRCMB*: Albelda SM, Sheppard D. Functional Genomics and Expression Profiling: *Am J Respir Cell Mol Biol* 2000; 23:265-69.

supervised / unsupervised learning classification, hierarchical / nonhierarchical clustering, principal component analysis, expression maps, pathway analysis, and self-organizing maps (Schena, 1999; Schena, 2003). These attempts are necessary when considering a protein does not always have a single biochemical function or cellular role and acts in conjunction with other proteins and molecules; elucidating co-regulated expression of individual genes is a powerful means for establishing possible biological networks associated with stages of a disease or an experimental treatment ('hypothesis generation'). Such mathematical modeling also provides potential for sample classification from patients with pre-defined clinical conditions for molecular profiling of a disease from the most significant signatures retrieved from microarray results.

b. Principal component analysis

A potential informative strength of microarray-generated data is the identification of co-regulation or relationships in gene expression. Principal component analysis (PCA) reduces the dimensionality of multivariate data into smaller sets of three-dimensional hypothetical constructs or principal components (PCs) visualized by standard graphical techniques (PROC PRINCOMP, SAS, Madison WI) (Timm, 2002). Coordinates are assigned to best represent the internal variability in the data **(Figure 1.4)**; multi-dimensional relationships between gene expression levels are maintained in the new three-dimensional representation within each component. The co-variances explained by the identified components are equal to their 'eigenvalues' (visually depicted in 'scree-plots'); the sum of all eigenvalues accounts for 100% of the original variance. Gene variables with the greatest variance tend to load heavily on the first principal component; uncorrelated variables load on different components. PCA can provide functional clues to unknown cDNAs based on how closely they associate with known genes.

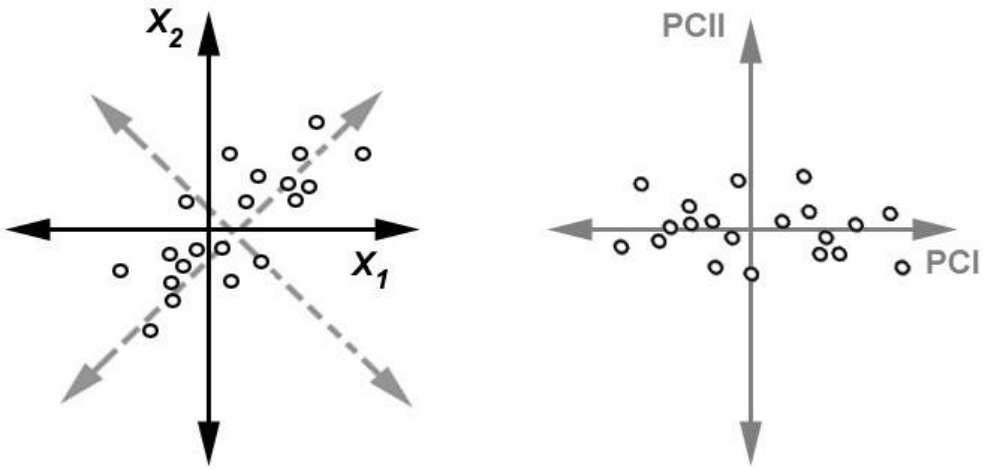

Figure 1.4 - Geometric schematic of principal component analysis.

New principal component (PC) coordinate axes (I and II) are designated to re-project multidimensional data sets and account for maximal variance.

1.H. Rationale for research

The consequences of joint conditions that progress to OA are economically consuming and can compromise quality of life of the affected animals. The synovium and articular cartilage are biologically interactive and together contribute to proper joint function. Elucidating disruptions in molecular, metabolic, and physiologic conditions of homeostasis are crucial to understanding the processes that may occur in these tissues during OA initiation and pathogenesis. The presented research encompasses the study of recombinant equine IL-1 (EqIL-1) induced changes in proteoglycan and prostaglandin metabolism in articular cartilage and steady state transcript levels in cultured chondrocyte and *in-vivo* stimulated synovium. These characterizations of proximal EqIL-1 mediated effects on ECM catabolism and gene expression levels in models of OA and an acute synovitis may be helpful in the identification of anti-IL-1 directed therapies and improved methods for the early diagnosis of joint disease.

CHAPTER II: Effects of equine recombinant interleukin-1a and interleukin-1b on proteoglycan metabolism and prostaglandin E_2 synthesis in equine articular cartilage explants

Modified and re-printed with permission, *AJVR*, Vol 63 (4), April 2002, 551-558

2.A. Abstract

The objectives of this study were to evaluate the effects of equine recombinant interleukin-1α (EqIL-1α) and recombinant interleukin-1β (EqIL-1β) on proteoglycan metabolism and prostaglandin E_2 (PGE_2) synthesis by equine articular chondrocytes in explant culture. Expression constructs containing cDNA sequences encoding EqIL-1α and EqIL-1β were generated, prokaryotically expressed, and the recombinant proteins purified. Near full-thickness articular cartilage explants (~ 50 mg), harvested from stifle joints of a 2-year-old and a 5-year-old horse, were separately randomized to receive EqIL-1α or EqIL-1β treatments (0 to 500 ng/ml). Proteoglycan release was evaluated by 1,9-dimethylmethylene blue spectrophotometric analysis of explant media glycosaminoglycan (GAG) concentration and release of ^{35}S-sulfate-labeled GAG to explant media. Proteoglycan synthesis was assessed by quantification of ^{35}S-sulfate incorporation into proteoglycan. Explant media PGE_2 concentrations were evaluated using a PGE_2-specific enzyme-linked immunoassay. Data were collected at 48-hour intervals and normalized by DNA content. Proteoglycan release was induced by EqIL-1α and rEqIL-1β at concentrations ≥ 0.1 ng/ml, with 38 to 76% and 88 to 98% of total GAG released by 4 and 6 days, respectively ($p<0.001$). Inhibition of proteoglycan synthesis (42 to 64%) was observed at IL-1 concentrations ≥ 0.1 ng/ml at 2 and 4 days ($p<0.001$). Increased PGE_2 concentrations were observed at IL-1 concentrations ≥ 1.0 ng/ml at 2 and 4 days ($p<0.001$). Equine IL-1 induced potent concentration-dependent derangement of equine chondrocyte metabolism *in-vitro*. These findings suggest this

model may be suitable for the *in-vitro* study of the pathogenesis and treatment of joint disease in horses.

2.B. Background

Interleukin-1 (IL-1) has been widely implicated with roles in the regulation of inflammatory and immunologic responses to injury and disease (Dinarello, 1994a, 1996). The agonist members of the IL-1 family, IL-1α and IL-1β, have been demonstrated to evoke signal transduction in response to binding only a few transmembrane receptors (i.e. IL-1RI) per cell and to induce pleiotropic cell-type dependent effects at picomolar and femtomolar concentrations (Dinarello, 1994a).

IL-1 mediates a number of pro-inflammatory and early pathogenic responses thought to be involved in the initiation of joint disease in man and other animals (Gowen, *et al.*, 1984; Wood, *et al.*, 1985; Pettipher, *et al.*, 1986; McIlwraith, 1987; Towle, *et al.*, 1987; May, *et al.*, 1992a; Dinarello, 1996), including the induction (Chang, *et al.*, 1986) and synthesis (Lyons-Giordano, *et al.*, 1989) of phospholipase A_2, and increased synthesis of cyclooxygenase, prostaglandin E_2 (PGE_2), and thromboxane B_2 (Chin and Lin, 1988; Campbell, *et al.*, 1990). Additionally, IL-1 has been shown to increase the production of tissue plasminogen activator, urinary plasminogen activator (Bunning, *et al.*, 1987; Campbell, *et al.*, 1988), and nitric oxide synthase (Platt, 1996), induce a dose-dependent release of articular cartilage extracellular matrix proteoglycan (PG) (Pasternak, *et al.*, 1986; Pettipher, *et al.*, 1986; Arner, 1994), inhibit PG synthesis by articular chondrocytes (Ikebe, *et al.*, 1986), and inhibit synthesis of hyaline cartilage specific collagen types II, IX, and XI (Tyler, *et al.*, 1990). Recombinant IL-1 has been shown to induce cartilage degradation associated with the increased induction (Caron, *et al.*, 1996; Richardson and Dodge, 2000) and secretion of zinc-dependent matrix metalloproteinase by chondrocytes and synoviocytes (Gowen, *et al.*, 1984; Campbell, *et al.*, 1986; Schnyder, *et al.*, 1987). It is suggested that during the development of naturally occurring osteoarthritis (OA), an imbalance in homeostatic degradative and repair

mechanisms ultimately result in the progressive and irreversible destruction of the articular cartilage (Tyler, 1985; Dean, *et al.*, 1989; Ronziere, *et al.*, 1990; Howell and Pelletier, 1993).

In-vivo (Morris, *et al.*, 1990; Alwan, *et al.*, 1991) and *in-vitro* (MacDonald, *et al.*, 1992; Morris and Treadwell, 1994; Neidel, *et al.*, 1994; Platt and Bayliss, 1994; Frisbie and Nixon, 1997; Hardy, *et al.*, 1998b) studies have supported the hypothesis that IL-1 may play an important role in the pathogenesis of OA in horses. High synovial fluid IL-1 concentrations were associated with spontaneously developing OA (Morris, *et al.*, 1990). High glycosaminoglycan (GAG) concentrations were detected in the synovial fluid, serum, and urine of horses with OA relative to clinically normal horses (Alwan, *et al.*, 1991). Previous investigations indicated the effects of human IL-1 on equine articular cartilage in explant culture to include inhibition of PG synthesis (MacDonald, *et al.*, 1992; Morris and Treadwell, 1994; Neidel, *et al.*, 1994; Platt and Bayliss, 1994; Frisbie and Nixon, 1997) and induction of PG degradation (MacDonald, *et al.*, 1992; Frisbie and Nixon, 1997; Frean, *et al.*, 2000). However, the concentrations of IL-1 required to elicit these effects on PG metabolism have varied. The results from one study suggested greater concentrations of IL-1 were necessary for the induction of PG degradation compared with the inhibition of PG synthesis (Morris and Treadwell, 1994). Results from another study suggested PG synthesis to be inhibited to a greater extent following treatment of equine articular cartilage explants with human IL-1β as compared to human IL-1α, although differences in protein bioactivity were not detected by an EL-4/CTLL murine lymphocyte bioassay (Platt and Bayliss, 1994).

The objectives of this study were to characterize recombinant equine IL-1α (EqIL-1α) and recombinant equine IL-1β (EqIL-1β) (Howard, *et al.*, 1998a) protein effects on PG metabolism and PGE_2 production by equine articular cartilage in explant culture. The qualitative and quantitative differences between EqIL-1α and EqIl-1β induced effects were evaluated and the appropriate conditions for use of these species-

homologous recombinant proteins in an EqIL-1 equine articular cartilage explant model for the study of joint disease pathogenesis and treatment in horses was characterized.

2.C. Methods and Materials

Expression construct design

Protein expression constructs for the production of the putative mature forms of EqIL-1α and EqIL-1β were generated by the polymerase chain reaction using previously described methods (Saiki, *et al.*, 1988; Howard, 1997). The templates used were the full-length cDNAs for EqIL-1α (pBluescript SK(+/-)/EqIL-1α) and EqIL-1β (pBluescript SK(+/-)/EqIL-1β) (Howard, *et al.*, 1998a). Synthetic primers were designed with overhangs producing *BamH1* and *HindIII* restriction enzyme sites and bracketing the predicted mature forms of the proteins: S-113 to F-270 for EqIL-1α and A-116 to A-268 for EqIL-1β (Howard, *et al.*, 1998a). A nucleotide sequence encoding a pentapeptide enterokinase cleavage site (D_4K) was placed immediately 5' to the amino terminus of the mature proteins (*refer to Appendix Figure A1*). The amplification products were cloned into pQE-30 (Howard, 1997) encoding a hexahistidyl peptide at the amino terminus of the translated fusion protein. Competent M15[pREP4] host cells (Qiagen Inc, Chatsworth, CA) were transformed with pQE-30/EqIL-1α and pQE-30/EqIL-1β and the nucleotide sequence of transformants was verified using the Sanger dideoxy chain termination technique (Sanger, *et al.*, 1977).

Expression and purification of EqIL-1

The M15[pREP4] host cells transformed with the described pQE/EqIL-1α and pQE/EqIL-1β constructs were cultured in 1 L of Luria Bertani media. Expression of the recombinant proteins was induced by the addition of isopropyl β-D-thiogalactopyranoside (2 U/L). Recovered cells were lysed by sonication and lysates were loaded onto affinity chromatography columns containing nickel nitrilo-triacetic acid resin (Qiagen Inc, Chatsworth, CA). The columns were washed of unbound proteins and eluted with a 0.3 *M* imidazole solution. The fusion proteins were subjected to

enterokinase (Invitrogen Co, San Diego, CA) digestion (~ 7 U/ml) for 24 hours at 4°C, and dialyzed overnight against 2 changes of PBS solution at 4°C. Digest solutions (~ 5 ml volumes) were subjected to size exclusion fast protein liquid chromatography (High-load 16/60 Superdex 75 column, Pharmacia Biotech Inc, Uppsala, Sweden) using a PBS running buffer at a flow rate of 0.75 ml/min, 4°C. The final protein solutions were incubated with an endotoxin removal protein-linked resin (Limulus Amebocyte Lysate Assay, Associates of Cape Cod Inc, Falmouth, MA) for 24 hours, at 4°C, and the resin was separated by centrifugation.

Protein analysis

Protein purity and electrophoretic migration were evaluated by sodium dodecyl-sulfate polyacrylamide gel electrophoresis. Fast protein liquid chromatography fractions exhibiting single bands of protein, as detected by Coomassie blue staining and with electrophoretic migration consistent with the mature forms of EqIL-1, were pooled. Protein purity was further characterized by high-pressure reversed phase liquid chromatography (Ultrapore C_3 column, Beckman Instruments Inc, San Ramon, CA). The concentration of endotoxin in purified protein solutions was determined using a Limulus Amebocyte Lysate assay (Associates of Cape Cod Inc, Falmouth, MA). Final protein concentrations were determined using the Bradford spectrophotometric assay (Bradford, 1976).

Bioactivity of EqIL-1

Recombinant protein bioactivity was determined using a previously described murine T-cell mitogenesis bioassay (Hopkins and Humphreys, 1989). Briefly, D10(N4)M murine T-lymphocytes (Dr. Stephen Hopkins, University of Manchester Rheumatic Diseases Center, Manchester, UK) were cultured in RPMI 1640 media supplemented with 10% fetal bovine serum (Gibco BRL, Life Technologies Inc, Grand Island, NY), 0.02 *M* β-mercaptoethanol, concanavalin A (3 μg/ml), murine IL-1β (Gibco BRL, Life Technologies Inc, Grand Island, NY) (8 U/ml), human IL-2 (Gibco BRL, Life

Technologies Inc, Grand Island, NY) (20 U/ml), and 10% penicillin-streptomycin at 37°C, 5% CO_2. Cells in log phase growth were plated in quadruplicate at 1 X 10^4 cells/well in 96-well plates with serial dilutions of IL-1 treated media. Spectrophotometric absorption was measured at 570 and 600 nm (116 hours) following the addition of an alamar blue dye solution (Biosource international, Camarillo, CA). The difference in absorbances at 570 and 600 nm, corresponding to the amounts of the reduced and oxidized forms of the dye respectively, were used as the estimate of mitogenesis:

$$\text{Absorbance}_{\text{final}} = A_{570} - A_{600}$$

The mean oxidative responses to EqIL-1 were plotted as functions of log dilutions relative to murine IL-1β (1×10^7 U/mg).

Explant culture

Two separate experiments were conducted to characterize the effects of EqIL-1 on equine articular cartilage explants in culture. Near full-thickness articular cartilage was aseptically removed from the stifle joints of a 2-year old (HORSE #1) and a 5-year old horse (HORSE #2) euthanized for reasons unrelated to joint disease (Virginia-Maryland Regional College of Veterinary Medicine, Blacksburg, VA). Cartilage was harvested in Gey's balanced salt solution (Gibco BRL, Life Technologies Inc, Grand Island, NY) cut into explants of similar wet weight (~ 50 mg), and randomly assigned to 24-well plates. Explants were equilibrated at 37°C, 5% CO_2 for 48 hours in a modified culture media (Kawcak, *et al.*, 1996): high-glucose Dulbecco's medium supplemented with 10% fetal bovine serum (Gibco BRL, Life Technologies Inc, Grand Island, NY), 0.24 mM ascorbic acid, 1.78 mM L-glutamine, 0.14 mM α-ketoglutaric acid, 21.5 mM HEPES, and 57 U/ml penicillin / 57 ug/ml streptomycin. Media alone (controls) or media containing EqIL-1α or EqIL-1β at 0.1, 1.0, 10, 50, 100, and 500 ng/ml concentrations (HORSE #1) and 0.01, 0.1, 1.0, 10, and 100 ng/ml (HORSE #2) were

added to quadruplicate wells (2 ml / well). Media was replenished at 48 hour intervals for proteoglycan degradation analyses; final media samples and explants were harvested at Day 4 (HORSE #2) and Day 6 (HORSE #1). Media was replenished at 48 hour intervals for proteoglycan synthesis analyses; explants were harvested at Day 2 (HORSE #2) and both Day 2 and Day 4 (HORSE #1). All samples were stored at -20°C.

Spectrophotometric analysis

Harvested media samples were incubated at 65°C for 4 hours with an equal volume of papain (Sigma, St. Louis, MO) (0.5 mg/ml) in digest buffer (50 m*M* $NaPO_4$, 2 m*M* N-acetyl cysteine, 4 m*M* EDTA disodium salt, pH 6.5). Harvested explants were incubated at 65°C for 4 hours in digest buffer (1 ml/10 mg wet weight) containing papain (0.5 mg/ml). Aliquots of digested media (200 µl) and explants (50 µl) were analyzed for GAG content using a modification of a 1,9-dimethylmethylene blue (DMMB) (Aldrich Chemical Co, Milwalkee, WI) labeling technique (Farndale, *et al.*, 1982). Sulfated GAG concentrations were determined by absorbance readings at 525 nm relative to a shark chondroitin-4-sulfate standard curve (0 to 50 µg/ml). Each sample was analyzed in triplicate. The GAG release data for both experiments were expressed as normalized raw values as well as proportions of available explant GAG released to the media as follows (e.g. for Day 2):

$$\text{Day 2 GAG Release} = \frac{\text{Day 2 GAG}}{\text{Days 2} + 4 + 6 + \text{explant GAG}}$$

Additionally, cumulative GAG release data for both experiments were expressed as proportions of the total available GAG over the experimental periods as follows:

$$\text{Cumulative GAG Release} = \frac{\text{Days 2} + 4 + 6\ \text{GAG}}{\text{Days 2} + 4 + 6 + \text{explant GAG}}$$

[^{35}S]O_4 release

Explants were incubated with ^{35}S-sulfate labeled $NaSO_4$ (20 µCi/ml) for 48 hours prior to the addition of EqIL-1. Harvested media and explant samples were papain-

digested using the conditions previously described for the DMMB spectrophotometric analysis. Aliquots (25 µl) of papain-digested cartilage and media samples were added to 96-well, 0.45-µm filter-bottomed plates and precipitated using an Alcian blue dye solution (0.2% [wt/vol] Alcian blue (Gibco BRL, Life Technologies Inc, Grand Island, NY), 0.05 *M* sodium acetate, 0.085 *M* $MgCl_2$). The precipitate was recovered by vacuum filtration and a multi-well punch system (Multiscreen assay system, Millipore, Bedford, MA). Emissions were recorded using a beta-scintillation counter. Each sample was analyzed in triplicate. Data were expressed as normalized raw values and as the proportion of ^{35}S-sulfate released to the media at each media change and for the cumulative experimental period, as described for the DMMB analysis.

^{35}S-incorporation

Explants were incubated with [^{35}S] $NaSO_4$ (40 uCi/ well) for 16 hours prior to explant harvest at the end of the experimental periods (Day 2 and Day 4 for HORSE #1 and Day 2 for HORSE #2). Explant digestion, GAG precipitation, and scintillation counting was conducted as previously described. All samples were analyzed in triplicate.

DNA quantification

Explant DNA concentrations were evaluated using a previously reported technique (Kim, *et al.*, 1998). Briefly, aliquots of papain-digested cartilage samples (100 ul) were added to a 0.1 ug/ml solution of Hoeschst 33258 dye (Hoeschst 33258, Molecular Probes, Eugene, OR) in 10 mM Tris, 1 mM Na_2EDTA, 0.1 mM NaCl, pH 7.4 (2 mls). Spectrofluorometry was performed using an excitation wavelength of 365 nm with detection of emission at 458 nm. Concentrations of DNA were determined relative to a calf thymus DNA standard curve (0-100 ug/ml). All analyses were conducted in triplicate.

PGE_2 enzymeimmunoassay

PGE_2 concentrations released to media from explants at Days 2 and 4 (HORSE #2) were quantified using a commercially available enzyme-immunoassay kit (Amersham Pharmacia Biotech Inc, Piscataway, NJ). Media samples (50ul) were diluted in the provided assay buffer. The enzyme substrate 3,3',5,5' tetramethylbenzidine / hydrogen peroxide in 20% (v/v) dimethylformamide was added (150 ul) and duplicate absorbance values were read within 30 minutes on a UV spectrophotometer (450 nm). A standard curve (50-6400 pg/ml PGE_2) was generated by plotting percent bound conjugated-PGE_2 as a function of PGE_2 concentration on a semi-logarithmic scale. Final sample PGE_2 concentrations (pg/ml) were deduced from the standard curve.

Data analysis

Data were normalized by explant DNA content, with final units designated in 'ug GAG / ng DNA' and 'cpm / ng DNA'. Count data (cpm) were logarithmically transformed to ensure homogeneity of variance between treatment groups as determined by the Brown-Forsythe's test and scatter plotting. All other data displayed patterns of homogenized variance and were not modified. An analysis of variance using a statistical model ((protein effect) x (concentration effect) x (day effect)) was conducted (Statistical Analysis Software, SAS Institute, Cary, NC). Further comparisons within the modeling structure were conducted using Tukey's t-tests.

2.D. Results

Purified protein characterization

Yields of purified EqIL-1α and EqIL-1β were 93.3 ug and 3.8 mg respectively (1 L cultures), with an approximate 50-fold greater EqIL-1β yield. Final EqIL-1α and EqIL-1β protein concentrations were 4.24 ug/ml and 70.75 ug/ml, respectively. Purified EqIL-1α and EqIL-1β exhibited electrophoretic migrations by SDS-PAGE with that expected for the mature form of the proteins (*refer to Appendix figure A2*). Protein purity

was estimated at near 100% for both EqIL-1α and EqIL-1β as determined by the detection of single peaks by HPLC (*refer to Appendix figure A3*). The specific bioactivities of EqIL-1α and EqIL-1β were 6.6 x 10^6 U/mg and 4.7 x 10^6 U/mg, respectively, as determined by the murine D10(N4)M T-cell mitogenesis bioassay **(Figure 2.1)**. Endotoxin concentrations were < 0.01 ng/ug of protein for both recombinant proteins.

DMMB spectrophotometric analysis

HORSE #1 - GAG release was observed for EqIL-1α and EqIL-1β concentrations ≥ 0.1 ng/ml at Day 2 ($p<0.0001$) and Day 4 ($p=0.0015$) **(Figure 2.2a)**. Day 6 media GAG concentrations were similar to control groups over all treatments ($p>0.48$). Significant differences between EqIL-1α and EqIL-1β treatment responses were not apparent, although a trend for greater GAG release from the EqIL-1α treatment groups was detected ($p=0.09$). Expression of the data as proportional release of GAG available indicated EqIL-1 induced similar effects on GAG release over the three treatment periods ($p=0.51$) **(Figure 2.2b)**. Near maximal cumulative release of GAG was detected (88-94%) relative to controls (mean release 42%) in response to EqIL-1 concentrations ≥ 0.1 ng/ml ($p<0.0001$) **(Figure 2.2b)**. These results corresponded to reduced GAG content of explants at Day 6 in all EqIL-1 treatment groups as compared to controls ($p<0.0001$) (data not shown).

HORSE #2 – Significant GAG release was observed from EqIL-1α and EqIL-1β treatment groups at concentrations ≥ 0.1 ng/ml on Day 2 ($p=0.0004$) and Day 4 ($p<0.005$), but not at the 0.01 ng/ml concentration **(Figure 2.3a)**. Significant differences in GAG release were not observed for groups treated with EqIL-1α versus EqIL-1β. The proportional release of GAG was significantly increased for groups treated with all concentrations of EqIL-1α and EqIL-1β Day 2 ($p<0.01$) and Day 4 ($p<0.004$) **(Figure 2.3b)**. Proportional GAG release in response to EqIL-1α and EqIL-1β was similar on Day 2 versus Day 4 ($p>0.11$). The range in mean cumulative GAG release was 38-67%

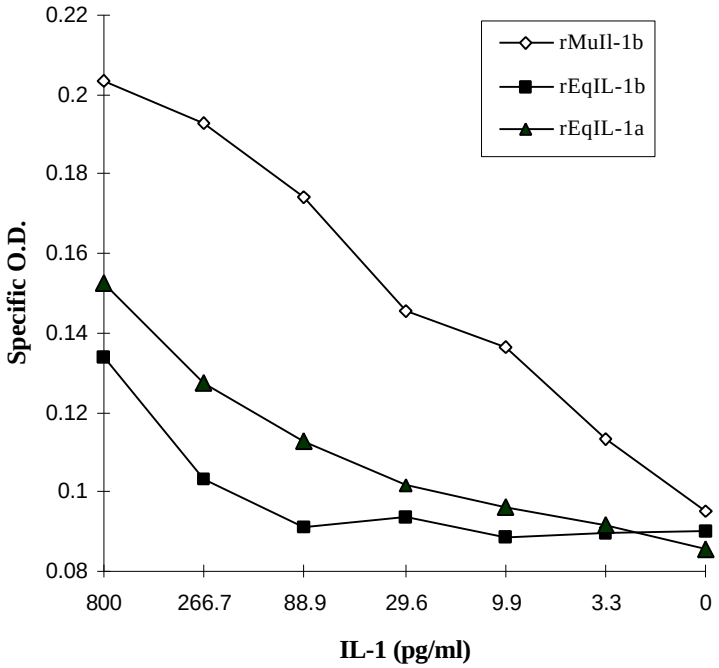

Figure 2.1 - Murine T-cell mitogenesis assay results.

Graph corresponds to recombinant equine interleukin-1 (rEqIL-1) bioactivities assessed relative to a murine interleukin-1β standard (rMuIL-1β): EqIL-1α = 6.6 x 10^6 U/mg (1.5 times less active than rMuIL-1β), EqIL-1β = 4.7 x 10^6 U/mg (2.1 times less active than rMuIL-1β). Data points reflect mean absorbance values of D10(N4)M T-cells plated in quadruplicate wells.

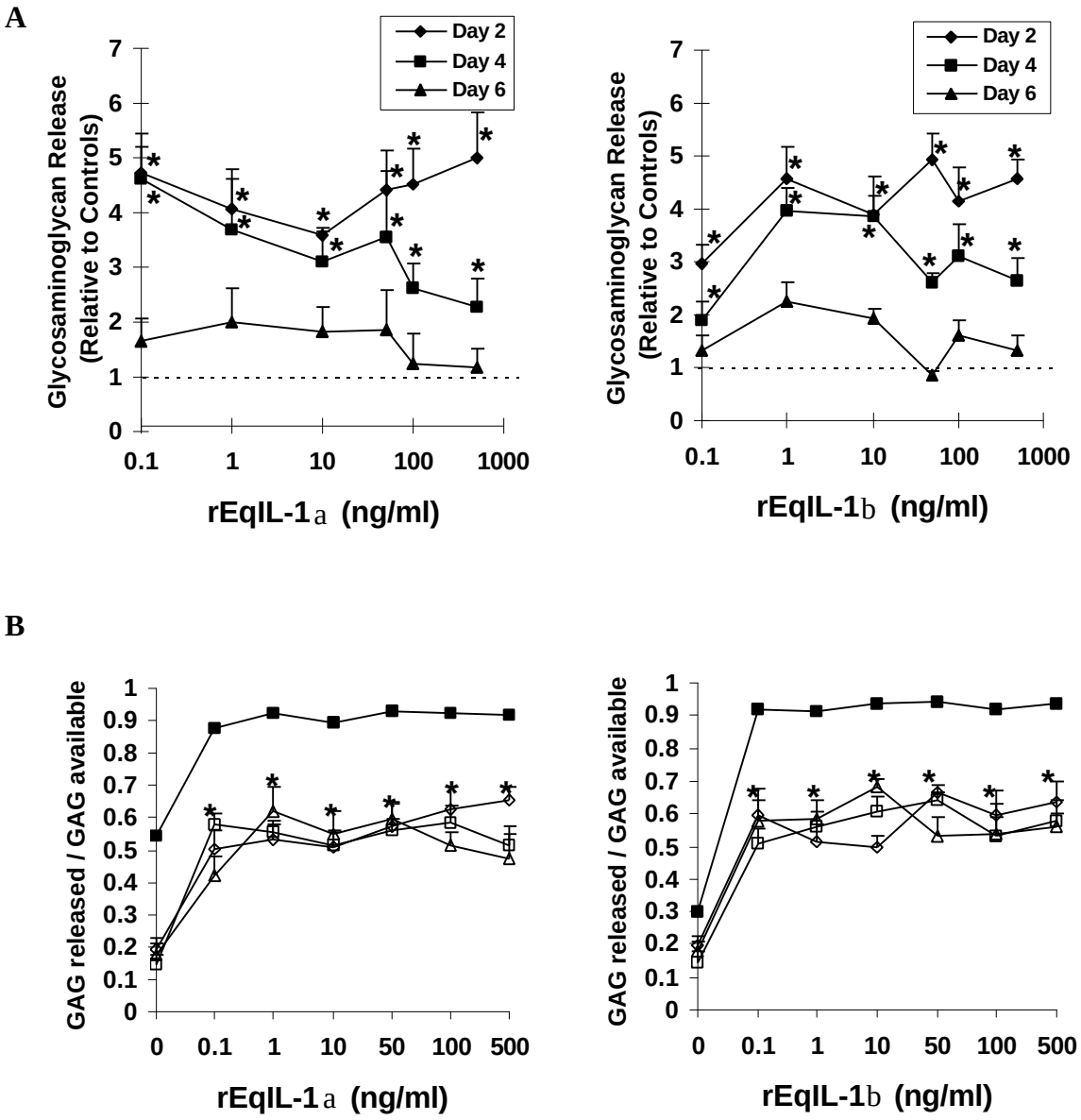

Figure 2.2 - Results of DMMB-spectrophotometric analysis (HORSE #1).

A) Raw normalized sulfated GAG concentrations detected in the media of equine articular cartilage explants exposed to EqIL-1 (0 to 500 ng/ml) at 2, 4, and 6 days. Dotted lines represent released GAG levels of control groups. B) Proportions of available GAG released in response to EqIL-1 (0 to 500 ng/ml). Open diamond = Day 2. Open square = Day 4. Open triangle = Day 6. Closed square = Cumulative release of available GAG after 6 days. Data points represent means and standard error values of quadruplicate wells normalized for DNA content. * denotes significance at $p<0.05$.

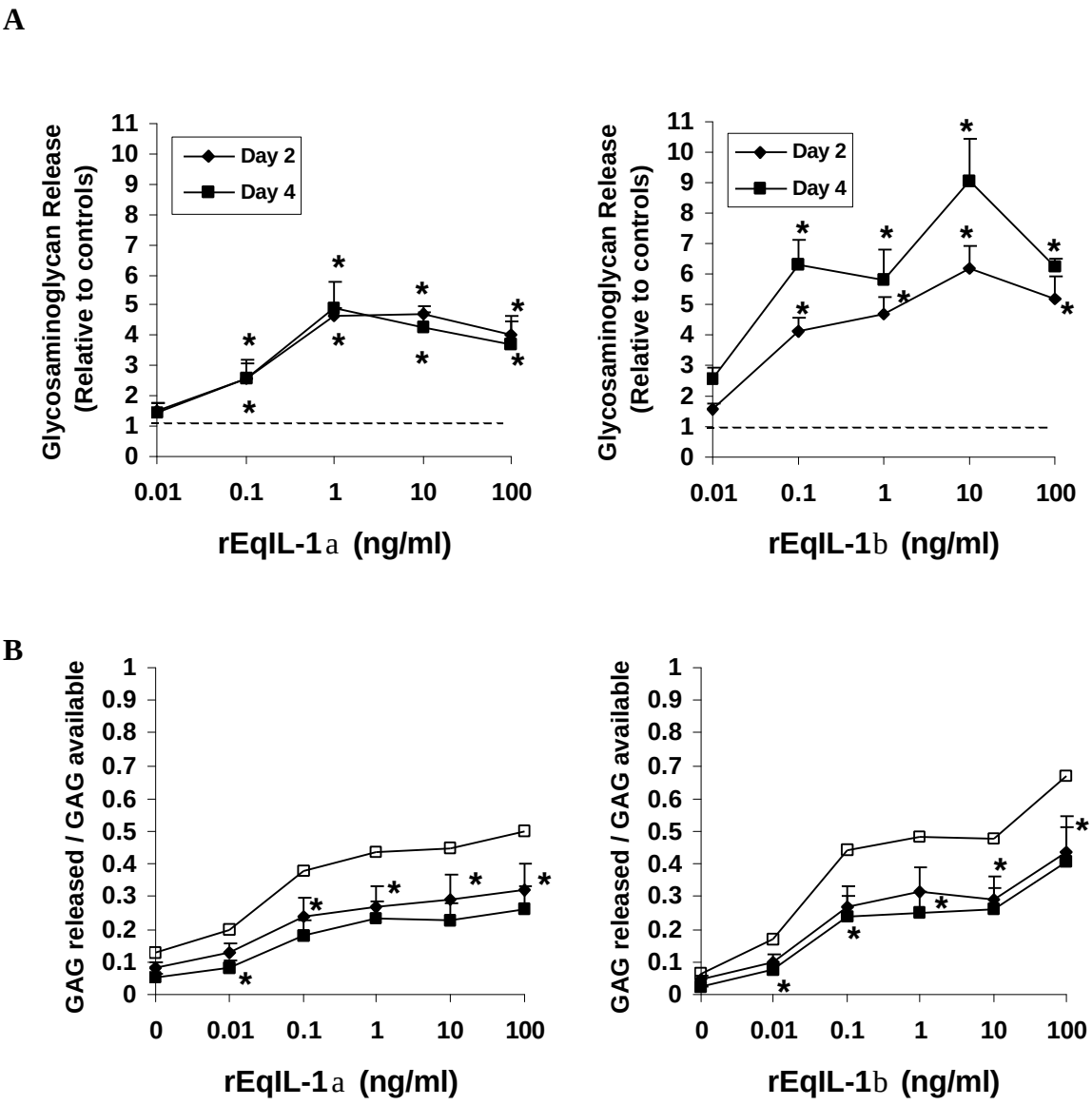

Figure 2.3 - Results of DMMB-spectrophotometric analysis (HORSE #2).

A) Raw normalized sulfated GAG concentrations detected in the media of equine articular cartilage explants exposed to EqIL-1 (0 to 100 ng/ml) at 2 and 4 days. Dotted lines represent released GAG levels of control groups. B) Proportions of available GAG released in response to EqIL-1 (0 to 100 ng/ml). Closed diamond = Day 2. Closed square = Day 4. Open square = Cumulative release of available GAG after 4 days. Data points represent means and standard error values of quadruplicate wells normalized for DNA content. * denotes significance at $p<0.05$.

for ≥ 0.1 ng/ml EqIL-1 treatment groups, 18% for 0.01 ng/ml treatments, and was 10% for the control group ($p<0.0006$) **(Figure 2.3b)**. These results corresponded to reduced GAG concentrations remaining in IL-1 treated explants on Day 4 for > 0.1 ng/ml concentrations ($p<0.013$) (data not shown).

$[^{35}S]O_4$ release

HORSE #1 – Release of $[^{35}S]O_4$-labeled GAG was increased at Day 2 ($p<0.0001$) and Day 4 ($p<0.0001$) in response to concentrations of EqIL-1 ≥ 0.1 ng/ml **(Figure 2.4a)**. Release of $[^{35}S]O_4$-labeled GAG on Day 6 was similar to controls among all IL-1 treatment concentrations ($p>0.14$). Significant differences in $[^{35}S]O_4$-labeled GAG release were not observed for EqIL-1α and EqIL-1β. Greater levels of $[^{35}S]O_4$-labeled GAG were detected at Day 2 than at Day 4 and Day 6 ($p<0.0001$); however, the proportional release of GAG was similar across the three time points ($p=0.87$) **(Figure 2.4b)**. The mean cumulative GAG release in EqIL-1 treatments groups ≥ 0.1 ng/ml ranged from 90–98% compared with 37% for the control group ($p<0.0001$) **(Figure 2.4b)**. A corresponding reduction in $[^{35}S]O_4$-labeled GAG remaining in the explants at Day 6 was detected for all EqIL-1 treatments ($p<0.0001$) (data not shown).

HORSE #2 - Significant $[^{35}S]O_4$-labeled GAG release was observed for EqIL-1α and EqIL-1β treatment groups at concentrations ≥ 0.1 ng/ml at Day 2 ($p<0.0001$) and Day 4 ($p<0.0003$), but not at 0.01 ng/ml **(Figure 2.5a)**. Significant differences in $[^{35}S]O_4$-labeled GAG release for EqIL-1α and EqIL-1β groups were not observed, although there was a tendency for increased release for EqIL-1α groups ($p=0.09$). Proportional release of available $[^{35}S]O_4$-labeled GAG was increased for concentrations of EqIL-1 tested on Day 2 and Day 4 ($p<0.0001$) **(Figure 2.5b)**. Similar proportions of available $[^{35}S]O_4$-labeled GAG were released at Day 2 and Day 4 evaluations ($p=0.81$) for EqIL-1 concentrations ≥ 0.1 ng/ml. Cumulative GAG release over the 4 day treatment period for concentrations of EqIL-1 ≥ 0.1 ng/ml were greater (50-76%) than 0.01 ng/ml (34%) and control groups (17%); these values for ≥ 0.01 ng/ml EqIL-1 were statistically greater than

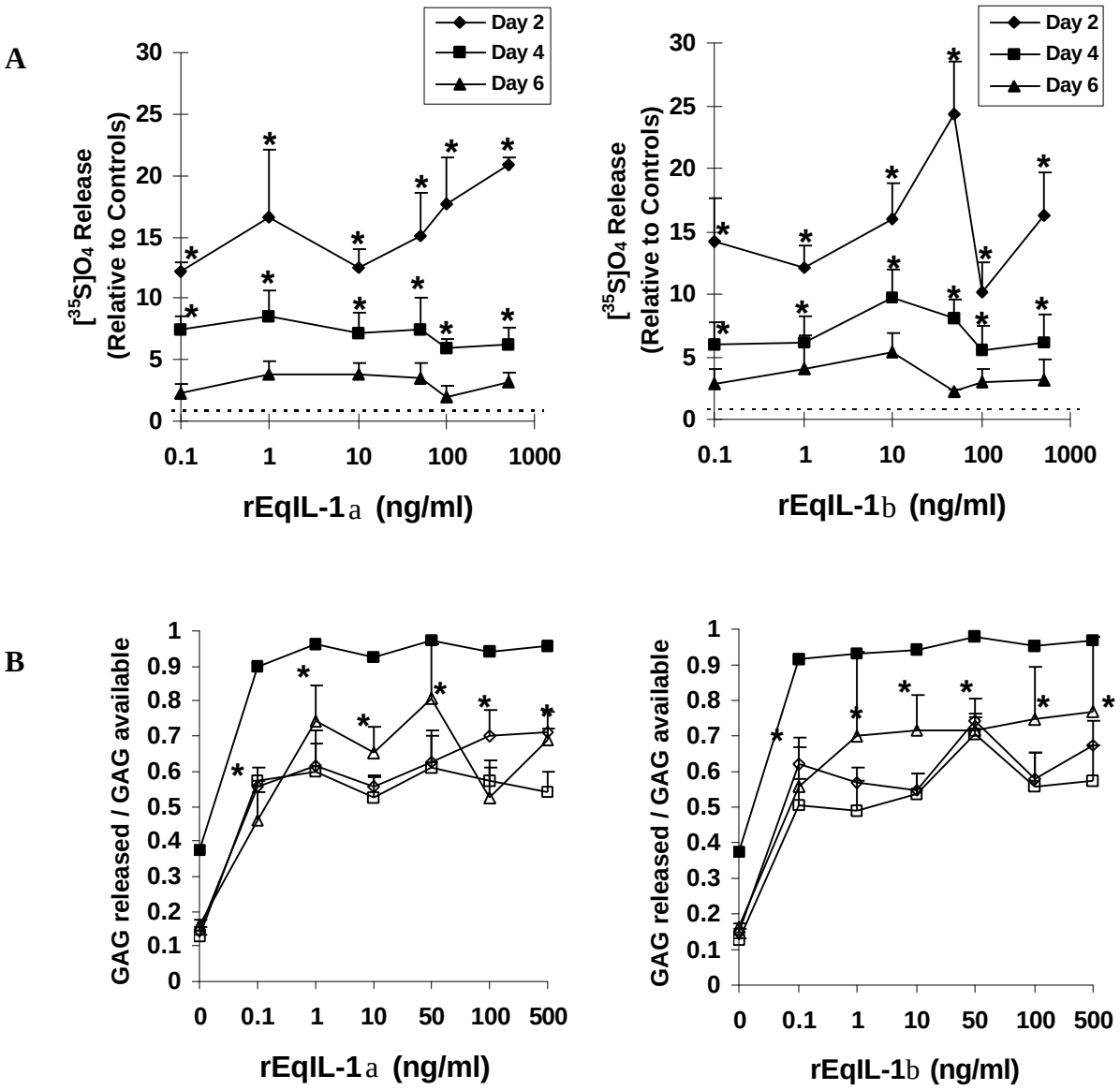

Figure 2.4 - Results of [^{35}S]O_4-sulfate-labeled GAG analysis (HORSE #1).

A) Raw normalized sulfated GAG concentrations detected in the media of equine articular cartilage explants exposed to EqIL-1 (0 to 500 ng/ml) at 2, 4, 6 days. Dotted lines represent released GAG levels of control groups. B) Proportions of available GAG released in response to EqIL-1 (0 to 500 ng/ml). Open diamond = Day 2. Open square = Day 4, Open triangle = Day 6. Closed square = Cumulative release of available GAG after 6 days. Data points represent the mean values of quadruplicate wells normalized for DNA content. * denotes significance at $p<0.05$.

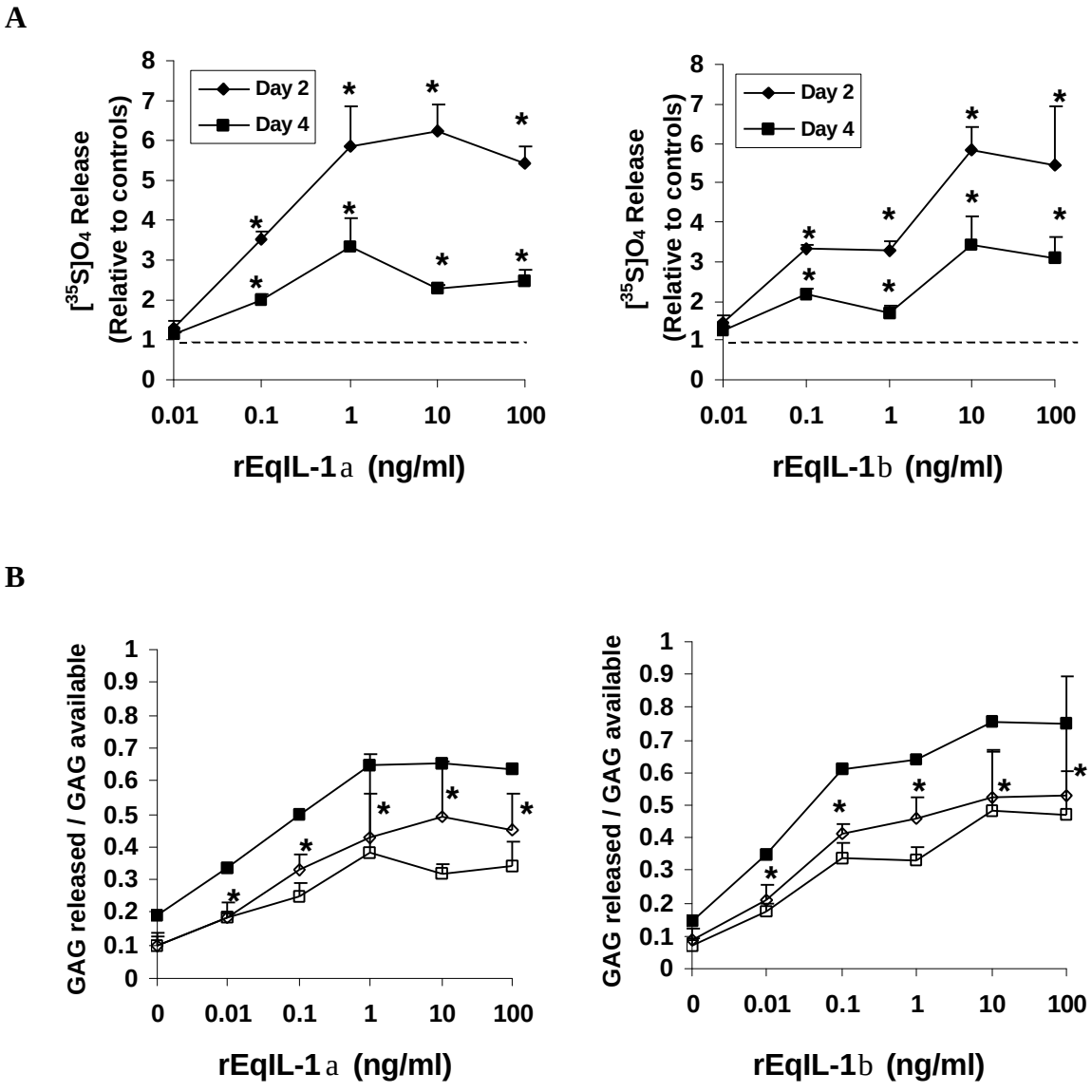

Figure 2.5 - Results of [^{35}S]O_4-sulfate-labeled GAG analysis (HORSE #2).

A) Raw normalized sulfated GAG concentrations detected in the media of equine articular cartilage explants exposed to EqIL-1 (0 to 100 ng/ml) at 2 and 4 days. Dotted lines represent released GAG levels of control groups. B) Proportions of available GAG released in response to EqIL-1 (0 to 100 ng/ml). Open diamond = Day 2. Open square = Day 4. Closed square = Cumulative release of available GAG after 4 days. Data points represent mean and standard error values of quadruplicate wells normalized for DNA content. * denotes significance at $p<0.05$.

controls ($p<0.0008$) **(Figure 2.5b)**. Decreased levels of $[^{35}S]O_4$-labeled GAG remained in the explants at Day 4 for EqIL-1 concentrations of $\geq$ 0.1ng/ml ($p<0.02$) (data not shown).

$[^{35}S]O_4$-incorporation

HORSE #1 – Incorporation of $[^{35}S]O_4$ was decreased in groups treated with EqIL-1α and EqIL-1β in concentrations $\geq$ 0.1 ng/ml compared with the untreated control group on Day 2 ($p=0.0002$) and Day 4 ($p=0.03$) **(Figure 2.6a)**. Recombinant EqIL-1α ($\geq$ 0.1 ng/ml) reduced $[^{35}S]O_4$ incorporation by > 58% at Day 2 and > 42% at Day 4. Recombinant EqIL-1β ($\geq$ 0.1 ng/ml) reduced $[^{35}S]O_4$ incorporation by > 47% at Day 2 and > 59% at Day 4. Both recombinant EqIL-1s induced a similar magnitude of inhibition of $[^{35}S]O_4$ incorporation ($p=0.36$) and exhibited a similar magnitude of effect for Day 2 and Day 4 observations ($p=0.7748$).

HORSE #2 - Incorporation of $[^{35}S]O_4$ was significantly reduced at Day 2 for EqIL-1 groups of $\geq$ 0.1 ng/ml concentrations ($p<0.0004$), but not at 0.01 ng/ml ($p=0.14$) **(Figure 2.6b)**. Mean $[^{35}S]O_4$ incorporation values were reduced by EqIL-1α and EqIL-1β ($\geq$ 0.1 ng/ml) by > 53% and > 64%, respectively. Differences in $[^{35}S]O_4$ incorporation were not detected for EqIL-1α relative to EqIL-1β.

PGE_2 assay

EqIL-1α and EqIL-1β induced dose-dependent PGE_2 release ($\geq$ 1.0 ng/ml concentrations) (HORSE #2) at Day 2 ($p<0.020$) and Day 4 ($p<0.0001$) **(Figure 2.7)**. Significant effects were not observed at 0.01 and 0.1 ng/ml concentrations at Day 2 or Day 4 evaluations. Significant differences in PGE_2 concentrations were not observed for EqIL-1α groups compared with EqIL-1β groups, although there was a trend for higher concentrations in EqIL-1β treatment groups ($p=0.08$).

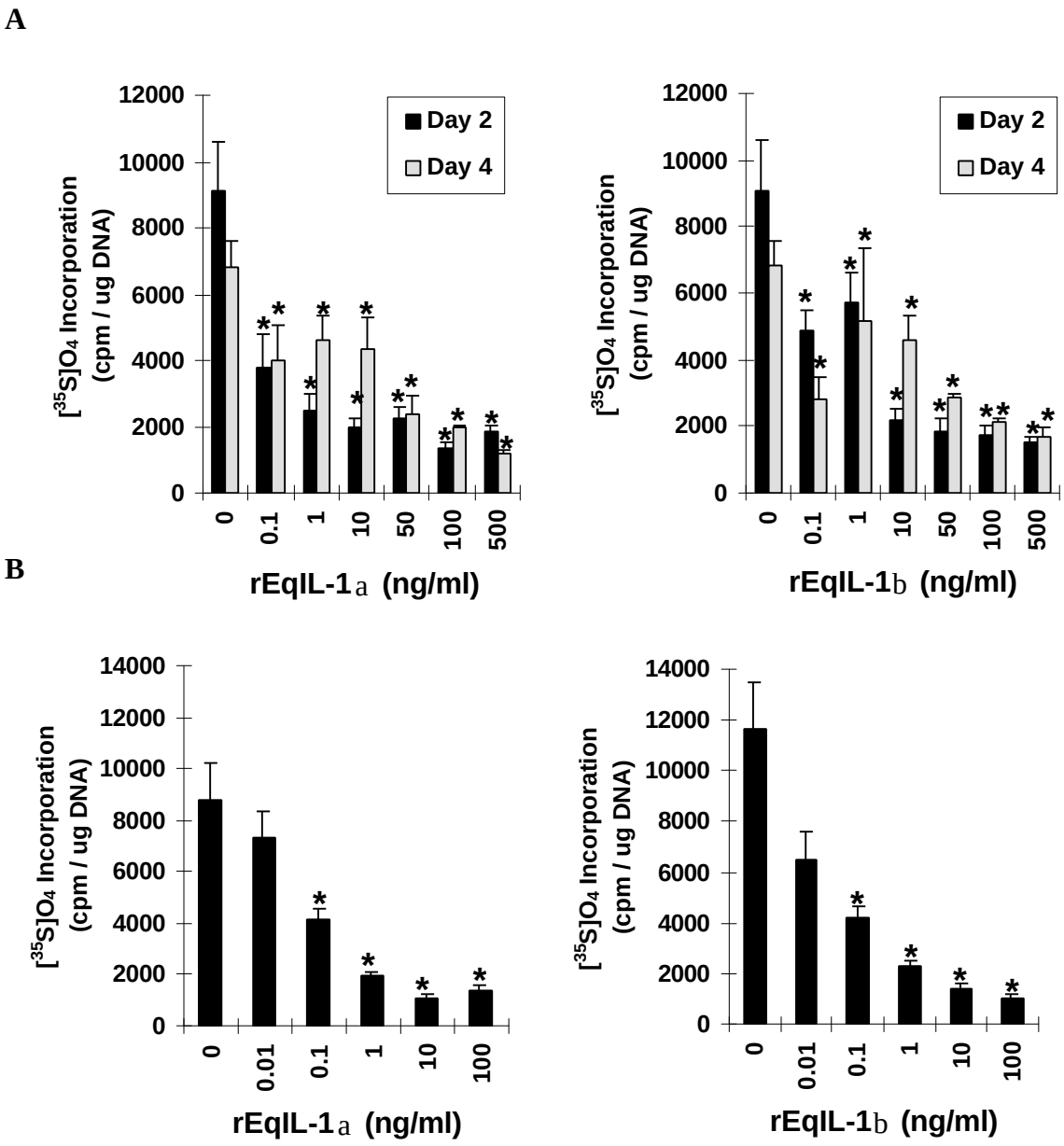

Figure 2.6 - Effects of EqIL-1 on proteoglycan synthesis.

^{35}S-sulfate incorporation in equine articular cartilage: A) Explants treated with EqIL-1 (0 to 500 ng/ml) at 2 and 4 days (HORSE #1). B) Explants treated with EqIL-1 (0 to 100 ng/ml) at 2 days (HORSE #2). Data points represent means and standard error values of quadruplicate wells normalized for DNA content. * denotes significance at $p<0.05$.

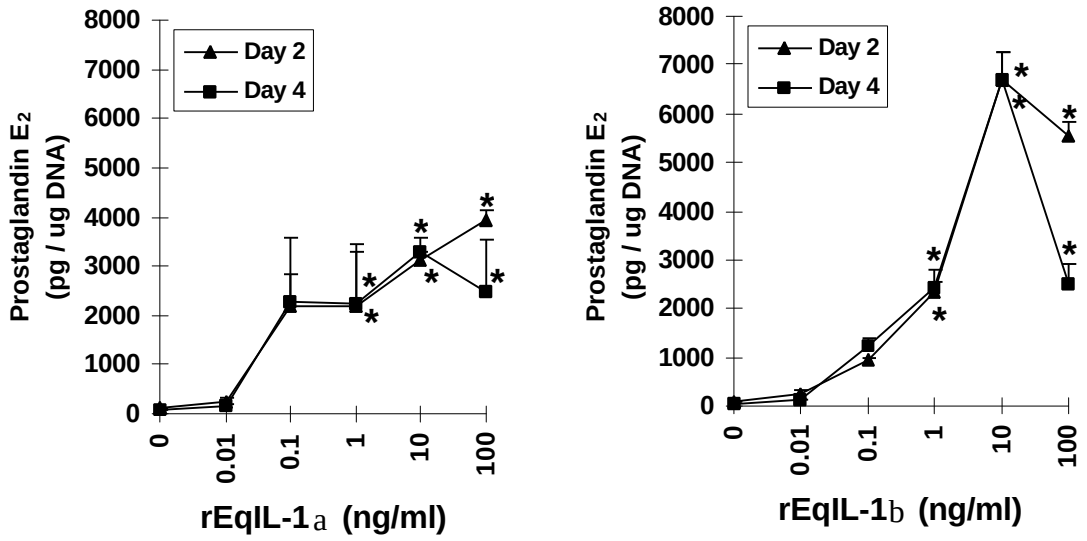

Figure 2.7 - Effects of EqIL-1 on prostaglandin E_2 concentrations.

Enzyme immunoassay analyzed PGE_2 release to the media from equine articular cartilage explants at days 2 and 4 in response to EqIL-1 (0 to 100 ng/ml) (HORSE #2). Data points represent means and standard error values of duplicate wells normalized for DNA content. * denotes significance at $p<0.05$.

Deoxyribonucleic acid assay

Mean DNA concentrations of papain-digested control and EqIL-1 treated explants (0.01 to 100 ng/ml) harvested at days 2 and 4 were not significantly different nor were EqIL-1 treated explants (0.1 to 500 ng/ml) harvested at days 2, 4, and 6.

2.E. Discussion

The results of this study indicated that EqIL-1α and EqIL-1β induced a dose-dependent derangement in proteoglycan metabolism and PGE_2 synthesis in equine articular cartilage in explant culture. These results suggest the EqIL-1/equine explant system may be a useful model for the *in-vitro* study of equine joint disease pathogenesis and treatment. Our findings are in general agreement with those of investigators who have demonstrated human IL-1 to induce PG degradation (MacDonald, *et al.*, 1992; Frisbie and Nixon, 1997; Frean, *et al.*, 2000) or to inhibit PG synthesis in equine articular cartilage explants (MacDonald, *et al.*, 1992; Morris and Treadwell, 1994; Neidel, *et al.*, 1994; Platt and Bayliss, 1994; Frisbie and Nixon, 1997). Near maximal responses for both PG degradation and inhibition of PG synthesis were observed at EqIL-1 concentrations greater than and equal to 100 pg/ml. The results of our study differ from those of previous studies in that significant effects on PG degradation and synthesis were observed at concentrations of EqIL-1 that were 40-100 times lower than the lowest HuIL-1 treatment concentrations reported to induce these effects (MacDonald, *et al.*, 1992; Neidel, *et al.*, 1994; Platt and Bayliss, 1994; Frisbie and Nixon, 1997). Additionally, the results of this study differ with a previous report suggesting inhibition of proteoglycan synthesis to occur at lower concentrations of HuIL-1 than concentrations resulting in significant PG degradation in equine articular cartilage explants (Morris and Treadwell, 1994). The current study was not designed to address the differences in effective concentrations of HuIL-1 and EqIL-1 on PG metabolism. Whether these potential differences had a biological basis or were reflections of different investigators and methodologies remains to be determined. However, our results would indicate lower

concentrations of EqIL-1 should be considered for equine articular cartilage explant studies compared with previously reported concentrations of HuIL-1.

It has been suggested that the biological response to IL-1 is to some extent a species-specific response (Lederer and Czuprynski, 1989; May, *et al.*, 1992b). The results of one study highlighted the preferential stimulation of bovine thymocytes and fibroblasts by bovine IL-1 compared with HuIL-1 (Lederer and Czuprynski, 1989). Another study demonstrated that equine thymocytes displayed increased sensitivity and proliferation to an equine mononuclear cell supernatant compared with HuIL-1 (May, *et al.*, 1992b). It has been proposed that a species-homologous equine IL-1 would be necessary to directly address the elucidation of the effects of IL-1 on chondrocyte metabolism in an equine system (May, *et al.*, 1992b). The observation of these investigators may be attributable to crucial differences in the amino acid sequences of equine and human IL-1, with amino acid sequence homology previously reported as 66.4% (Howard, *et al.*, 1998a) and 71.6% (Kato, *et al.*, 1995) for IL-1α and 66.7% (Kato, *et al.*, 1995) and 72.7% (Howard, *et al.*, 1998a) for IL-1β. These sequence differences may in turn confer changes in receptor binding and activation. Our results indicate that EqIL-1 has potent effects on equine articular cartilage metabolism and would appear to support the use of species-homologous IL-1 in such *in-vitro* studies. Further experiments are required to address the issue of species-specificity directly.

In this study, evaluation of the raw normalized data suggested the magnitude of GAG released to the explant media, as determined by DMMB spectrophotometry and the release of ^{35}S-sulfate-labeled GAG, was influenced by the duration of exposure to EqIL-1. Evaluation of these data alone might suggest a loss of responsiveness over time to EqIL-1. The magnitude of release of GAG would logically depend on the amount of degradative activity by chondrocytes, as well as the availability of substrate (ie, PG). Evaluation of the proportion of available GAG released to the explant media indicated that the release of GAG was similar over all time points evaluated. Approximately 75%

of the total GAG had been released by day 4 and 90% had been released by day 6. We concluded that the lack of effect evidenced by the day 6 raw normalized GAG release data was attributable to substrate depletion rather than a lack of chondrocyte EqIl-1 responsiveness.

The results of this study indicated that prokaryotic expression and native purification of recombinant equine IL-1α and IL-1β provided an acceptable yield of purified recombinant proteins exhibiting authentic IL-1 bioactivity. The yield of EqIL-1β in the present study exceeded that of EqIL-1α by approximately 40-fold. This difference in protein yield was not the result of differences in expression (data not shown) but was attributable to the reduced aqueous solubility of EqIL-1α compared with EqIL-1β. Methods of purification employing denaturing conditions would likely produce improved and similar yields of EqIL-1α and EqIL-1β. Purification under denaturing conditions requires accurate refolding of the protein for the restoration of the bioactivity. The yields and bioactivity, using the described methods, were acceptable, and the potential difficulty associated with renaturation of recombinant proteins was avoided.

It was important to ensure that the purified EqIL-1 proteins contained acceptable levels of lipopolysaccharide (LPS), since LPS has been shown to induce derangements in PG metabolism and eicosanoid production in equine articular cartilage explants that are qualitatively similar to those induced by IL-1 (MacDonald, *et al.*, 1994). The prokaryotic expression of recombinant protein in this study presented ample opportunity for LPS contamination derived from the host cell M15 strain of *Escherichia coli*. The described method for removal of LPS was effective in reducing the LPS concentration to < 0.01 ng/ug of protein. The manufacturer of a commercially available rHuIL-1 (Calbiochem-Novabiochem, San Diego, CA) indicates its product has < 0.1 ng LPS /ug protein, suggesting this commercially available IL-1 could contain up to ten times more LPS than the EqIL-1 used in this study. In an evaluation of the effects of *Salmonella typhosa* derived LPS on equine articular cartilage explants in culture, a dose-dependent decrease

in PG synthesis, dose-dependent increase in GAG release, and increase in PGE_2 synthesis was demonstrated (MacDonald, *et al.*, 1994). In the cited study, LPS (10 ng/ml) induced a significant reduction of PG synthesis in articular cartilage explants obtained from 10 of 15 horses, whereas the highest possible concentration of endotoxin that was associated with EqIL-1 treatment in the current study was 0.005 ng/ml. Therefore, the contribution of LPS to the observed effects of EqIL-1 on equine articular cartilage explants presented in this study should be considered negligible.

The D10(N4)M murine T-cell line has been previously shown to undergo mitogenesis in the presence of IL-1 with high sensitivity and specificity (Hopkins and Humphreys, 1989). Although the D10(N4)M bioassay was helpful in establishing that the purified recombinant proteins qualitatively exhibited authentic IL-1 bioactivity, the validity of the bioassay for the quantitative determination of equine IL-1 bioactivity was less certain. The bioactivity of the purified EqIL-1α and EqIL-1β was determined to possess 66% and 47%, respectively, the bioactivity of a recombinant murine IL-1β (1 X 10^7 U/mg). We did not directly determine whether the reduced responsiveness of the D10(N4)M cells to the rEqIL-1 was due to a relative decreased bioactivity of the proteins compared with murine IL-1β or to potential differences in responsiveness of the murine T-cells to murine and equine IL-1. Since the EqIL-1 bioactivity was not determined using an equine cell line and the EqIL-1 appeared to demonstrate good bioactivity on equine articular cartilage explants in a pilot study (data not presented), the treatments were applied on a mass/ml rather than bioactivity/ml basis. This approach appeared to be reasonable since significant differences were not observed in the effects induced by EqIL-1α and EqIL-1β despite the indication from the D10(N4)M bioassay that the bioactivity of EqIL-1β was 71% that of EqIL-1α. Trends were observed in this study suggesting EqIL-1α was more potent in its effect on inducing GAG release from explants of HORSE #1 ($p=0.09$) and $[^{35}S]O_4$ release from explants of HORSE #2 ($p=0.09$) compared with EqIL-1β. However, these differences were not significant nor consistent with the accompanying analyses of the $[^{35}S]O_4$ release for HORSE #1 or GAG release for

HORSE #2. Additionally, an opposite trend was observed suggesting PGE_2 synthesis was induced to a greater extent by EqIL-1β than EqIL-1α in the explants of HORSE #2 ($p=0.08$). It is unlikely that the experimental design used in this study evaluating EqIL-1 treatments applied in orders of magnitude of concentration difference and methods of analysis used were capable of detecting the 29% difference in bioactivity predicted by the D10(N4)M bioassay. Ultimately, it was unclear whether the 29% apparent difference in bioactivity of the EqIL-1s on D10(N4)M cells was attributable to differences in the quality of the protein preparations or was the result of biological differences in the murine cell responses to the different isoforms of EqIL-1. We conclude that the effects on proteoglycan metabolism and PGE_2 synthesis were similar for the two EqIL-1 proteins used in our study over all treatment conditions.

Because the yield of EqIL-1β exceeded that of EqIL-1α by 40-fold and the responses to the two proteins were similar, we intend to use EqIL-1β in future related studies. This conclusion is consistent with a previous study demonstrating similar effects of human monocyte derived IL-1α and IL-1β on cultured human connective tissue cells (Rupp, *et al.*, 1986), but conflicts with another similarly designed explant study suggesting HuIL-1α induced a greater magnitude of effects relative to HuIL-1β on equine articular cartilage explants (Platt and Bayliss, 1994). The two isoforms of human IL-1 have been shown to possess crucial similarities in structural topology and to bind with similar affinity to common transmembrane IL-1 receptors (Dinarello, 1994a). To the authors' knowledge, this information is unavailable for the equine IL-1 system, but it is reasonable to presume that a similar biological relationship is in operation for the horse.

Consistent with the findings of other investigators evaluating the effects of HuIL-1 on equine articular cartilage cells (May, *et al.*, 1992a; Hardy, *et al.*, 1998b), the results of our study indicate that EqIL-1 induced the dose-dependent synthesis and secretion of PGE_2 by chondrocytes in articular cartilage explant culture. Because the methods used in

our study did not include the determination of the amount of PGE_2 contained within the explants, the total synthesis of PGE_2 was not evaluated but only that portion released to the explant media. It is unknown how determination of total PGE_2 synthesis might have differed from our results.

The characteristics of the ideal *in-vitro* model for the study of joint disease are a subject for debate. An acceptable model ideally would resemble the course of naturally developing disease and be associated with as few confounding variables as possible. Tissues from a limited number of horses were evaluated in our study for the purpose of establishing the validity of the methods described. One should be cautioned against the rigid extrapolation of the results of our study to other environments or subjects. The combined pattern of effects of EqIL-1 on proteoglycan metabolism and PGE_2 synthesis observed in our study suggests that the EqIL-1/equine articular cartilage explant model may be useful for the study of the pathogenesis and treatment of joint disease in horses. Alterations in PG metabolism and PGE_2 synthesis are processes that have been associated with naturally developing joint disease in horses and ample evidence is available suggesting IL-1 may be an important effector in the pathogenesis of joint disease in horses. We suggest that the depletion of approximately 90% of the total GAG from the extra-cellular matrix of the cartilage explants over a period of 6 days or approximately 75% over 4 days represents a severe and acute insult. The indication that EqIL-1 induced PG degradation even at the 0.01 ng/ml concentration applied over an experimental period of 4 days has prompted related studies to refine this *in-vitro* system to more accurately represent the more insidious progression of joint problems in horses such as OA.

CHAPTER III: Modulated chondrocyte gene expression following *in-vitro* exposure to interleukin-1 proteins

3.A. Abstract

A central feature of osteoarthritis (OA) is the progressive and irreversible degeneration of articular cartilage. This degeneration has been suggested to be attributable in part to an imbalance in cytokine activity in affected tissues. A customized targeted cDNA array analysis was used to study the early effects of recombinant equine interleukin-1 alpha (EqIL-1α), beta (EqIL-1β), and receptor antagonist (EqIL-1ra) on transcription by equine articular chondrocytes *in-vitro*. Chondrocytes grown in monolayer were exposed to media containing either 0 or 10 ng/ml EqIL-1α, EqIL-1β, or EqIL-1ra for one hour at 37°C, 5% CO_2. Significantly increased mRNA levels for insulin-like growth factor-2, interleukin-6, bone-morphogenetic protein-4, bromodomain transcription factor, phosphoinositol-3-kinase, and β-actin were observed for the EqIL-1α group ($p<0.05$). The levels of thirteen additional genes were altered > 2-fold in the EqIL-1α group. Principal component analysis revealed five vectors to reflect ~ 95% of the total variation. One component corresponding to ~ 4% of the variation, appeared to relate to latent differentiative and growth transcriptional responses, and reflected a significant difference between EqIL-1α and EqIL-1β effects ($p=0.022$). These results add to the current body of knowledge of the role of IL-1 on chondrocyte biology and may facilitate the development of strategies for treatment and diagnosis of joint disease.

3.B. Background

Equine osteoarthritis (OA) is a complex progressive disease of diarthrodial joints, whereby the capacity of articular chondrocytes for repair of cartilage extracellular matrix (CECM) damage is exceeded by the destructive influences of the ongoing disease process (McIlwraith, 1987, 1996). The result is irreversible loss of the structural integrity and

biomechanical characteristics of a normal joint, including efficient load distribution, low coefficient of friction, and resistance to wear. The role of neutral zinc-dependent metalloproteinases (MMPs) in mediating the progressive destruction of both collagenous and proteoglycan components of the CECM has been previously described (Dean, *et al.*, 1989; Howell and Pelletier, 1993). Further characterization of processes that occur early in the pathogenesis of OA may facilitate the identification of potential markers for earlier diagnosis and more targeted therapies.

Interleukin-1 (IL-1) is a potent pro-inflammatory cytokine found in elevated concentrations in osteoarthritic joint effusions and is purported to be one of the primary mediators in the pathogenesis of OA (Pettipher, *et al.*, 1986; Morris, *et al.*, 1990; Alwan, *et al.*, 1991; Dinarello, 1996). IL-1 induces MMP transcription and inhibits proteoglycan and collagen synthesis by chondrocytes (Schnyder, *et al.*, 1987; Lotz, *et al.*, 1995; Lotz, 2001). Other IL-1 effects include activation of cytokines, growth factors, interferons, prostaglandins, and nitric oxide, that may further perpetuate and regulate inflammatory responses (Towle, *et al.*, 1987; Dinarello, 1994b; Fukuda, *et al.*, 1995; Platt, 1996). The inhibitory effects of IL-1 receptor antagonist (IL-1ra) on IL-1 mediated joint destruction further support IL-1 as the cytokine prototype for CECM catabolism in acute and chronic inflammation associated with OA (Arend, *et al.*, 1990; Abramson and Amin, 2002). Results of previous studies point to the complexity of IL-1 signaling pathways and the involvement of distinct transcriptional factors in activated expression of different genes (Lotz, *et al.*, 1995; O'Neill, 1995). Furthermore, IL-1 signaling and effects on gene expression may vary with cell-type and be influenced by a variety of micro-environmental factors (Lotz, *et al.*, 1995; Stokes, *et al.*, 2002).

This study was conducted to investigate changes in steady state mRNA levels in equine articular chondrocytes after a 1-hour exposure to recombinant equine interleukin-1 (alpha, beta, and receptor antagonist) using a custom cDNA array analysis. These results may assist in efforts toward identification of potential points of intervention for anti-IL-1

therapies for various stages of joint disease in horses. We propose that the construction of the described targeted cDNA array may be a useful tool to study of equine OA, with potential applications for research focusing on the role of IL-1 cytokines in human arthritides.

3.C. Materials and Methods

Recombinant equine interleukin-1

Expression constructs for the nucleotide sequences encoding the putative mature forms of equine interleukin-1 alpha (EqIL-1α), interleukin-1 beta (EqIL-1β), and interleukin-1 receptor antagonist (EqIL-1ra) were previously cloned (Howard, *et al.*, 1998a, b) (*refer to Appendix figure A1*). Recombinant proteins were expressed, purified under native conditions, and evaluated for purity and concentrations using sodium dodecyl-polyacylamide gel electrophoresis, high-pressure liquid chromatography, and spectrophotometric analysis (Takafuji, *et al.*, 2002) (*refer to Appendix figures A2,3*). A murine T-cell mitogenesis assay was used to quantify protein bioactivity (Takafuji, *et al.*, 2002). Endotoxin levels were determined to be < 0.1 ng/ug using a limulus amebocyte lysate assay (Associates of Cape Cod, Inc, Falmouth MA). Protein stocks were stored in phosphate buffered saline at –70°C prior to use.

Target compilation

One hundred sixty-five cDNA clones corresponding to genes purported to have a role in joint disease pathobiology were compiled (*refer to Appendix II.B.1 and Table AVI*). Strategies used for target cDNA acquisition included plaque hybridization screening an equine peripheral blood mononuclear cell cDNA library, subtractive hybridization using EqIL-1β stimulated and unstimulated synovium (*refer to Chapter V*), donations from colleagues, and purchase from commercial sources (American Tissue Culture Collection, Manassas VA and Incyte Genomic Inc, La Jolla CA). The cDNA array included a range of pro-inflammatory cytokines and chemokines, CECM components or proteins involved in CECM metabolism, regulators of signal transduction,

nuclear transcription factors, and cell cycle regulators. All target clones were originally derived by priming to the poly A region of nucleotide sequences. One house-keeping target cDNA (equine glyceraldehyde-3-phosphate dehydrogenase (GAPDH)), three positive hybridization controls (cDNA from chondrocytes, synovium, cartilage), and one negative hybridization control (plasmid DNA) were also included.

Array printing

Target cDNAs were amplified using standard polymerase chain reaction (PCR) methods using either sequence-specific or vector-specific primers (0.4 uM), 2 mM $MgCl_2$, and Taq DNA polymerase (2.5U) (Promega Corporation, Madison WI) (initial denaturation of 94°C for 5 minutes and 35 cycles of: 94°C for 1 minute, 55°C for 1 minute, 72°C for 1.5 minutes, final extension of 72°C for 10 minutes). Amplicons were purified using standard chloroform extraction and ethanol precipitation, quantified relative to a mass ladder (Low mass™ DNA ladder, Invitrogen Co, Carlsbad CA), subjected to alkali denaturation (300 uM NaOH), and immobilized to charged nylon membranes (Hybond™-XL, Amersham, Piscataway NJ) at similar mass (2.5 ng). Printing was conducted in duplicate on each membrane (Vicky library printer, V&P Scientific, San Diego CA), followed by UV crosslinking (70,000 ujoules/cm^2) (*refer to Appendix II.B.3*).

Primary chondrocyte isolation and culture

Near full-thickness articular cartilage was aseptically removed from stifle joints of three adult horses (2-5 years, mean 4 years) euthanized for reasons unrelated to joint disease (VA-MD Regional College of Veterinary Medicine, Blacksburg, VA). Articular cartilage chondrocytes were liberated from the ECM by collagenase digestion (1.0%) at 37°C, 16 hours in a modified procedure (Nixon, *et al.*, 1992). Yields ranged from 3-6 x 10^6 chondrocytes / gram cartilage (wet weight). Chondrocytes were assessed for viability by trypan blue exclusion (88-95 %), cultured for 2-4 passages, and cryogenically stored. Cells were thawed and seeded in high-density (1 x 10^5 cells/cm^2) onto 60-mm diameter

dishes, 37°C, 5 % CO_2 in a low glucose Dulbecco's modified eagle medium with 10 % fetal bovine serum, 4 mM L-glutamine, 21.5 mM HEPES buffer, penicillin (57 U/ml) / streptomycin (57 μg/ml), and ascorbic acid (50 ug/ml), pH 7.2. Media was replaced every 3-4 days until monolayers reached confluency (6-8 days). Cells were passaged 1-2 more times prior to initiation of the experiment (passage 5-7). Separate monolayers from each of the 3 horses were rinsed with Dulbecco's phosphate buffered solution immediately prior to treatment with experimental media alone or media supplemented with IL-1 (EqIL-1α, EqIL-1β, or EqIL-1ra) at 10 ng/ml concentrations. Experimental media was devoid of serum and supplemented with 0.2 % lactalbumin hydrolysate to remove residual serum components and their possible effects on gene expression. Monolayers were harvested after 1 hour with Trizol™ (1 ml) and stored at -70°C. Genomic DNA concentrations were analyzed using a Hoechst 33258 dye fluorescent assay (EX 360 nm, EM 465 nm) against a calf thymus DNA standard curve (0-100 ug/ml) (Molecular Probes, Eugene OR) (*refer to Appendix III*).

Probe preparation

Total RNA from monolayer cultures were precipitated from Trizol™ solubilized aqueous fractions using isopropanol, as per the manufacturer's instructions (Invitrogen Corporation, San Diego, CA) (*refer to Appendix II.C.1*). Total RNA (10 ug, $A_{260nm/A280nm}$ > 1.8) was combined with an oligo (d)T primer (2 ug) and incubated with Powerscript™ reverse transcriptase (300 U) (CLONTECH Laboratories, Palo Alto, CA), dNTPs (1 mM each dCTP, dGTP, dTTP), and DTT (3.3 mM) at 37°C for 90 minutes. The cDNA was directly radiolabeled using [α-^{32}P]-dATP (20 uCi, Redivue™, Amersham, NJ), with incorporation efficiencies ranging from 20-60 % (*refer to Appendix II.C.3*). Probes were separated from unincorporated label by sephadex column chromatography and were heat denatured (95°C for 5 minutes) prior to hybridization.

Hybridization

Duplicate membranes for each labeled probe were pre-hybridized in a modified Church buffer (0.5 M sodium phosphate, 7 % SDS, 10 mM EDTA, 100 ug/ml herring sperm DNA) at 65°C for 1 hour. Hybridization reactions were conducted in 35 mm x 150 mm glass tubes at 65°C for 16 hours, 8-10 rpm/minute (*refer to Appendix II.C.4*). Membranes were washed in increasing stringency: 2X SSC / 0.1% SDS (2X 5 min, 25°C), 1X SSC / 0.1% SDS (1X 15min, 42°C), 0.1X SSC / 0.1% SDS (2X 10 min, 65°C) and air-dried. Membranes were exposed to a phosphorimaging screen (2 hours), scanned, and analyzed (Storm 820 phosphorimager and ImageQuant^{TM} software, Amersham Pharmacia Biotech, Piscataway NJ). A separate assessment of the hybridization system using titrated concentrations of labeled probe indicated approximate sensitivity to range from 0.001-0.01 ng (*refer to Appendix II.D.1 and Figure A4*).

Collagen analysis

Protein fractions precipitated from the organic layer of Trizol^{TM} solubilized monolayers were subjected to digestions with pepsin at 4°C for 16 hours (1 mg/ml) (Sigma-Aldrich Corporation, St. Louis, MO) and pancreatic elastase at 35°C for 30 minutes (1 mg/ml) (Worthington Biochemical Corporation, Lakewood, NJ). Isolated collagens were analyzed by enzyme-linked immunoassay at 490 nm relative to a purified equine standard curve for type II collagen (0-0.2 ug/ml) (Capture ELISA kit, Chondrex Inc, Redmond WA). Duplicate measurements were averaged and control and equine IL-1 treated group means were compared using Student's t-tests (α=0.05). Reverse-transcriptase polymerase chain reaction (RT-PCR) was also employed to quantify mRNA levels for type I and type II collagen (see below).

RT-PCR

Primers were designed to partial coding regions of reported equine nucleotide sequences for seven genes exhibiting altered transcript levels in the EqIL-1α or EqIL-1ra

groups as detected by cDNA array analysis (*refer to Appendix II.C.6)* (PrimerSelect, DNASTAR, Madison WI). Aliquots of reverse transcribed RNA (4 ug) (Universal RiboClone® cDNA synthesis system, Promega Corporation, Madison WI) were added to reactions containing gene-specific primers (0.4 uM), 50 mM KCl, 10 mM Tris-HCl, 0.2 mM dNTPs, and 2.5U Taq polymerase (Eppendorf Scientific Inc, Westbury NY) (50 ul volumes). An optimized number of cycles was carried out for each primer pair: 95°C for 1 minute, 48-61°C for 1.5 minutes, 72°C for 1.5 minutes, and a final extension at 72°C for 10 minutes. Optimum cycle numbers were determined by the addition of 0.1 uCi [α-^{32}P]-dATP (Amersham Pharmacia Biotech, Piscataway NJ) and Cerenkov counting of aliquots taken at 20, 25, 30, and 35 cycles (*refer to Appendix Table AVIII*) (Ko, 1995). Twenty microliter aliquots of the optimized reactions were run on 1.5% agarose gels and quantified by densitometry following correction for GAPDH (ImageJ 1.30v, National Institutes of Health, Bethesda MD). Equine IL-1 treated and control group means were compared using Student's t-tests (α=0.05). Data were presented as means of the ratios of EqIL-1 relative to controls.

Statistical analysis

A one-stage mixed linear analysis of variance (ANOVA) was conducted to detect differences in signal intensities. Statistical analysis involved modeling genes as fixed effects in a subplot, and horse and IL-1 treatment effects in the whole-plot sampling structure (Statistical Analysis Software, SAS Institute, Cary, NC). Pairwise gene comparisons were ordered using an arbitrary cutoff (α= 0.05); mean differences were depicted on a log base 2 scale in a modified volcano plot corrected for one error term. Data were log-transformed and EqIL-1 treatment effects were evaluated for replicate signal intensity correlation prior to analysis **(Figure 3.1)**. Mean signal intensities were calculated from four hybridization values normalized to the mean signal intensities of equine GAPDH. Appropriateness of GAPDH normalization was determined by assessing signal variation of house-keeping targets across IL-1 stimuli, membranes, and horses. Possible bias in the hybridization system was addressed (*refer to Appendix II.D.2*

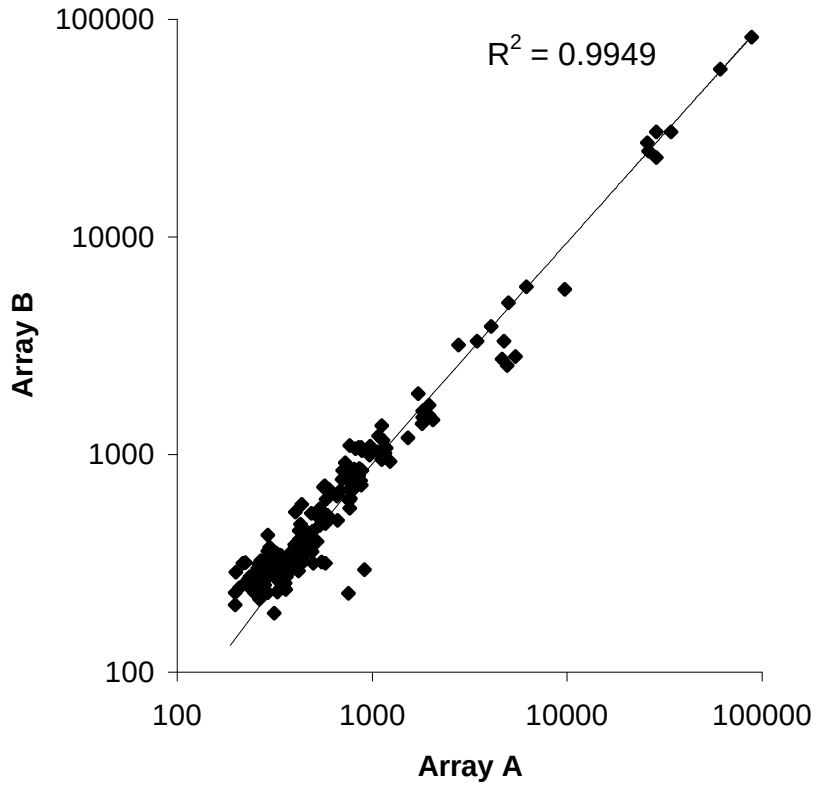

Figure 3.1 - Replicate array hybridization analysis.

Duplicate data points from a single membrane hybridized with EqIL-1β stimulated labeled cDNA from one horse. Results are representative of duplicate membranes and are typical of replicate analyses across horses and EqIL-1 stimuli.

and Figure A5). Principal component analysis (PCA) was conducted to identify latent trends in EqIL-1 modulated gene expression levels (PROC PRINCOMP, Statistical Analysis Software, SAS Institute, Cary, NC). Principal component score means from the three horses were compared using an ANOVA (α=0.05).

3.D. Results

Signal normalization

It was critical to identify a constitutively expressed housekeeping target cDNA for normalization of signal intensities between arrays being compared. The overall variance in data corresponding to the equine and murine forms of GAPDH and β-actin was assessed. Equine GAPDH yielded the least variable signal intensities across the three horses, the four stimuli within one horse, between spots on the same membrane, and across membranes **(Table 3.1)**. Importantly, signal intensities corresponding to the four stimuli were not significantly different across all membranes (p=0.6556). From these combined evaluations, equine GAPDH was determined to be the most appropriate house-keeping target for proper data normalization of the stimulated chondrocyte mRNA populations being analyzed within this newly described hybridization system.

cDNA array data analysis

Increased target signal intensities were predominantly observed in the EqIL-1α and EqIL-1β groups relative to media treated control groups, while decreased target signal intensities were predominantly observed in the EqIL-1ra group **(Figure 3.2)**. Hybridization signal intensities corresponding to targets for phosphoinositol 3-kinase (PI-3K), bone morphogenetic protein-4 (BMP-4), insulin-like growth factor-2 (IGF-II), interleukin-6 (IL-6), bromodomain transcription factor (BPTF), and β-actin were significantly higher in the EqIL-1α groups relative to the control groups **(Table 3.2)** and relative to the EqIL-1ra group ($p<0.01$) (data not shown), but similar to those for the EqIL-1β group. Signal intensities for 13 additional targets were increased > 2-fold in the EqIL-1α group relative to controls, but these differences were not statistically significant.

Table 3.1 - cDNA array signal normalization assessment.

Estimated variance	***eq GAPDH****	***eq b-actin***	***mu GAPDH***	***mu b -actin***
Horse-to-horse	***0.9218***	1.5041	1.0529	1.4363
Stimuli within a horse	***0.6797***	1.2219	0.6933	0.1554
Membrane-to membrane witihin a stimulus	***-0.03496***	-0.04701	-0.07249	-0.4019
Spot-to-spot within a membrane	***0.193***	0.2181	0.3275	5.9037
Stimuli across membranes (p-value)	***0.6556***	0.4905	0.7326	0.2287

* Results indicate equine GAPDH to correspond to the smallest estimated variance over the tested comparisons, and to be the least variable across untreated control and EqIL-1 stimuli by ANOVA.

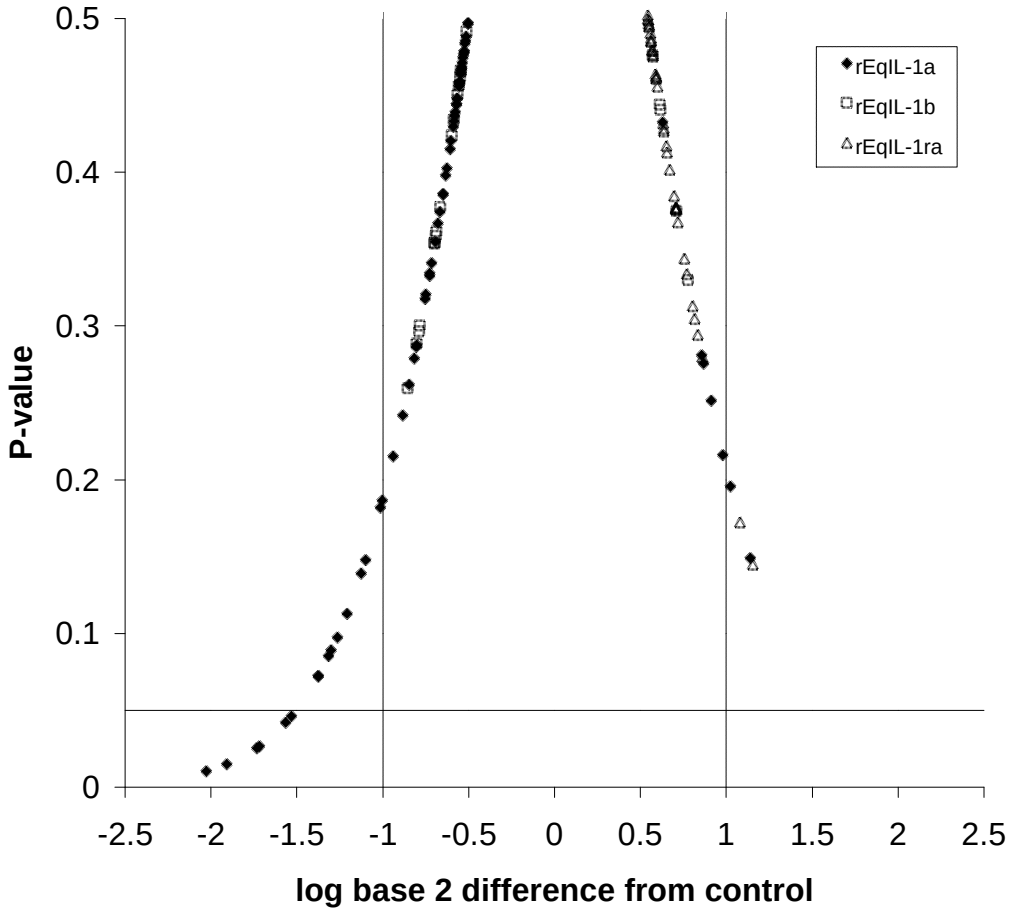

Figure 3.2 - ANOVA pairwise comparisons.

Log-transformed EqIL-1 treatment group mRNA levels relative to control. Negative x-axis values correspond to increased mRNA levels and positive values correspond to decreased mRNA levels; a one-unit difference corresponds to an approximate 2-fold difference. Significance is denoted by horizontal line at p=0.05.

Table 3.2 - EqIL-1 treated group signal intensities relative to controls.

Gene	*Genbank*	*IL-1 to control*	*Fold change*
Phosphoinositol 3-kinase related kinase (PI-3K)	AF506975	IL-1α	+ 3.7 *
Bone morphogenetic protein-4 (BMP-4)	AA473799	IL-1α	+ 2.8 *
Insulin-like growth factor-2 (IGF-II)	AA059967	IL-1α	+ 3.3 *
Interleukin-6 (IL-6)	U64794	IL-1α	+ 3.5 *
Bromodomain transcription factor (BPTF)	AY246719	IL-1α	+ 4.0 *
β-actin	AF035774	IL-1α	+ 2.8 *
R-ras	AA432641	IL-1α	+ 2.3
G-beta protein	AY246708	IL-1α	+ 2.5
Transketolase	AY343543	IL-1α	+ 2.3
Elongation factor (E2f1)	AA396123	IL-1α	+ 2.5
N-myc/STAT interactor	AY246724	IL-1α	+ 2.6
cDNA subtracted library fragment 42 (EST #42)	AY246806	IL-1α	+ 2.5
IL-12 p35 subunit	AI050362	IL-1α	+ 2.0
Interleukin-1 converting enzyme (ICE)	AF090119	IL-1α	+ 2.3
Cytochrome C oxidase IV (COXIV)	AY246701	IL-1α	+ 2.1
Major histocompatibility complex I (MHCI)	M95410	IL-1α	- 2.0
Tumor necrosis factor receptor factor-5 (TRAF5)	AA170423	IL-1α	- 2.1
Transforming growth factor beta receptor 2 (TGFβR2)	AY246716	IL-1ra	- 2.3
Tissue inhibitor of matrix metalloproteinase-1 (TIMP-1)	U95039	IL-1ra	- 2.1

Targets corresponding to mRNA level ratio differences > 2-fold are listed. * denotes significance at $p < 0.05$ by ANOVA.

The signal intensities corresponding to the major histocompatibility complex I (MHCI) and tumor necrosis factor receptor-5 (TRAF-5) were lower in the EqIL-1α groups relative to controls; however, these effects were not statistically significant **(Table 3.2)**. A non-significant decrease in signal intensities for transforming growth factor beta receptor-2 (TGFβR2) and tissue inhibitor of matrix metalloproteinase-1 (TIMP-1) targets was observed for the EqIL-1ra group relative to controls **(Table 3.2)**.

PCA

Five principal components representing ~ 95% of the total variation were identified (data not shown). Within the fourth component reflecting ~ 4 % of the total variation, a significant difference between principal component scores was observed between the EqIL-1α and EqIL-1β groups across the three horses (p=0.022) **(Figure 3.3)**. Genes positively loading on the component corresponded to greater mean values for the EqIL-1β group compared with the EqIL-1α group (i.e. higher IL-1β/IL-1α fold change); the reverse was also observed, with negative loading genes corresponding to targets with higher relative signal intensities in the EqIL-1α group (i.e. lower IL-1β/IL-1α fold change) **(Table 3.3)**. Greater than two-fold difference in signal intensity for aggrecan and cartilage oligomeric protein (COMP) targets were observed for the EqIL-1α group relative to the EqIL-1β group, although these differences were not significant **(Table 3.3)**. No significant stimuli effects were detected in the other four components evaluated (not shown).

RT-PCR

A non-significant increase in mRNA levels corresponding to BMP-4 (+1.1-fold), IGF-II (+1.1-fold), BPTF (+1.1-fold), IL-6 (+1.7-fold), β-actin (+1.1-fold), and PI-3-K (+1.1-fold) was detected by RT-PCR for the EqIL-1α groups relative to media treated control groups. A non-significant decrease in mRNA levels was detected by RT-PCR for

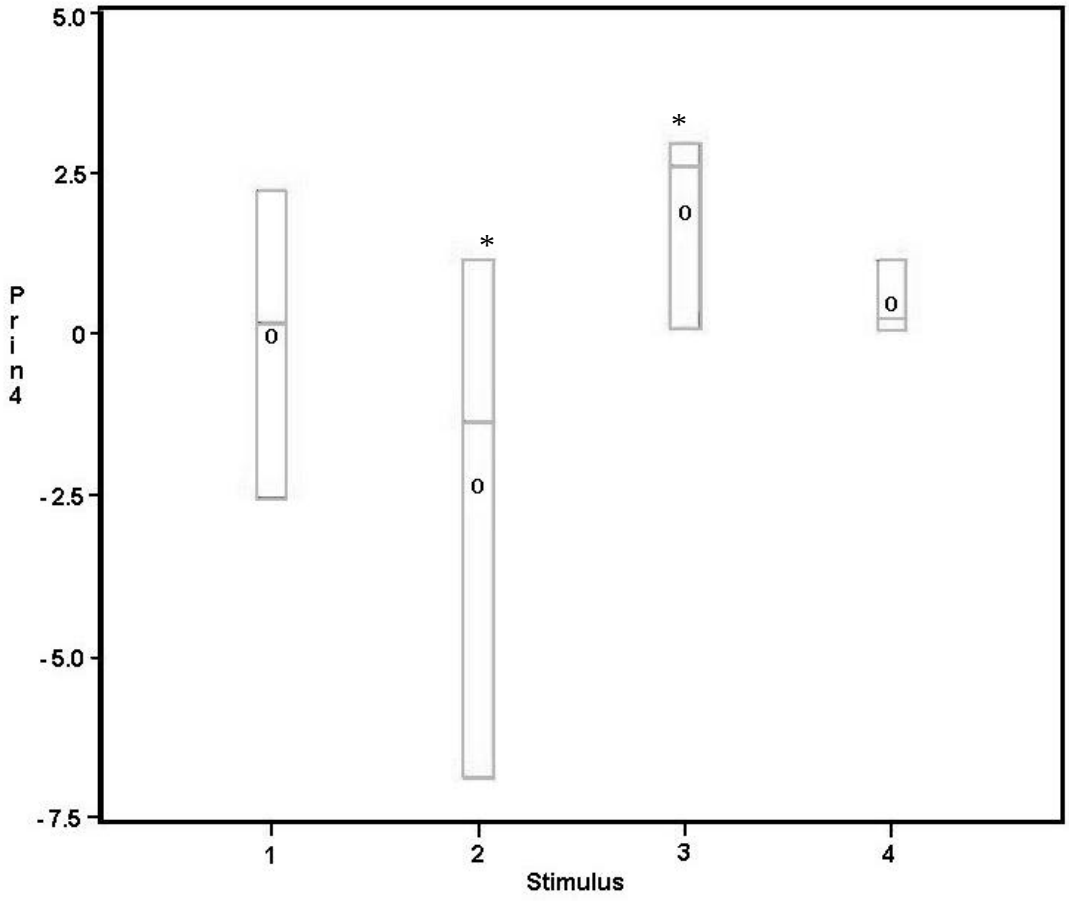

Figure 3.3 - Graphically depicted scores for principal component 4 (Prin4).

Box-plots represent principal component scores for the three horses across the four stimuli tested: stimulus 1= untreated, 2= EqIL-1α, 3= EqIL-1β, 4= EqIL-1ra. Circles and horizontal lines correspond to mean and median values, respectively. Boxes correspond to 95% interquartile ranges. * denotes significant effect between EqIL-1α and EqIL-1β scores, $p = 0.022$.

Table 3.3 - Principal component 4 (PC4) results.

Gene	*Genbank*	*PC4 correlation*	*IL-1b / IL-1a fold change*
Folate binding protein-1	AA139715	0.18	+ 1.53
TNF receptor associated factor-5 (TRAF-5)	AA170423	0.18	+ 1.44
Decorin (DSPGII)	AF038127	0.16	+ 1.31
IKBα	AA204405	0.13	+ 1.21
STAT-1	AA386678	0.12	+ 1.61
Indian Hedgehog protein (Ihh)	AA245525	0.12	+ 1.01
Folate binding protein-2	AA015571	0.12	+ 1.15
Caspase-9	AI155822	0.12	+ 1.31
Growth arrest specific protein (GAS)	AA087048	0.12	+ 1.68
Epidermal growth factor (EGF)	AI648855	0.11	+ 1.02
Phosphoprotein (C8FW)	AF506971	-0.29	- 1.34
Gelsolin	AY246741	-0.22	- 1.74
Matrix metalloproteinase-2 (MMP-2)	AJ010314	-0.21	- 1.44
Aggrecan	AF040637	-0.18	- 2.11
c-NOS	Not available	-0.15	- 1.38
Actin filament capping protein	AF506976	-0.14	- 1.09
Galactocerebrosidase (GALC)	AF506974	-0.14	- 1.41
Cartilage oligomeric protein (COMP)	AB040453	-0.13	- 2.04
Cullin 4B (CUL4B)	AF513243	-0.12	- 1.59
Fibronectin (FN1)	AA275041	-0.12	- 1.50

Listed cDNAs correspond to the ten genes most positively and negatively correlated with PC4. Fold changes reflect the original log-transformed signal intensities of EqIL-1β relative to EqIL-1α stimulated chondrocytes.

MHCI (-1.1-fold) in the EqIL-1α group and TIMP-1 (-1.3-fold) in the EqIL-1ra treatment group. Messenger RNA for type I collagen (α1 and α2 chains) was detected in control and EqIL-1 stimulated chondrocytes from all 3 horses by RT-PCR, but concentrations were not significantly different across treatment groups. Type II collagen mRNA was not detected by RT-PCR through 40 cycles of amplification (data not shown).

Collagen content

Significant differences were not detected between untreated control and EqIL-1 treated chondrocyte monolayer type II collagen epitope concentrations.

3.E. Discussion

The primary objectives of this study were to investigate early IL-1 induced changes in articular chondrocyte gene expression levels, and to evaluate differences in effect of the three EqIL-1 proteins. The overall increased expression observed for the EqIL-1α and EqIL-1β groups as compared to control and EqIL-1 receptor antagonist groups **(Figure 3.2)** support previous reports of stimulatory effects of IL-1 on chondrocyte transcription (Goldring, *et al.*, 1994; Fukuda, *et al.*, 1995; Margerie, *et al.*, 1997; Vincenti and Brinckerhoff, 2001). The more potent effects of EqIL-1α over EqIL-1β observed in this study may be explained by the ~ 40% greater bioactivity of the EqIL-1α protein preparation used in this study or possible differences in protein tertiary folding conformations (Dinarello, 1994a; Takafuji, *et al.*, 2002). Interleukin-1ra binds to the same receptors as the two IL-1 agonists without undergoing receptor mediated internalization and inducing signaling events presumably affecting transcription (Dripps, *et al.*, 1991). Thus, the observed suppressive effects of IL-1ra on expression relative to controls presumably was the result of inhibition of endogenous IL-1, and highlights the importance of this naturally occurring antagonist in regulating IL-1 effects in articular chondrocytes (Arend, *et al.*, 1990; Murata, *et al.*, 2003).

Increased levels of mRNA corresponding to cytokines, growth factors, signaling proteins, and a microfilament component were observed after one hour of exposure to EqIL-1α **(Table 3.2)**. The increase in interleukin-6 (IL-6) transcript levels in this study is consistent with the reports of IL-1 activated IL-6 expression and synthesis in chondrocytes *in-vitro* and elevated levels of IL-6 in osteoarthritic synovial fluids (Bender, *et al.*, 1990; Guerne, *et al.*, 1990; Van de Loo, *et al.*, 1997; Vincenti and Brinckerhoff, 2001). Local effects of IL-6 on cartilage pathophysiology remain uncertain, since conflicting results exist for its possible roles in IL-1 mediated proteoglycan synthesis suppression; the ubiquitous ability of chondrocytes to produce IL-6 has suggested potential roles of this cytokine in cartilage ECM homeostasis and activation of T-cells within the joint (Guerne, *et al.*, 1990; Nietfeld, *et al.*, 1990; Van de Loo, *et al.*, 1997). Insulin growth factor-II was demonstrated to stimulate cartilage matrix synthesis, glucose uptake, cellular growth, and production of autocrine factors promoting cellular survival (Bhaumick and Bala, 1991; Loeser and Shanker, 2000). Bone morphogenic protein-4, a member of the transforming growth factor beta family, is noted with contributions to ECM anabolism, autocrine stimulated preservation of the chondrogenic phenotype, and weak mitogenic effects on chondrocytes cultured in monolayer (Luyten, *et al.*, 1994; Shukunami, *et al.*, 2000). Thus, up-regulated IGF-II and BMP-4 expression levels may suggest the initiation of growth factor-mediated ECM anabolism counter to CECM degradative processes after one hour of IL-1 stimulation. Altered β-actin expression levels may support reports of IL-1 to induce changes in chondrocyte actin cytoskeletal architecture, with consequent effects on morphology, differentiative mechanisms, and gene expression (Mallein-Gerin, *et al.*, 1991; Svoboda, 1998; Cimpean, *et al.*, 2000). Increased mRNA levels for PI-3-kinase is consistent with previous reports describing the role of protein kinase C pathways in IL-1 signal transduction (O'Neill, 1995; Svoboda, 1998).

Principal component analysis is a sophisticated mathematical reduction of multi-dimensional data in the effort to identify trends in expression level patterns and

relationships between individual genes (Timm, 2002). Of the ten genes most positively correlated and likely to contribute to the identified principal component in response to EqIL-1β, the majority related to general cellular metabolic, growth, and apoptotic processes **(Table 3.3)**. Three of these genes function in IL-1β/Toll receptor/IL-1 receptor signaling and NFKB / JNK activation (O'Neill, 1995; Chung, *et al.*, 2002). The co-expression of the small proteoglycan decorin and Indian hedgehog within this identified component may suggest an underlying transcriptional mechanism for IL-1β mediated phenotypic changes in isolated chondrocytes (Kronenberg, *et al.*, 1997; Bock, *et al.*, 2001). Of the ten transcripts most negatively correlated with the component, the majority corresponds to cartilage-specific ECM components and CECM metabolic enzymes **(Table 3.2)**. Together, these results suggest that IL-1β may contribute to growth and de-differentiation transcriptional processes, whereas IL-1α may influence opposing pro-differentiation responses in cultured chondrocytes. IL-1β, but not IL-1α, was observed to promote growth in the adrenal cortex; divergent biological effects of the two IL-1 agonists have also been reported in immune response activation (Boraschi, *et al.*, 1990; Zieleniewski, *et al.*, 1995a, b). Clearly, this hypothesis is preliminary, but might suggest against using the two IL-1 proteins interchangeably in similar *in-vitro* expression studies without careful interpretation. Further investigations into signal transduction mechanisms may help to elucidate these observed early subtle differences in response to IL-1α and IL-1β.

Shortcomings of the *in-vitro* culture and cDNA array analysis systems described in this study are acknowledged. As an equine chondrocyte cell line is not currently available, a heterogeneous population derived from the harvested near full-thickness articular cartilage from the three horses may have contributed to inherent variability in transcript levels (Fukuda, *et al.*, 1995). Genes transcribed below the ~ 0.01 ng estimated detection range of this cDNA array system may have been a limiting factor for binding to quadruplicate targets. Also, increased signal variation between replicate data points may have lowered the number of detected significant pairwise comparisons (*refer to Appendix*

II.D.2 and Figure A5). The majority of transcript levels altered > 2-fold by EqIL-1 treatments **(Table 3.2)** presented weak baseline hybridization signal intensities (data not shown), demonstrating the ability of this system to detect expression level effects despite the described technical limitations.

Chondrocytes de-differentiate toward a fibroblastic / pre-chondrogenic phenotype following isolation from intact CECM and passaging in adherent culture, characterized by increased type I collagen and decreased type II collagen expression (Castagnola, *et al.*, 1988; Mallein-Gerin, *et al.*, 1991; Binette, *et al.*, 1998). Attempts were made in this study to minimize de-differentiation, by plating at high cellular densities and using low glucose media supplemented with ascorbic acid (Castagnola, *et al.*, 1988; Vincenti and Brinckerhoff, 2001). ELISA-based methods detected low concentrations of type II collagen epitopes in the cell lysate protein fractions. Additionally, transcripts corresponding to the large proteoglycan aggrecan were detected at moderate baseline levels in the 3 horses by cDNA array analysis (not shown), suggesting some degree of maintenance of a cartilage-specific phenotype. However, results of RT-PCR detected type I collagen but not type II collagen expression levels, indeed supporting the notion that heterogeneous populations of de-differentiating chondrocytes were likely used in this study. This was an anticipated finding since the cells had been stored, thawed, and passaged 5-7 times prior to initiation of experimental conditions. It has been suggested that passaged chondrocytes may exhibit responses similar to that of de-differentiated osteoarthritic cells; thus, it is possible that the *in-vitro* culture system used in this study may have simulated the response of later stage diseased chondrocytes (Luyten, *et al.*, 1994; Binette, *et al.*, 1998).

Complementary DNA array analysis enables the parallel evaluation of expression levels of a number of genes at a time. The genes on this cDNA array were selected based on their purported involvement in pathophysiologic processes in joint disease, but it is recognized that the vast majority of actively expressed transcripts likely remained

unstudied with this targeted approach. PCA results suggest a potential divergence in EqIL-1α and EqIL-1β biological responses, which comparison of signal intensities alone were unable to demonstrate. Our results indicate that IL-1 may be a principal effector in stimulatory and pathologic responses in chondrocytes, and may support further investigation into the use of IL-1ra in anti-IL-1 directed therapies for OA (Thompson, *et al.*, 1992; Abramson and Amin, 2002). These results provide baseline information for future expression-based studies and may help to further elucidate complex IL-1 regulated inflammation and joint disease processes in horses.

3.F. Acknowledgments

The authors thank Dr. David Horohov, DVM, Louisiana State University, College of Veterinary Medicine, Baton Rouge, LA, for donation of equine IL-6 and β-actin cDNAs, Dr. Dean W. Richardson, DVM, University of Pennsylvania School of Veterinary Medicine, Kennett Square, PA for donation of equine aggrecan and decorin cDNAs, Dr. Nobushige Ishida, DVM, PhD, Laboratory of Molecular and Cellular Biology, Equine Research Institute, Tokami-Cho, Utsunomiya, Tochigi, Japan for donation of a COMP cDNA, and Dr. Peter Clegg, DVM, Department of Veterinary Clinical Science and Animal Husbandry, University of Liverpool, Leahurst, Neston, UK for donation of equine MMP-2 and c-NOS cDNAs.

CHAPTER IV: Temporal effect of equine interleukin-1b on gene expression in articular chondrocytes

4.A. Abstract

The specific transcriptional events underlying cytokine-driven inflammation and production of enzymatic factors responsible for the irreversible degradation of articular cartilage associated with osteoarthritis remain undefined. The objective of this study was to investigate the effects of recombinant equine IL-1β (EqIL-1β) on high-density passaged equine chondrocyte steady state mRNA levels over time (1, 3, and 6 hours). Reverse-transcribed radiolabeled cDNA from chondrocytes treated with media or EqIL-1β was hybridized to a customized 380-target cDNA array. Means of duplicate log-transformed hybridization signals were normalized to signals corresponding to equine glyceraldehyde 3-phosphate dehydrogenase (GAPDH). Differentially expressed transcripts were identified using a two-stage mixed linear analysis of variance model with Bonferroni correction for multiplicity (α=0.05) (Statistical Analysis Software, Cary, NC). Signal intensities for seven cDNA targets were significantly increased after 6 hours of EqIL-1β stimulation ($p<0.00004$): cullin 4B, ferritin, matrix metalloproteinase-13, intermediate early response-2, transforming growth factor beta-2, tumor necrosis factor receptor associated factor-1, and an expressed sequence tag (AY246802). A time-dependent increase in the number of transcripts altered > 2-fold in response to EqIL-1β was observed: one transcript was increased at 1 hour, 2 transcripts were increased at 3 hours, and 102 transcripts were altered after 6 hours. Principal component analysis revealed five components to reflect ~ 88 % of the total variation. The third component, explaining ~ 10 % of the variation, was proposed to reflect EqIL-1β induced transcription of cell-cycle regulatory proteins relative to controls ($p=0.0179$). These results contribute to current knowledge of IL-1β regulated gene expression in equine chondrocytes, and provide insights into possible anti-IL-1 approaches for treatment of joint disease.

4.B. Background

Osteoarthritis (OA) is characterized by changes in subchondral bone and degradation of the proteoglycan and collagen frameworks of articular cartilage that gradually overcomes the capacity for chondrocytic synthetic repair (Dean, *et al.*, 1989; Hamerman, 1993; Howell and Pelletier, 1993; Platt, 1996). Zinc-dependent neutral matrix metalloproteinases (MMPs) cleave specific collagen and proteoglycan components of the cartilage extracellular matrix (CECM). Excessive production of MMPs and additional proteases may outweigh inhibitory mechanisms (e.g. tissue inhibitor of metalloproteinases (TIMPs), progressing to an irreversible degradation of the CECM (Dean, *et al.*, 1989; Martel-Pelletier, *et al.*, 1994; DiBattista, *et al.*, 1995a). Activated synoviocytes, infiltrating inflammatory cells, and articular cartilage chondrocytes produce increased levels of cytokines and soluble factors that propagate inflammatory cascades and can contribute to local tissue destruction.

Interleukin-1 (IL-1) is an inflammatory cytokine detected in elevated concentrations in effusions from diseased joints in horses (Morris, *et al.*, 1990; Alwan, *et al.*, 1991). IL-1 is implicated in CECM catabolism and OA pathogenesis, by inducing production of MMPs and suppressing proteoglycan and collagen synthesis in articular chondrocytes (Pasternak, *et al.*, 1986; Tyler and Benton, 1988; Tyler, *et al.*, 1990; Platt and Bayliss, 1994; Taskiran, *et al.*, 1994). In cartilage and cultured chondrocytes, IL-1 was demonstrated to induce synthesis of cytokines, nitric oxide synthase, plasminogen activators, and prostaglandin E_2 via cyclooxygenase activation (Pasternak, *et al.*, 1986; Campbell, *et al.*, 1988; Campbell, *et al.*, 1990; Palmer, *et al.*, 1993; Hardy, *et al.*, 1998b). The naturally occuring IL-1 receptor antagonist was shown to reduce IL-1 induced articular cartilage ECM degradation, further implicating the crucial role of this cytokine in the pathogenesis of OA (Thompson, *et al.*, 1992; Abramson and Amin, 2002).

The objectives of this study were to investigate the temporal effects of recombinant equine IL-1β (EqIL-1β) on equine chondrocyte steady state mRNA levels (1-6 hours) using a custom targeted cDNA array analysis. Efforts were directed toward the identification of proximal IL-1 effects on chondrocyte gene expression as a model system for the study of IL-1 regulated cartilage biology. The results of this study may have promising applications for possible anti-IL-1 directed therapies and may identify potential markers for the diagnosis of joint disease in horses and other species.

4.C. Materials and Methods

Recombinant equine interleukin-1

The mature putative nucleotide sequence encoding EqIL-1β was previously cloned (Howard, *et al.*, 1998a) (*refer to Appendix I*). The native protein was purified and evaluated for purity using sodium dodecyl-polyacylamide gel electrophoresis and high-pressure liquid chromatography (Takafuji, *et al.*, 2002). Protein concentration and bioactivity (4.7×10^6 U/mg) was determined using spectrophotometric analysis and a T-cell mitogenesis assay, respectively (Takafuji, *et al.*, 2002). Endotoxin levels were determined to be at acceptable levels using a limulus amebocyte lysate assay (Associates of Cape Cod, Inc, Falmouth MA) (< 0.1 ng/ug). Protein stocks were stored in phosphate buffered saline at –70°C.

Target probe compilation

Three hundred and eighty cDNAs corresponding to genes with purported roles in joint disease pathobiology were compiled using a combination of strategies (*refer to Appendix II.B.2, and Table AVII*): plaque hybridization screening an equine peripheral blood mononuclear cell cDNA library, subtractive hybridization using EqIL-1β stimulated and unstimulated synovium (*Chapter V*), donation by colleagues, and purchase from commercial sources (American Tissue Culture Collection, Manassas VA and Incyte Genomic Inc, La Jolla CA). The targeted cDNA array included a range of inflammatory cytokines and chemokines, CECM components or proteins involved in modulation of

CECM metabolism, nuclear transcription factors, and cell cycle regulators. All target clones were originally derived by priming to the poly A region of nucleotide sequences. One house-keeping target cDNA (equine glyceraldehyde-3-phosphate dehydrogenase (GAPDH), 1 positive hybridization control (chondrocyte cDNA), 1 positive labeling control (poly A oligo), 1 negative hybridization control (plasmid DNA), and 1 negative printing control (printing solution alone) were also included.

Array printing

Target cDNAs were amplified using standard polymerase chain reaction methods, using either sequence-specific or vector-specific primers (0.4 uM), $MgCl_2$ (2 mM), and Taq polymerase (2.5U) (Promega Corporation, Madison WI). Thermocycler conditions included an initial denaturation at 94°C for 5 minutes and 35 cycles of: 94°C for 1 minute, 55°C for 1 minute, 72°C for 1.5 minutes, with a final extension of 72°C for 10 minutes). Amplicons were purified using standard chloroform extraction and ethanol precipitation, run on agarose gels relative to a mass ladder (Low mass™ DNA ladder, Invitrogen Co, Carlsbad CA), and heat denatured (95°C for 10 minutes). Targets were transferred to charged nylon membranes (Hybond™-XL, Amersham, Piscataway NJ) at similar mass (2.5 ng) using a 96-pin library copier (Vicky library printing device, V&P Scientific, San Diego CA) and immobilized by UV crosslinking (70,000 ujoules/cm^2) (*refer to Appendix II.B.3*).

Primary chondrocyte isolation and culture

Near full-thickness articular cartilage was aseptically removed from stifle joints of three adult horses (2-5 years, mean 4 years) euthanized for reasons unrelated to joint disease (VA-MD Regional College of Veterinary Medicine, Blacksburg, VA). Chondrocytes were liberated from the CECM by collagenase digestion (1.0%) at 37°C for 16 hours in a modified procedure (Nixon, *et al.*, 1992), with yields ranging from 3-6 x 10^6 chondrocytes / gram cartilage (wet weight). Chondrocytes were assessed for viability by trypan blue exclusion (88-95%), passaged (2-4 times), and cryogenically stored. The

cells were thawed and seeded in high-density (1 x 10^5 cells/cm^2) onto 60-mm diameter culture dishes, 37°C, 5% CO_2 in a low-glucose Dulbecco's modified eagle medium supplemented with 10% fetal bovine serum, 4 mM L-glutamine, 21.5 mM HEPES buffer, penicillin (57 U/ml) / streptomycin (57 μg/ml), and ascorbic acid (50 ug/ml), pH 7.2. The media was replaced every 3-4 days until monolayers were confluent (6-8 days). The cells were passaged 1-2 more times (passage 5-7) prior to initiation of the experiment. Chondrocyte monolayers from the 3 horses were rinsed with Dulbecco's phosphate buffered solution immediately prior to treatment with media alone or media supplemented with EqIL-1β at 1.0 ng/ml. Experimental media lacked serum and was supplemented with 0.2% lactalbumin hydrolysate to remove residual serum components prior to EqIL-1β experimental treatments. Monolayers were harvested after 1, 3, and 6 hours into Trizol™ (1 ml), and stored at –70°C. Cellular density of monolayer cultures was assessed by measurements of genomic DNA concentrations using a Hoechst 33258 dye fluorescent assay (EX 360 nm, EM 465 nm) (*refer to Appendix III*).

Probe preparation

Total RNA was precipitated with isopropanol from Trizol™ treated samples, as per the manufacturer's instructions (Invitrogen Corporation, San Diego, CA) (*refer to Appendix II.C.1*). Total RNA (10 ug, $A_{260nm/A280nm} > 1.8$) was combined with an oligo (d)T primer (2 ug) and reverse transcribed using Powerscript™ reverse transcriptase (300 U), dNTPs (1 mM each dCTP, dGTP, dTTP), and DTT (3.3 mM) incubated at 37°C for 90 minutes. The cDNA was directly radiolabeled by incorporation of [α-^{32}P]-dATP (20 uCi, Redivue™, Amersham, NJ) (*refer to Appendix II.C.3*). Probes were separated from unincorporated label by sephadex column chromatography and were heat denatured (95°C for 5 minutes) prior to hybridization.

Hybridization

Duplicate membranes for each labeled probe sample were pre-hybridized in a modified Church buffer (0.5 M sodium phosphate, 7 % SDS, 10 mM EDTA, 100 ug/ml

herring sperm DNA) at 65°C for 1 hour. Hybridization reactions were conducted in 35 mm x 150 mm glass tubes at 65°C for 16 hours, 8-10 rpm/minute (*refer to Appendix II.C.4*). The membranes were washed in increasing stringency: 2X SSC / 0.1% SDS (2X 5 min, 25°C), 1X SSC / 0.1% SDS (1X 15min, 42°C), 0.1X SSC / 0.1% SDS (2X 10 min, 65°C) and air-dried. Membranes were exposed to a phosphorimaging screen (2 hours), scanned, and analyzed (Storm 820 phosphorimager and ImageQuant™ software, Amersham Pharmacia Biotech, Piscataway NJ). A separate assessment of the hybridization system using titrated concentrations of labeled probe indicated approximate sensitivity to range from 0.001-0.01 ng (*refer to Appendix II.D.1 and Figure A4*).

RT-PCR

The level of mRNA corresponding to selected genes in EqIL-1β treated and control groups was analyzed using RT-PCR as verification of the results of cDNA array analysis. Additionally, the steady state mRNA levels for type I and II collagens were assessed by RT-PCR. Primers were designed to partial coding regions of eleven reported equine nucleotide sequences: GAPDH, matrix metalloproteinases-1, -3, and -13 (MMP-1, MMP-3, and MMP-13), ferritin, bone morphogenetic protein-4 (BMP-4), osteoclast stimulating factor (OSF), major histocompatibility complex I (MHCI), type I collagen, A1 chain, type I collagen A2 chain, and type II collagen (*refer to Appendix II.C.6*) (PrimerSelect, DNASTAR, Madison WI). Aliquots of reverse transcribed RNA (4 ug) (Universal RiboClone® cDNA synthesis system, Promega Corporation, Madison WI) were added to reactions containing gene-specific primers (0.4 uM), 50 mM KCl, 10 mM Tris-HCl, 0.2 mM dNTPs, and 2.5U Taq polymerase (Eppendorf Scientific Inc, Westbury NY) (50 ul volumes). The following thermocycler conditions were repeated for primer pair optimized numbers of cycles: 95°C for 1 minute, 48-61°C for 1.5 minutes, 72°C for 1.5 minutes, and a final extension at 72°C for 10 minutes. Optimal cycle numbers were determined by the addition of 0.1 uCi [α-^{32}P]-dATP (Amersham Pharmacia Biotech, Piscataway NJ) and Cerenkov counting of aliquots taken at 20, 25, 30, and 35 cycles (*refer to Appendix Table AVIII*) (Ko, 1995). Twenty microliter aliquots were run on

1.5% agarose gels and quantified by densitometry following correction for GAPDH (ImageJ 1.30v, National Institutes of Health, Bethesda MD). Equine IL-1β treated and media control group means were compared at each of the three time points using Student's t-tests (α=0.05). Data were presented as mean ratios of EqIL-1β and untreated control groups at 1, 3 and 6 hours.

Glycosaminoglycan release

Glycosaminoglycan (GAG) release to the culture media harvested at 1, 3, and 6 hours after treatment was quantified using a described DMMB binding assay and spectrophotometric analysis (525 nm) (Farndale, *et al.*, 1982). Samples were papain-digested at 65°C for 4 hours (0.5 mg/ml) (Sigma-Aldrich, St. Louis, MO) in a digest buffer of 50 mM $NaPO_4$, 2 mM N-acetyl cysteine, 4 mM EDTA disodium salt, pH 6.5. Digested media samples were further diluted (1:6) in digest buffer in microtiter plates (100ul volumes), and a 0.05 mM DMMB solution in 0.03 M sodium formate, 2 mM formic acid, pH 3.5 was added (100ul). Sulfated GAG concentrations were determined relative to a shark chondroitin-4-sulfate standard curve (0-50 ug/ml). Triplicate measurements were averaged and EqIL-1β and control group means were compared at each of the three time points using Student's t-tests (α=0.05).

Prostaglandin E_2 synthesis

Prostaglandin E_2 (PGE_2) release to the culture media at 1, 3, and 6 hours after treatment was evaluated using a competitive binding enzyme immunoassay (Amersham, Piscataway NJ). Media samples (50ul) were added to provided 3,3',5,5' tetramethylbenzidine / hydrogen peroxide in 20% (v/v) dimethylformamide (150 ul), and absorbance was determined (duplicate measures) within 30 minutes on a UV spectrophotometer (450 nm). A standard curve (50-6400 pg/ml PGE_2) was generated by plotting percent bound conjugated-PGE_2 as a function of PGE_2 concentration on a semi-logarithmic scale. Final sample PGE_2 concentrations (pg / ml) were deduced from the

standard curve. Equine IL-1β and control group means were compared at each of the three time points using Student's t-tests (α=0.05).

Collagen analysis

Protein fractions precipitated from organic layers of Trizol™ solubilized monolayers were subjected to digestions with pepsin at 4°C for 16 hours (1 mg/ml) (Sigma-Aldrich Corporation, St. Louis, MO) and pancreatic elastase at 35°C for 30 minutes (1 mg/ml) (Worthington Biochemical Corporation, Lakewood, NJ). Protein digests were analyzed by enzyme-linked immunoassay at 490 nm relative to a purified equine standard curve for type II collagen (0-0.2 ug/ml) (Capture ELISA kit, Chondrex Inc, Redmond WA). Duplicate measurements were averaged for each sample and control and EqIL-1β group means were compared at each of the three time points using Student's t-tests (α=0.05).

Statistical analysis

Signal intensities were log-transformed and normalized to the variables of horse and membrane (within a horse) using a two-stage mixed linear analysis of variance (ANOVA) (Wolfinger, *et al.*, 2001; Chu, *et al.*, 2002). Array data were analyzed with gene designated as fixed subplot effects and EqIL-1β and time treatments defined in the whole-plot sampling structure (Statistical Analysis Software, SAS Institute, Cary, NC). Pairwise gene comparisons were ordered using Bonferroni correction for multiplicity (α=0.05), and differences in means were depicted on a log base 2 scale in modified volcano plots. Mean signal intensities were calculated from two hybridization values normalized to the mean signal intensities of equine GAPDH. Appropriateness of GAPDH normalization was determined by assessing signal variation of house-keeping targets in control and EqIL-1β stimulated cultures, membranes, and horses. Possible bias in the hybridization system was addressed (*Appendix II.D.2 and Figure A6*).

In the effort to reduce the multivariate dimensionality of the data and to explore potential co-regulated gene expression levels, principal component analysis (PCA) was

conducted (Timm, 2002) (PROC PRINCOMP, Statistical Analysis Software, SAS Institute, Cary, NC). Principal component score means from the three horses and the three time points, as well as the 6-hour time point means alone, were compared using an ANOVA (α=0.05).

4.D. Results

cDNA array data analysis

The levels of mRNA corresponding to seven genes were significantly greater in the EqIL-1β treated groups relative to controls at 6 hours: cullin 4B (CUL4B) (AF513243), ferritin (FERR) (AY112742), MMP-13 (AF034087), intermediate early response-2 (IER-2) (AA038052), transforming growth factor beta 2 (TGFβ2) (AI323791), TNF receptor-associated factor-1 (TRAF-1) (AA183167), and an expressed sequence tag (AY246802) **(Figure 4.1)**. Signal intensities for an additional 102 cDNA targets changed > 2-fold at 6 hours; however, these changes were not significant **(Table 4.1)**. Significant differences in signal intensities were not detected at the 1-hour exposure, although one target corresponding to an expressed sequence tag, EST82 (AY246844), was increased in the EqIL-1β group relative to controls (+ 2.01-fold). After 3 hours of EqIL-1β stimulation, two transcript levels were increased relative to controls: MMP-13 (+ 2.53-fold) and serum amyloid A (+ 2.04-fold) (AY246757), but these effects were not significant. Baseline log-transformed signal intensities for MMP-13 were slightly higher than those for MMP-1 in both control and EqIL-1β groups over the three time points (p=0.035) **(Figure 4.2a)**.

PCA

Five components were shown to represent ~ 88% of the total variation (data not shown). The third component reflected ~10% of the variation, and a significant EqIL-1β induced increase in principal component scores relative to controls across the three horses was detected (p=0.0179). Identification of the ten most positively and negatively correlated cDNAs suggested this component to reflect co-regulated transcription of cell-

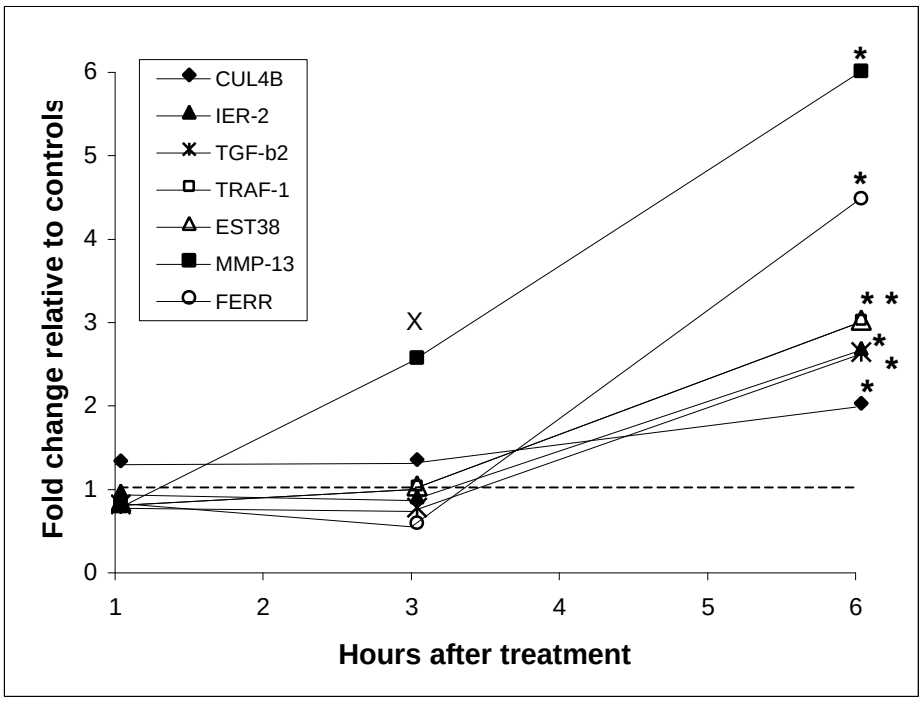

Figure 4.1 - ANOVA results at 1, 3, and 6 hours.

Data represent mean fold change in signal intensity in response to EqIL-1β. * denotes significance at $p<0.05$ relative to controls. ^{X} denotes a non-significant > 2-fold change relative to controls. Dotted reference line corresponds to approximate control signal intensities.

Table 4.1 - EqIL-1β induced mRNA levels > 2-fold over controls (6 hours).

cDNA	Genbank	Fold change	p-value
Serum amyloid A (SAA)	AY246757	4.01	0.0013
Cyclin D2 (CcnD2)	W98440	3.38	0.0007
EST72	AY246836	3.24	0.0002
EST53	AY246817	2.70	0.0284
Protein kinase C delta (PKCd)	AA616214	2.64	0.0004
Transmembrane protein (TMP)	Not available	2.63	0.004
Nuclear factor kappa beta-1, p105 (NFKB-1)	AA276822	2.61	0.0002
EST37	AY246801	2.59	0.0347
Guanine nucleotide binding protein	AY246708	2.57	0.0038
Fibroblast growth factor receptor I (FGFRI)	AY246707	2.55	0.0083
EST3	AY246767	2.55	0.024
Cadherin-2 (Cad2)	AA242226	2.54	0.0008
Pre-mRNA processing 8 (Prp8)	Not available	2.54	0.0176
Caspase 7	AI131763	2.53	0.0007
EST19	AY246783	2.53	0.0457
Platelet derived growth factor A (PDGFA)	AI583995	2.52	0.0139
Cyclin B1- G2/M specific (CcnB1)	AA396324	2.51	0.0024
EST22	AY246786	2.51	<.0001
EST59	AY246823	2.51	0.0085
EST5	AY246769	2.47	0.0372
EST35	AY246799	2.47	0.0919
BCL-2 antagonist of cell death (BAD)	BF117194	2.46	0.0002
Retinoid X-receptor alpha (rxya)	AA209592	2.46	0.0002
p53	AA896672	2.44	<.0001
Major histocompatibility complex I (MHCI)	Not available	2.43	0.0006
EST18	AY246782	2.43	0.1208
Nucleolin (NCL)	AY246725	2.42	0.0335
Wildtype p53 activated fragment 1 (p21)	AA792520	2.41	0.0005
Protein phosphatase type IB, beta isoform (PP1B)	Not available	2.41	0.1401
Caspase 11	AI0212244	2.40	0.0004
c-rel protooncogene	AI247359	2.39	0.0002
Prostaglandin D synthase (PGDS)	AI323558	2.37	0.0074
Protein kinase C alpha (PKCa)	AI894239	2.37	0.0008
Growth arrest specific protein (GAS)	AA087048	2.36	0.0025
EST2	AY246766	2.35	0.0341
EST62	AY246826	2.34	0.0024
Ras homolog gene family, member A (A-ras)	Not available	2.33	0.1756
EST20	AY246784	2.33	0.1195
Matrix metalloproteinase-3 (MMP-3)	U62529	2.32	0.0096
Interleukin-12, p40 subunit (IL-12-40)	AA267353	2.32	0.0031
Elongation factor 1 alpha (EF1a)	AY246720	2.32	0.0177
Pibosomal protein L41 (RPL41)	AY246729	2.31	0.0254
EST30	AY246794	2.30	0.0028
Integrin beta 1 (Ib1)	AA23903	2.29	<.0001
EST34	AY246798	2.29	0.1657
Granulocyte chemotactic protein-2 (GCP2)	AY114351	2.28	0.0112
EST21	AY246785	2.28	0.0357
Glia maturation factor B (GMFB)	Not available	2.27	0.0534
Folate binding protein-2 (Fol2)	AA015571	2.26	0.0002
Fibronectin (FN1)	AA275041	2.25	<.0001
Bone morphogenetic protein-4 (BMP-4)	AA473799	2.23	0.0002

Table 4.1 (cont) – EqIL-1β induced mRNA levels > 2-fold over controls (6 hours).

cDNA	Genbank	Fold change	p-value
Growth arrest specific protein-2 (GAS-2)	AA423395	2.23	0.0107
Proteosome subunit, alpha type 4 (PSMA4)	Not available	2.23	0.0415
EST46	AY246810	2.23	0.0048
Zinc finger protein (ZFP)	AY246739	2.21	0.0427
EST4	AY246768	2.21	0.0758
EST36	AY246800	2.20	0.0747
Cell division cycle control protein 2a (cdc2a)	AA035888	2.19	0.0028
EST54	AY246818	2.19	0.0097
EST51	AY246815	2.18	0.1955
EST82	AY246844	2.17	0.1007
EST41	AY246805	2.17	0.0145
EST50	AY246814	2.17	0.1895
Matrix metalloproteinase-1 (MMP-1)	AY246754 - AY246756	2.16	0.0361
c-abl	AW209918	2.16	0.0405
N-myc/STAT interactor	AY246724	2.16	0.0104
EST63	AY246827	2.16	0.0291
Interleukin-12, p35 subunit (IL-12-35)	AI050362	2.15	0.0053
Glutathione peroxidase, plasma isoform (GPx-3)	AY246750	2.15	0.0073
EST67	AY246831	2.15	0.1855
Cyclin G (CcnG)	AA067318	2.13	0.0051
Platelet derived growth factor B (PDGFB)	AA162467	2.13	0.0038
Liprin	Not available	2.13	0.084
Cadherin-3 (Cad3)	W12889	2.12	0.0035
Dihydrofolate reductase (DHFR)	AA920415	2.12	0.0004
Fibroblast growth factor-1 (FGF-1)	AA261582	2.12	0.0025
Folate binding protein-1 (Fol1)	AA139715	2.12	0.011
Growth differentiation factor-1 (GDF-1)	W65054	2.12	0.0033
LPS induced TNF alpha factor (LITAF)	AF503366	2.11	0.0023
r-ras	AA32641	2.11	0.0006
Manganese superoxide dismutase (Mn-SOD)	AY246751 - AY246753	2.11	0.0297
EST70	AY246834	2.11	0.0604
Zinc finger protein 216 (ZNP216)	Not available	2.09	0.0413
G-protein regulator	Not available	2.08	0.2187
Nitric oxide synthase-3 (Nos-3)	AA177420	2.07	0.0421
Early growth response 2 (Egr-2)	AA727313	2.06	0.0354
TNF receptor-associated factor 2a (TRAF2A)	AA165848	2.06	0.0005
Integrin beta 2 (Ib2)	AA467489	2.05	0.0025
Indian hedgehog protein (Ihh)	AA245525	2.05	0.0037
Seven in absentia homolog (Siah-2)	AY246715	2.05	0.1625
EST55	AY246819	2.05	0.0348
Selenoprotein P (SEPP1)	Not available	2.04	0.0964
Osteoclast stimulating factor (OSF)	Not available	2.04	0.0291
Insulin-like growth factor binding protein-5 (IGFBP-5)	Not available	2.03	0.012
Annexin V (AA5)	AA002439	2.03	0.0019
Interleukin-15 (IL-15)	AA862763	2.03	0.0023
WW domain binding protein 11 (SNP70)	AY246738	2.03	0.0175
p21/H-ras-1 transforming protein	AI116111	2.02	0.0071
Platelet activating factor acetylhydrolase (PAFA)	Not available	2.02	0.0628
BTAF1 RNA polymerase II	Not available	2.01	0.1553
Vesicle associated membrane protein, A (VAMPA)	Not available	2.01	0.0865
EST64	AY246828	2.01	0.0472

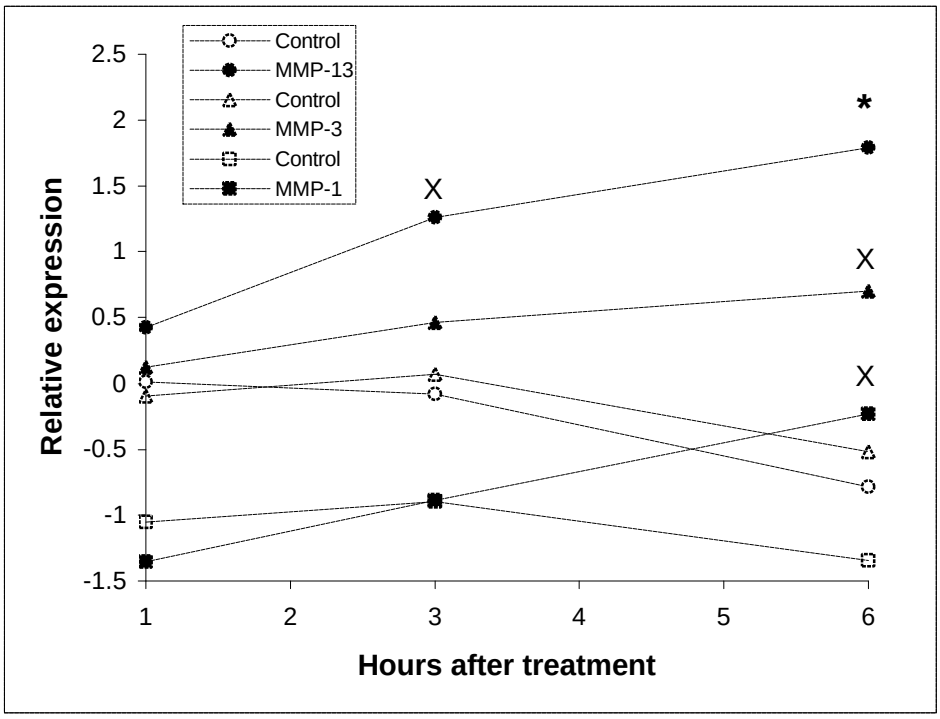

Figure 4.2a - Relative matrix metalloproteinase (MMP) mRNA levels.

Data represent means of log-transformed, GAPDH normalized signal intensities for control (open symbols) relative to EqIL-1β treated groups (closed symbols) for MMP-13 (circle), MMP-3 (triangle), and MMP-1 (square) at each 1, 3, and 6 hour time points. * denotes significance at $p<0.05$. ^{X} denotes a non-significant > 2-fold change.

cycle arrest regulatory proteins **(Table 4.2)**. Similar PCA and ANOVA analysis on the 6-hour data alone resulted in the identification of the same component and loading genes (not shown).

RT-PCR

Significantly increased transcript levels were detected for MMP-1 and MMP-13 (at 6 hours), MMP-3 (at 3 and 6 hours), BMP-4 (at 6 hours), and ferritin (at 6 hours) in EqIL-1β treated groups relative to media controls **(Figures 4.2b, 4.3)**. Non-significant increases in EqIL-1β stimulated mRNA levels corresponding to OSF and MHCI were detected by RT-PCR **(Figure 4.3)**. Significant differences were not observed between amplified mRNA levels in EqIL-1β treated and untreated control chondrocytes for type I collagen, A1 chain and type I collagen, A2 chain at each of the three time points (data not shown). Type II collagen was not detected by RT-PCR after 40 cycles of amplification in control or EqIL-1 treated groups over all time points (data not shown).

Glycosaminoglycan release

Significant differences in GAG concentrations were not detected in culture media harvested from EqIL-1β stimulated chondrocytes relative to media treated controls at each of the 1, 3, and 6-hour time points (data not shown). In addition, no differences in GAG release were detected between the three time points.

PGE_2 release

A time-dependent increase in PGE_2 concentrations was detected in the culture media of the EqIL-1β groups relative to control groups at the 3 and 6-hour evaluations, but not at the 1-hour evaluation **(Figure 4.4)**.

Collagen quantification

Significant differences in concentrations of type II collagen epitopes were not detected in control versus EqIL-1β groups after 1 and 3 hours of exposure. However,

Table 4.2 - Ten most positively and negatively loading cDNAs on principal component 3 (PC3).

cDNA	Genbank	PC3 correlation	Fold change
p53	AA896672	0.12187	2.44
Transforming growth factor beta 2 (TGFβ2)	AI323791	0.11134	2.60
Indian hedgehog protein (Ihh)	AA245525	0.11035	2.05
Caspase 6	AA914450	0.10908	1.79
Retinoblastoma 1 (Rb1)	AA427019	0.10877	1.81
Mitochondrial ribosomal protein Rnase	Not available	0.10855	1.72
Rho-A transforming protein	AA162923	0.1063	1.81
p21	AA792520	0.10562	2.41
Protein kinase C, delta subunit (PKCδ)	AA616214	0.10482	2.64
Interleukin-9 receptor	AA106013	0.10456	2.00
Dermatopontin (DPT)	Not available	-0.10535	-1.25
EST15	AY246779	-0.09235	-1.71
EST16	AY246780	-0.08909	-1.50
PCTAIRE protein kinase 1	AY246710	-0.08772	-1.18
EST14	AY246778	-0.08673	-1.93
EST31	AY246795	-0.08671	-1.65
Tumor associated calcium signal transducer	Not available	-0.08643	-0.75
EST33	AY246797	-0.08605	-1.55
Tumor rejection antigen (gp96)	AY246760	-0.08393	-1.44
EST27	AY246791	-0.08367	-1.02

Fold changes represent original log-transformed signal intensity EqIL-1β group means relative to control group means at 6 hours.

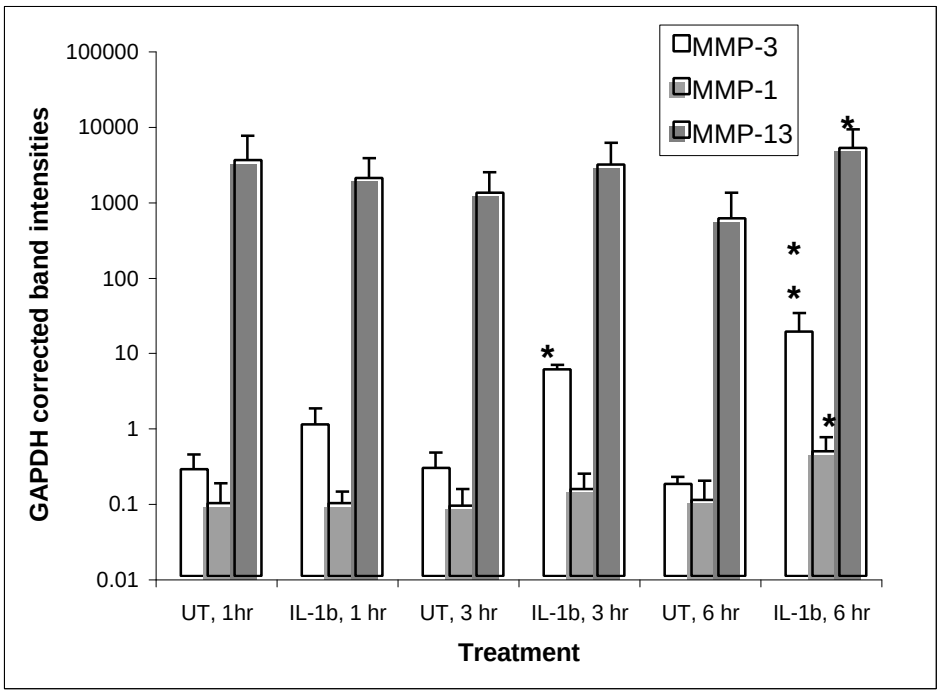

Figure 4.2b - RT-PCR analysis of MMP mRNA levels.

Data represent log-transformed, GAPDH normalized amplified intensities and standard deviations for untreated (UT) compared to EqIL-1β treated chondrocytes at 1, 3, and 6-hour time points. * denotes significance, $p<0.05$. ** denotes significance, $p<0.001$.

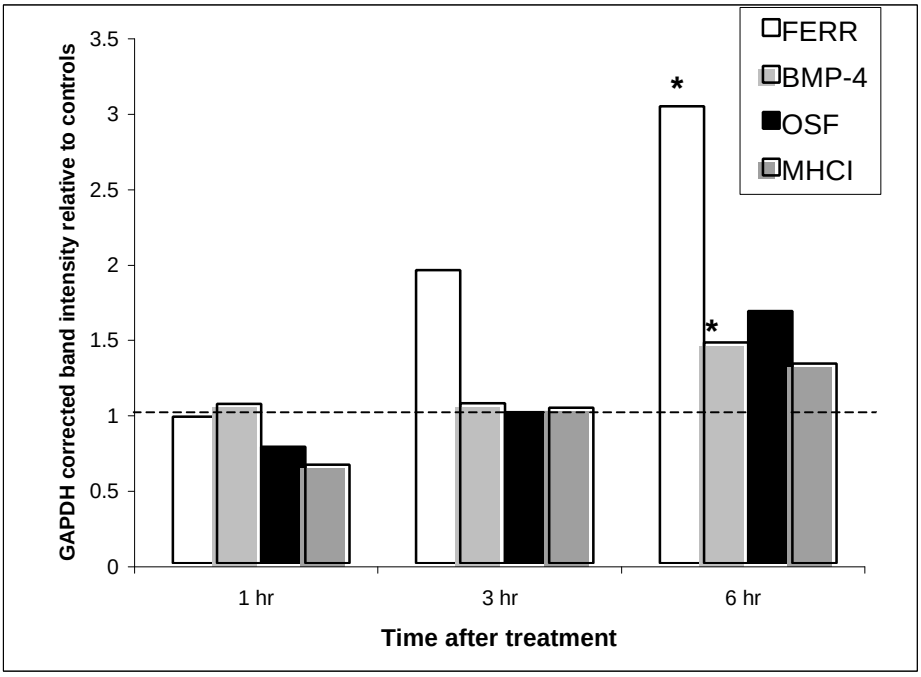

Figure 4.3 - RT-PCR analysis of selected transcripts increased in response to EqIL-1β as detected by cDNA array analysis.

Data represent GAPDH normalized amplified intensities of EqIL-1β relative to media treated controls. * denotes significance, $p<0.05$. Dotted reference line corresponds to approximate amplified intensities of controls.

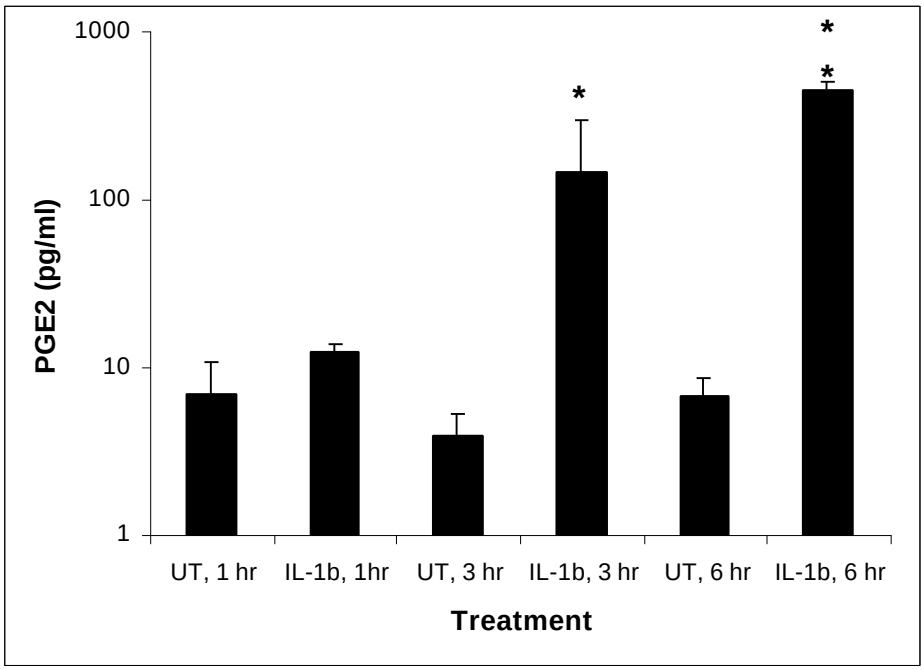

Figure 4.4 - PGE_2 concentrations in culture media at 1, 3, and 6 hours.

Data represent means and standard deviations from duplicate readings for untreated (UT) controls compared to EqIL-1β stimulated chondrocytes at each of the 1, 3, and 6-hour time points. * denotes significance at $p<0.05$. ** denotes significance at $p<0.001$.

type II collagen concentrations were decreased in the EqIL-1β group at 6 hours **(Figure 4.5)**.

4.E. Discussion

The temporal effects of EqIL-1β on steady state mRNA levels in monolayer cultured equine articular chondrocytes was visually apparent by plotting the data relative to untreated controls over time in modified volcano plots **(Figure 4.6)**. Significant differences were not apparent at 1 and 3 hours, suggesting that a 6-hour minimum EqIL-1β stimulation (at 1.0 ng/ml) may be required for the detection of altered mRNA levels using the described targeted cDNA array and chondrocyte culture methodologies. Thus, the most proximal effects of exogenous EqIL-1β on chondrocyte gene expression levels were likely represented, satisfying the primary objectives of this study.

Increased MMP-1, -3, and -13 mRNA levels, in conjunction with unaltered mRNA levels for TIMP-1 and TIMP-2 (data not shown), may reflect EqIL-1β induced changes in transcription associated with protease imbalances and de-regulated ECM catabolism in disease (Dean, *et al.*, 1989; Richardson and Dodge, 2000). The finding that EqIL-1β increased mRNA levels for MMP-1, MMP-3, and MMP-13 agrees with reports describing human IL-1β stimulated MMP expression in cultured chondrocytes (Caron, *et al.*, 1996; Flannery, *et al.*, 1999a; Richardson and Dodge, 2000). The lower steady-state mRNA levels for MMP-1 relative to MMP-13 **(Figure 4.2a, 4.2b)** are consistent with low basal transcript levels reported for MMP-1 in osteoarthritic chondrocytes (Tardif, *et al.*, 1999).

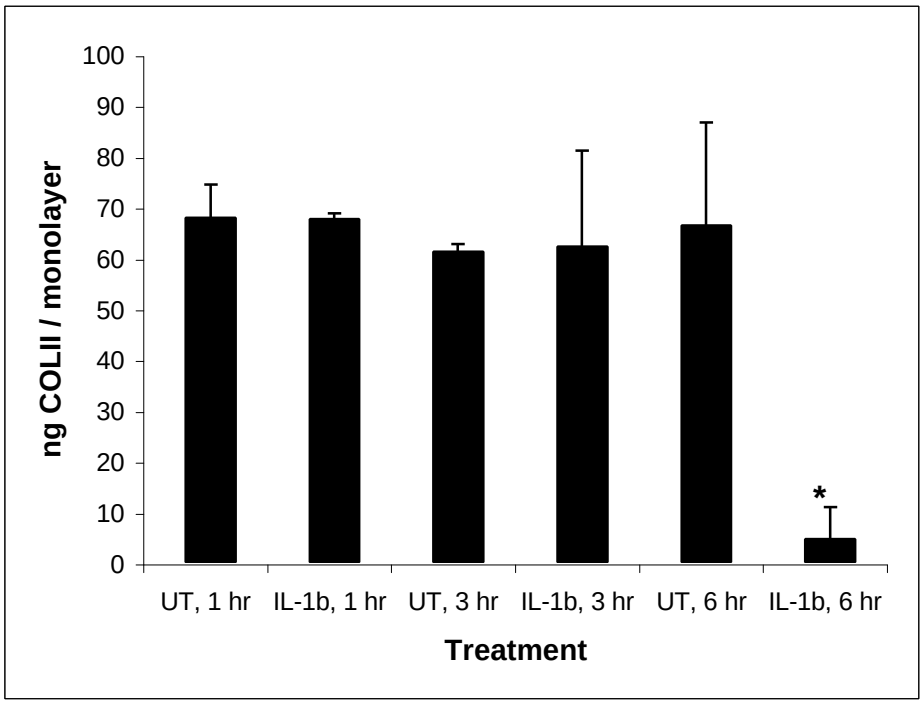

Figure 4.5 - ELISA results for type II collagen in chondrocyte monolayers.

Data represent means and standard deviations of duplicate measurements of untreated (UT) controls relative to EqIL-1β treated cells at each of the 1, 3, and 6-hour time points. * denotes significance, $p<0.05$.

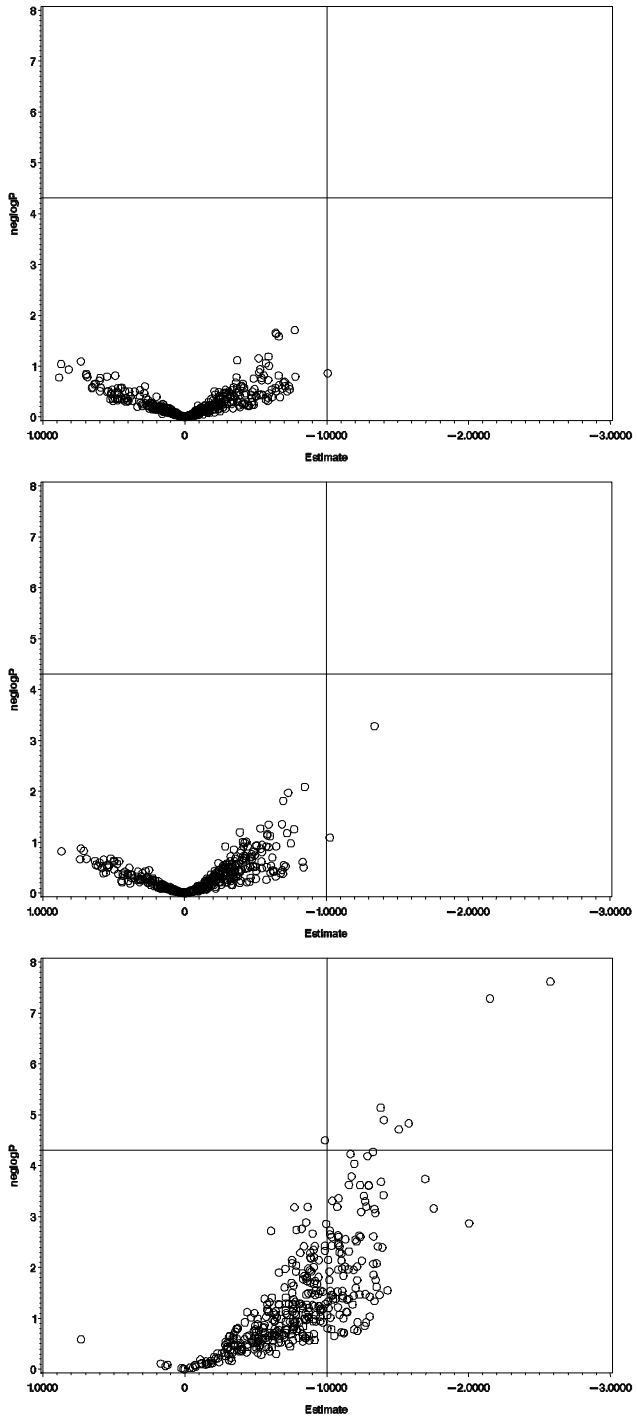

Figure 4.6 - Volcano plots for EqIL-1β induced mRNA levels over time.

Log-transformed EqIL-1β treated mRNA levels relative to controls after 1 (upper panel), 3 (middle panel), and 6 (lower panel) hours. Negative x-axes values correspond to decreased mRNA levels, positive values correspond to increased mRNA levels; a one-unit difference corresponds to an approximate 2-fold difference. Y-axes reflect p-values (negative log base 10). Significance is denoted by horizontal line at p=0.00004.

Unique roles of MMP-1 in ECM catabolism during inflammation, and MMP-13 in the remodeling phases of joint disease have been proposed (Tardif, *et al.*, 1999). Variations in MMP-1/MMP-13 articular cartilage topographic distributions and promoter site sequences have been suggested (Moldovan, *et al.*, 1997; Tardif, *et al.*, 1999; Mengshol, *et al.*, 2000). In addition, transcriptional regulation by distinct TGFβ isoforms has been reported (i.e. TGFβ2 induced MMP-13, and TGFβ1 induced MMP-1 synthesis) (Tardif, *et al.*, 1999). Thus, the significant increases of TGFβ2 and MMP-13 mRNA levels in our study may support the existence of a mechanism for greater increased transcript levels detected for MMP-13 at 6 hours (Tardif, *et al.*, 1999).

Principal component analysis is a mathematical means to detect coordinated patterns in gene expression in large multivariate data, while accounting for the majority of internal variability. The majority of the ten most positively correlated genes on the third described component are suggested to contribute to cell-cycle regulation **(Table 4.2)**. p53 is a well-defined tumor suppressor gene which can activate transcription of the cyclin/cyclin-dependent kinase inhibitor p21 to block G1 to S cell-cycle transitions. Upon extensive DNA damage, p53 effects are linked to apoptosis cascade events. The unphosphorylated retinoblastoma (Rb) protein is important for regulated inhibition of G1 to S cell-cycle transitions. Mutations within p53 and Rb are linked to a range of cancers. Thus, the co-expression of p53, p21, Rb, together with caspase 6, may suggest a chondrocytic mechanism for cell-cycle arrest and apoptotic cascade activation induced byEqIL-1β. Co-expression of TGFβ2 within this component may reflect a growth factor mediated suppression of exogenous IL-1 induced proliferation in passaged, de-differentiated chondrocytes (Guerne, *et al.*, 1994), and growth stimulatory processes proposed after a 1-hour exposure to EqIL-1β (at 10 ng/ml) (*refer to Chapter III*). Of the ten most negatively correlated genes loading on the identified component, two correspond to tumor-associated proteins and might suggest a de-regulation of cell-cycle entry **(Table 4.2)**. Identification of this principal component using input data from all three time points, as well as the filtered time 6-hour data (not shown), together reinforce

the likelihood of this component to describe co-regulated gene expression induced by EqIL-1β in this study.

IL-1 signaling is complex and likely involves multiple cis regulatory and trans acting factors in the transduction pathways involved in specific gene transcriptional activation (O'Neill, 1995). The significant increase in immediate early response-2 (IER-2) transcript levels relative to untreated controls may be the first indication of the role of this transcription factor in chondrocyte signaling **(Figure 4.1)**. Significant increases in TNF receptor associated factor -1 (TRAF-1) transcript levels support a role for this group of adaptor proteins in IL-1/Toll-receptor associated signaling **(Figure 4.1)** (Chung, *et al.*, 2002). Further evidence for MAP kinase, NFKB, tyrosine kinase, and G-protein involvement in IL-1β signaling is provided by the greater than 2-fold increase in transcript levels after 6 hours **(Table 4.1)** (Lotz, 2001). Increased protein kinase C transcript levels at 6 hours may indicate downstream stimulation by increased PGE_2 levels released to the culture media as early as 3 hours after EqIL-1β treatment **(Figure 4.4)**.

EqIL-1β stimulated > 2-fold increases in mRNA levels corresponding to growth factors and anti-inflammatory related genes after 6 hours **(Table 4.1)**, which may suggest chondrocytic induction of specific ECM anabolic processes to counteract increased MMP-mediated ECM degradation. The significant increase in TGFβ2 transcript levels at 6 hours **(Figure 4.1)** may reflect growth factor mediated ECM protection and anabolic effects (van Beuningen, *et al.*, 1993). Increased expression levels for manganese superoxide dismutase, glutathione peroxidase, and fibroblast growth factor receptor I, directly correlate with increased transcript levels detected in EqIL-1β stimulated synovium after 6 hours (*refer to Chapter V*). Reduced responsiveness of osteoarthritic cartilage to the ECM protective effects of insulin-like growth factor-1 (IGF-1) has been suggested to result from increased IGF binding protein synthesis rather than reduced receptor levels (Martel-Pelletier, *et al.*, 1998). Thus, increased insulin-like growth factor

binding protein-5 (IGFBP-5) transcript levels may suggest a mechanism for modulated responses of IL-1 exposed chondrocytes to the ECM anabolic effects of IGFs (Sunic, *et al.*, 1998).

Significant decreases in type II collagen concentrations **(Figure 4.5)** and increases in PGE_2 levels **(Figure 4.4)** demonstrate the stimulatory effects of EqIL-1β on ECM catabolism and inflammatory cascades. The lack of significant difference between EqIL-1β induced GAG release relative to controls was likely due to the complex nature of IL-1 influenced proteoglycan metabolism in passaged chondrocytes over the observed culture periods (Richardson and Dodge, 2000). The duration of culture was possibly not long enough to observe the translation, activation, and proteolytic processes corresponding to the increased MMP mRNA levels detected at 6 hours. In addition, IL-1 has been shown to both induce GAG degradation and inhibit GAG synthesis in cartilage (Tyler, 1985; Platt and Bayliss, 1994). It was shown that newly synthesized non-collagenous proteins were directly released to the media instead of being incorporated into the small amount of existing pericellular ECM between cells in monolayer culture (Lefebvre, *et al.*, 1990a, b). Thus, the combination of slightly decreased GAG production and slightly increased GAG release possibly negated detectable differences in levels in media harvested across the evaluated treatments and time points.

In this study, a targeted cDNA array analysis was used for the parallel evaluation of changes in chondrocyte steady state mRNA levels induced by EqIL-1β over time. These results, in conjunction with RT-PCR verification, may suggest MMP-1, -3, -13, and ferritin heavy chain (an iron metabolic-related protein), as possible transcriptional markers for elevated EqIL-1 activity in chondrocytes. Results also indicate a number of cDNA expressed sequence tags may be involved in EqIL-1β / chondrocyte biology. Future studies are necessary to elucidate their identity or biological function. In addition, these results specify increased mRNA levels of growth factors and free radical oxidative scavenging systems in normal, non-diseased chondrocytes that may contribute to the

regulation of exogenous EqIL-1β. These genes may warrant further investigation into their potential application in anti-inflammatory therapy of naturally occurring joint disease.

4.F. Acknowledgements

The authors thank Dean W. Richardson, DVM, University of Pennsylvania School of Veterinary Medicine, Kennett Square, PA for donation of equine MMP-1, MMP-3, and MMP-13 cDNAs. We also thank Ms. Kristi L. Seat for technical assistance.

CHAPTER V: Differential gene expression in an equine interleukin-1b induced model of synovitis

5.A. Abstract

Steady-state mRNA levels in equine synovium resulting from an exposure to recombinant equine interleukin-1β (EqIL-1β) were profiled using suppression subtractive hybridization polymerase chain reaction (SSH-PCR). Equine IL-1β (100 ng) was injected into the middle carpal joint space of an 18-month old horse clinically free of joint disease. Synovium was collected from the injected and the contralateral un-injected joints after 6 hours. Messenger RNA (~ 400 ng) was isolated and reverse transcribed (PCR-Select^{TM} cDNA Subtraction Kit, CLONTECH, CA). Double-stranded cDNA was enzymatically digested and sequential hybridizations of cDNAs derived from EqIL-1β injected and un-injected synovium were conducted, followed by two PCR cycles for enrichment of differentially expressed transcripts. Fifty-seven genes with homology to existing nucleotide sequences and 91 novel expressed sequence tags were identified (Genbank AY246701-246855). Results were verified and SSH-PCR efficiency assessed using a combination of cDNA array hybridization and semi-quantitative RT-PCR. Our data support the hypothesis that IL-1 may play an important role in the pathogenesis of joint disease and suggests this *in-vivo* IL-1β induced model of acute synovitis may be useful in the study of equine joint disease and inflammatory joint diseases in humans.

5.B. Background

Synovitis is a common cause of lameness in horses that if persistent, may precipitate the initial biochemical and morphological changes associated with osteoarthritis (OA). Some degree of synovitis is associated with all stages of OA and other joint diseases in horses (McIlwraith, 1996). Synovial tissues are subjected to a variety of biomechanical and biochemical stimuli that influence the metabolism of

synovial fibroblasts; these stimuli, when excessive or imbalanced, may play important roles in joint disease pathophysiology (Evans, 1992; McIlwraith, 1996). Activated synovial fibroblasts stimulate articular cartilage chondrocytes to secrete cytokines, soluble pro-inflammatory mediators and matrix metalloproteinases (MMPs) that degrade collagen and proteoglycan structures of articular cartilage and synovial tissues. Synovitis is accompanied by hypertrophy of the synovial intima and subintima, invasion by stimulated leukocytes; these cells assist in perpetuation of the inflammatory response by secreting lysosomal enzymes and oxygen radicals, and mediating immune-regulated responses (McIlwraith, 1996; Hardy, *et al.*, 1998a).

Interleukin-1 (IL-1) is a cytokine that has been repeatedly implicated in initiation of inflammation and tissue destruction associated with joint disease in man and animals (McIlwraith, 1987; Dinarello, 1996; Platt, 1996). IL-1 promotes catabolism of extracellular matrix (ECM) components of articular cartilage and other joint connective tissues by induction of reactive oxygen species, MMPs, and serine and cysteine proteases, while also inhibiting new ECM synthesis and local tissue repair. The reported effects of IL-1 suggest this cytokine to contribute to the regulation of acute and chronic inflammation in joints, in part, through its effect on synovial fibroblasts, articular chondrocytes, and activated macrophages and T cells (Wood, *et al.*, 1985; Platt, 1996; Fernandes, *et al.*, 2002).

The objective of this study was to profile changes in mRNA levels in equine synovium resulting from a recombinant equine interleukin-1β (EqIL-1β) stimulation as an *in-vivo* model of an acute synovitis. This was accomplished using suppression subtractive hybridization polymerase chain reaction (SSH-PCR), a robust means to identify differential transcripts unique to an affected tissue (Diatchenko, *et al.*, 1996; Gurskaya, *et al.*, 1996; Tkatchenko, *et al.*, 2000). Messenger RNAs common to treated ('tester') and reference untreated ('driver') populations are first removed via a series of cDNA hybridizations. Unique cDNAs are exponentially enriched and non-specific

amplification is suppressed by PCR methods. Enrichment is proposed to exceed 1000-fold following one round of hybridization, providing advantages to traditional representational differential analysis methodologies and enabling the retrieval of both rare and highly abundant differentially expressed transcripts on a high-throughput scale (Diatchenko, *et al.*, 1996). These efforts have resulted in the generation of a battery of equine cDNAs that may facilitate further array-based investigations for improved diagnoses and treatments for OA and may have important implications for the study of joint disease in horses and humans.

5.C. Materials and Methods

IL-1 injection and tissue collection

The right middle carpal joint of an 18-month old gelding was aseptically prepared and injected with 100 ng of rEqIL-1β dissolved in phosphate buffered saline (1 ml); the protein had been previously expressed, purified, and characterized in our laboratory (Howard, *et al.*, 1998a; Takafuji, *et al.*, 2002). The horse was donated to the VA-MD Regional College of Veterinary Medicine, Blacksburg, VA for reasons unrelated to joint disease. Six hours after injection of EqIL-1β, the horse was evaluated for clinical evidence of acute synovitis and anesthesized using a combination of intraveneously administered xylazine HCl, ketamine, and guaifenesin. Synovium was sharply excised from both middle carpal joints prior to euthanasia by lethal injection of sodium pentobarbital. The tissues (~ 2 grams wet weight) were flash-frozen in liquid nitrogen, pulverized using a cooled mortar and pestle, and stored in Trizol™ (Invitrogen Corporation, Carlsbad CA) at -70°C. Synovial fluid was collected from the injected joint for routine analysis.

Suppression subtractive hybridization

Subtractive hybridization was conducted in forward and reverse orientations to detect transcripts unique to the EqIL-1β injected (synovium forward = 'SF') and the uninjected (synovium reverse = 'SR') tissues. Isolated mRNA fractions (400 ng)

(Nucleotrap™ mRNA isolation kit, CLONTECH Laboratories Inc, Palo Alto CA) were added to oligo d(T) primed reverse transcription and second strand cDNA synthesis reactions (PCR-Select cDNA Subtraction Kit, CLONTECH Laboratories Inc, Palo Alto CA). Double-stranded cDNA samples were subjected to restriction enzyme digestion (RsaI) at 37°C for 16 hours. Adapter nucleotide sequences were separately ligated to EqIL-1β injected and uninjected tissue cDNAs for subtractive hybridization in the two orientations. Denatured ligated tester cDNAs were hybridized to denatured unligated driver cDNAs at 68°C for 24 hours; the second hybridization involved the addition of denatured driver and incubation at 68°C for 16 hours.

PCR amplification

Unique cDNAs were amplified using a high-fidelity Taq DNA polymerase (50X Advantage™ cDNA Polymerase Mix, CLONTECH Laboratories Inc, Palo Alto CA) and primers complementing adaptor sequences (10 uM) (30 cycles of: 94°C for 1 minute, 66°C for 1 minute, 72°C for 2 minutes, final extension at 68°C for 5 minutes). A second amplification was conducted using nested primer pairs (10 uM) (15 cycles of: 94°C for 1 minute, 66°C for 1 minute, 72°C for 2 minutes, final extension at 68°C for 5 minutes). Aliquots of secondary PCR reactions were cloned into linearized pCR2.1-TOPO vector (Invitrogen Corporation, Carlsbad CA) at 25°C for 30 minutes. Competent *E.Coli* TOP10 cells were transformed and plated onto Luria bertani agar supplemented with ampicillin (100 ug/ml) and X-Gal (100 ug/ml) at 37°C.

Clone processing

White colonies were cultured in 96-well microtiter plates in terrific broth (150 ul) with ampicillin (100 ug/ml) at 37°C for 16 hours and transferred to nylon membranes (Hybond™-N, Amersham Pharmacia Biotech, Piscataway NJ) using a library copier (V&P Scientific, San Diego CA). Bacteria were grown on membranes on agar / ampicllin / X-gal plates at 37°C for 16 hours. The membrane-bound cells were lysed, and cDNA denatured (0.5 M NaOH/1.5 M NaCl, 10 minutes), neutralized (1 M Tris-

Cl/1.5 M NaCl, pH 7.2, 5 minutes), and rinsed (2X SSPE, 10 minutes) using previously reported methods (Tkatchenko, *et al.*, 2000). Membranes were treated with proteinase K (250 ug/ml) at 37° for 3 hours, individually rinsed (5X SSC/0.5% SDS, 25°C), air-dried, and UV crosslinked (70,000 uJ/cm^2). Membranes were washed with shaking (5X SSC/0.5% SDS, 50°C for 30 minutes) and (0.1X SSC/0.5 % SDS, 50°C for 30 minutes), and allowed to air dry.

Differential hybridization screening

Hybridization probes were generated by random-primed labeling of forward and reverse subtracted cDNA libraries ('SF' and 'SR') (Prime-a-gene® labeling system, Promega Corporation, Madison WI) with incorporation of ^{32}P-labeled dATP (35 uCi, Redivue™, Amersham Pharmacia Biotech, Piscataway NJ). Bacterial colony membranes were hybridized with heat denatured (95°C, 5 minutes) labeled probes in 50% formamide, 0.12 M Na_2PO_4, 0.25 M NaCl, 7% SDS at 42°C for 16 hours, washed at 42°C (2X SSC/0.1% SDS for 30 minutes; 0.5X SSC/0.1% SDS for 30 minutes; 0.1X SSC/0.1% SDS for 30 minutes). Membranes were exposed to a phosphorimaging screen for 2 hours and digitized (Storm 820 phosphorimager, Amersham Pharmacia Biotech, Piscataway NJ). Clones displaying detectable signals after hybridization with the correctly oriented probe were transferred to new 96-well microtiter plates, fixed to nylon membranes, and subjected to a second round of hybridization, as previously described **(Figure 5.1)**. Clones passing the second round of screening were processed for nucleotide sequence determination.

Sequence analysis

Selected bacterial colonies were used to inoculate aliquots of terrific broth (2 mls) supplemented with ampicillin (100 ug/ml) and incubated at 37°C, 180 rpm for 16 hours. Plasmid DNA was isolated using alkaline lysis-based methods (Wizard™ Purification System, Promega Corporation, Madison WI). Single-pass sequence analysis was conducted using an upstream vector primer and ABI BigDye fluorescent-tagged

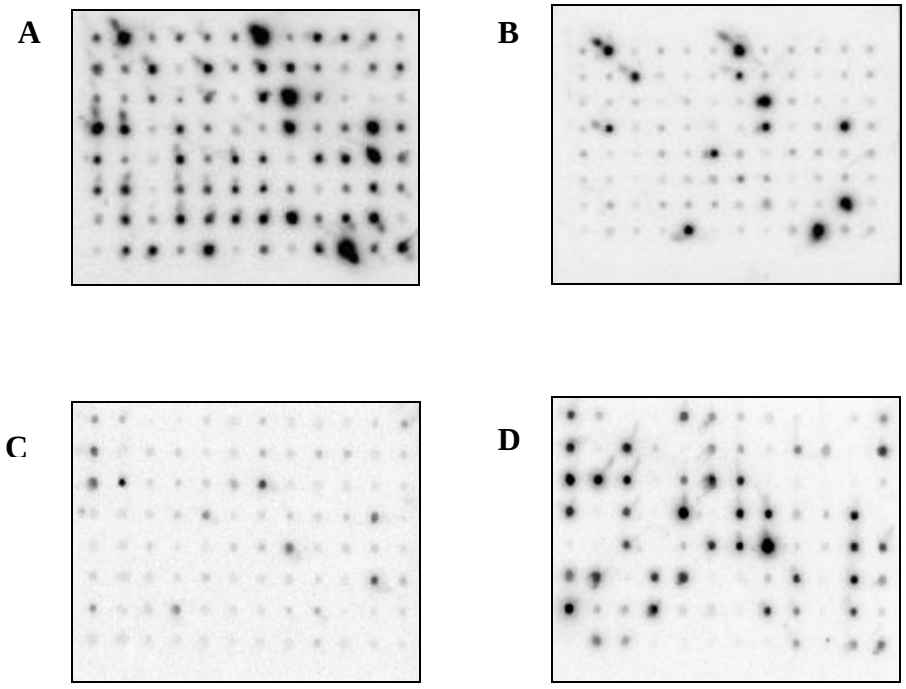

Figure 5.1 - Examples of hybridized 96-colony arrays.

EqIL-1β forward subtracted (A, B) and reverse subtracted (C, D) clones hybridized with subtracted cDNA labeled probes (A, C = Synovium Forward, 'SF'; B, D = Synovium Reverse, 'SR'). Clones displaying strong hybridization signals with the correct labeled probe were selected for the second round of screening. Target clones hybridizing with both probes were not further characterized.

chemistry (Virginia Bioinformatics Institute, DNA Sequencing Core Facility, Blacksburg, VA). Downstream vector primed sequence analysis was also conducted for cDNAs > 500 base pairs in length. Contiguous nucleotide sequences were identified (SeqMan, DNASTAR Inc, Madison WI), and data were aligned to nucleotide and translated protein sequence databases (BLAST, National Center for Biotechnology Institute, Rockville, MD). Repetitive elements and satellite clones were removed from further characterization.

Clone redundancy

Initial sequence analysis results indicated a high redundancy of cDNAs corresponding to collagenase-1 (MMP-1) in the forward subtracted cDNA library ('SF'). Clones corresponding to three non-overlapping segments of protein coding sequence were characterized: 372 bp (AY246754), 197 bp (AY246755), 333 bp (AY246756), corresponding to nucleotides 1622>1254, 1223>1098, and 765>1097 respectively, of equine MMP-1 (AF148882). The multiple clones were PCR-amplified, purified, equally combined by mass, and radiolabeled by methods described for array target probe generation (below). Bacterial clones displaying hybridization signals above the calculated mean for each membrane analyzed were not processed for sequence analysis (data not shown).

cDNA array analysis

a. Target printing

Differential expression observed by SSH-PCR was verified by cDNA array analysis. Identified cDNAs were amplified by PCR using vector-specific primers (0.4 uM), 2.0 mM $MgCl_2$, and Taq DNA polymerase (Promega Corporation, Madison WI) (2.5U) (initial denaturation 94°C for 5 minutes and 35 cycles of: 94°C for 1 minute, 57°C for 1.5 minutes, 72°C for 1.5 minutes, final extension at 72°C for 10 minutes). PCR products were purified by standard chloroform extractions and quantified by agarose gel electrophoresis / ethidium bromide visualization (Low mass™ DNA ladder, Invitrogen

Corporation, Carlsbad, CA). For the three instances where multiple non-overlapping clones corresponded to an individual gene, mixtures consisting of equivalent amplified masses of each respective cDNA were made. Target cDNAs (2.5 ng) were heat denatured (95°C for 10 minutes), transferred to positively charged nylon membranes (Hybond^{TM}-XL, Amersham Pharmacia Biotech, Piscataway NJ) using a library copier (V&P Scientific, San Diego CA), and UV cross-linked (70,000 ujoules/cm^2). Additional equine cDNA clones (72), compiled from donations and other cDNA library screening methods (not shown), and corresponding to genes with purported roles in inflammation and joint disease pathophysiology, were similarly arrayed.

b. Hybridization

Subtracted cDNA libraries ('SF' and 'SR') were random-primed labeled (Prime-a-gene® labeling system, Promega Corporation, Madison WI) (^{32}P-labeled dATP, 35 uCi, Redivue^{TM}, Amersham Pharmacia Biotech, Piscataway NJ). Arrays were pre-hybridized in 0.5M Na_2HPO_4, 7% SDS, 10mM EDTA, 100 ug/ml herring sperm DNA at 65°C for 1 hour. Labeled probes were heat denatured (95°C, 5 minutes) and added to the hybridization reactions at 65°C for 16 hours. Arrays were washed with increasing stringency: 2X SSC / 0.1% SDS at room temperature (2 X 5 minutes), 0.5X SSC / 0.1% SDS at 42°C (1 X 15 minutes), and 0.1X SSC / 0.1% SDS at 65°C (2 X 10 minutes). Data from two separate membranes were averaged following a 2-hour exposure to a phosphorimaging screen, as previously described. Data were adjusted for probe specific activities (50-75% radionuclide incorporation), and were presented as ratios of forward relative to reverse subtracted probe hybridization signals ('SF / SR') (refer to Table 5.2).

Reverse transcriptase-PCR

A subset of differentially expressed transcripts detected by cDNA array analysis, but not by SSH-PCR, was evaluated by reverse transcriptase-PCR (RT-PCR). Primers corresponding to partial coding regions for equine glyceraldehyde-3-phosphate dehydrogenase (GAPDH), β-actin, biglycan, ferritin, IL-1β, MMP-3, tissue inhibitor of

matrix metalloproteinase-1 (TIMP-1), and one gene isolated by SSH-PCR, equine MMP-1 (AY246754), were compiled (PrimerSelect, DNASTAR, Madison WI) (*refer to Appendix Table AVIII*). Aliquots (2.5 ul) of reverse transcribed RNA (4 ug) from EqIL-1β injected and uninjected synovium samples (Universal RiboClone® cDNA synthesis system, Promega Corporation, Madison WI) were added to PCR reactions consisting of gene-specific primers (0.4 uM), 50 mM KCl, 10 mM Tris-HCl, 0.2 mM dNTPs, and 2.5 U Taq polymerase (Eppendorf Scientific Inc, Westbury NY) (50 ul volumes). Optimal cycling numbers for each primer pair were determined with the addition of 0.1 uCi ^{32}P-dATP (Amersham Pharmacia Biotech, Piscataway NJ) and Cerenkov counting of amplified products at 20, 25, 30, and 35 cycles (Ko, 1995). Reaction mixtures were denatured at 95°C for 5 minutes, followed by optimal number of cycles: 95°C for 1 minute, 50-61°C for 1.5 minutes, 72°C for 1.5 minutes, and a final extension at 72°C for 10 minutes. Amplified products were detected on 1.5 % agarose gels by ethidium bromide staining, assessed densitometrically, and normalized to the signal for GAPDH (ImageJ 1.30v, National Institutes of Health, Bethesda MD).

5.D. Results

Clinical evaluation

Six hours post EqIL-1β injection, the horse displayed grade 2/5 lameness during subjective gait evaluation, moderate synovial effusion, and periarticular swelling on joint palpation. Synovial fluid removed from the injected joint had markedly elevated neutrophil cell counts (35 x 10^9 cells/mm^3).

Clone characterization

Of the 1536 colonies initially selected, 1127 displayed detectable signals after the first round of screening **(Table 5.1)**. After the second hybridization round, 662 colonies remained; a subset (208) was identified as matrix metalloproteinase-1 (MMP-1). Differentially expressed cDNAs corresponding to 148 genes or expressed sequence tags (ESTs) were identified by sequence analysis and submitted to the Genbank public

Table 5.1 - Colony screening results.

Total number of white colonies analyzed	1536
Clones with detectable signal (1^{st} round)	1127
Total differential clones (2^{nd} round)	662
Total clones sequenced	454
Percent MMP-1 clones (includes redundant probe hybridization strategy)	31%
Number of cDNA contigs	58
Number of expressed sequence tags	91

database (AY246701-AY246855) **(Table 5.2)**. Lengths of cDNAs ranged from 50-914bp (mean=354 bp). Fifty-seven clones exhibited homology to nucleotide and protein database sequences (AY246701-AY246764), of which 76% were derived from the forward subtracted cDNA library ('SF'). Ninety-one clones lacked homology to existing mammalian or prokaryotic databases and were designated as expressed sequence tags (ESTs) #1-91, of which 82% were derived from the forward subtracted cDNA library (AY246765-AY246855) ('SF').

cDNA array analysis

Relative differences in signal intensities between the two subtracted libraries corresponding to a negative control plasmid DNA target ranged from - 1.6 to + 1.6-fold. This range was determined to be an indication of non-specific hybridization; therefore, a > 2-fold difference in signal intensity was designated as a threshold for detectable effects. Complementary DNA array analysis confirmed altered gene expression direction ('up / down') associated with EqIL-1β stimulation for all differential transcripts identified by SSH-PCR **(Table 5.2)** and ESTs (data not shown). cDNA array hybridization results corresponding to six genes **(Table 5.2)** and fifteen ESTs (data not shown) fell within the noise of the hybridization system (fold difference < 2.0); however, the direction of change in gene expression correlated with SSH-PCR results.

Hybridization of the labeled subtracted library probes ('SF and SR') to 72 additional cDNA arrayed targets demonstrated differential expression of twelve genes (> 2-fold difference) that were not detected using SSH-PCR. These included IL-1β = + 7.1-fold (ECU92481), TIMP-1 = + 6.3-fold (ECU95039), ferritin = + 4.7-fold (AY112742), MMP-3 = + 30.0-fold (ECU62529), granulocyte chemotactic protein-2 = + 9.7-fold (AY114351), biglycan = + 5.6-fold (AF035934), β-actin = + 3.1-fold (AF035774), capping protein actin-filament = + 2.2-fold (AF506976), decorin = + 2.8-fold (AF038127), ribosomal protein L5 = + 9.0-fold (AY113682), ubiquitin = + 2.4-fold (AF506969), and zinc finger protein-9 = + 2.9-fold (AF513861) **(Figure 5.2)**.

Table 5.2 - SSH-PCR results and cDNA array verification of differential expression.

	Genbank accession		Homology (%)	Expression direction	Fold change (SF/SR)
		Metabolic / growth regulation			
1	AY246701	Cytochrome C oxidase subunit IV isoform (COX4)	89 (b)	Up	2.9
2	AY246702	Lactate dehydrogenase B (LDHB)	92 (h)	Up	2.6
3	AY246703	Proliferation-associated protein 2G4 (Pa2g4)	100 (m)	Up	2.2
4	AY246704	Retinoblastoma-associated protein-1	94 (h)	Down	-2.5
5	AY246705	Ubiquitin homolog (fau)	93 (p)	Up	3.3
		Intracellular signaling			
6	AY246706	Grb-2 associated binder-1 protein (Gab-1)	95 (h)	Down	-1.1
7	AY246707	Basic fibroblast growth factor receptor 1 (FGFRI)	94 (h)	Up	2.6
8	AY246708	G-beta like protein, guanine nucleotide binding	90 (p)	Up	3.7
9	AY246709	Growth factor receptor tyrosine kinase (KIDR)	88 (h)	Down	-2.0
10	AY246710	PCTAIRE protein kinase 1	94 (h)	Down	-3.3
11	AY246711	Pleckstrin (p47)	86 (h)	Up	4.6
12	AY246712	Protein phosphatase 1 (PPP1), catalytic subunit	97 (h)	Up	2.9
13	AY246713-14	Serine-threonine kinase (STE20)	90 (h)	Down	-2.5
14	AY246715	Seven in absentia homolog (Siah2)	94 (h)	Up	2.4
15	AY246716	Transforming growth factor beta receptor 2 (TGFbR2)	93 (h)	Down	-1.1
		Transcription / translation			
16	AY246717	Acidic ribosomal protein P2 (RPP2)	97 (h)	Down	-2.5
17	AY246718	Bromodomain containing 1 nuclear protein (BDNF)	88 (m)	Up	2.4
18	AY246719	Bromodomain transcription factor (BPTF)	98 (h)	Up	3.1
19	AY246720	Elongation factor 1a (EF1a)	94 (b)	Down	-1.4
20	AY246721	Heterogenous ribonucleoprotein D-like (hnRNPD)	94 (h)	Up	1.5
21	AY246722	Histone H3.3B	98 (h)	Up	3.3
22	AY246723	HnRNP core protein A1 (HCP-1)	94 (h)	Up	2.4
23	AY246724	N-myc / STAT interactor	84 (h)	Down	-5.0
24	AY246725	Nucleolin	90 (h)	Down	-2.0
25	AY246726	Ribosomal protein L17	92 (h)	Down	-5.0
26	AY246727	Ribosomal protein L19	87 (h)	Up	2.9
27	AY246728	Ribosomal protein L35a	92 (r)	Up	3.1
28	AY246729	Ribosomal protein L41	91 (h)	Up	2.9
29	AY246730	Ribosomal protein L7	89 (h)	Up	2.6
30	AY246731	Ribosomal protein S12	85 (m)	Up	4.2
31	AY246732	Ribosomal protein S26	94 (h)	Up	18.0
32	AY246733	Ribosomal protein S9	82 (h)	Up	2.9
33	AY246734	Ring finger protein	96 (m)	Down	-1.7
34	AY246735	RNA binding protein, ewing sarcoma (EWS)	96 (h)	Up	2.6
35	AY246736	Signal transducer and activator of transcription, acute-phase response factor (STAT3)	96 (h)	Up	3.5
36	AY246737	SRB7 suppressor of RNA polymerase B homolog	88 (h)	Up	2.6
37	AY246738	WW domain binding protein 11 (SNP70)	94 (h)	Down	-2.0
38	AY246739	Zinc finger protein	93(h)	Up	3.3
		Cytoskeletal regulation			
39	AY246740	Calpactin I light chain (p11)	93 (b)	Up	2.2
40	AY246741	Gelsolin, actin-depolymerizing factor (ADF)	100 (e)	Down	-2.0
41	AY246742	Kinesin, heavy chain-like protein (KHCHP)	90 (h)	Down	-3.3
42	AY246743	Thymosin b4	94 (h)	Up	3.3
		Extracellular matrix metabolism			
43	AY246744	Laminin, b1	89 (h)	Up	2.0
44	AY246745	Proteoglycan 4 (megakaryocyte stimulating factor)	92 (h)	Up	3.5
45	AY246746	Syntenin, syndecan binding protein	97 (h)	Up	4.4
46	AY246747	Tenascin C (hexabrachion)	90 (h)	Up	2.4
		Inflammatory / Immune response			
47	AY246748	b-2 microglobulin	96 (e)	Up	6.8
48	AY246749	Complement C1s (CC1s)	85 (h)	Up	2.9
49	AY246750	Glutathione peroxidase 3, plasma isoform (GPx-3)	86 (b)	Down	-1.4
50	AY246751-53, AY246758-59	Manganese superoxide dismutase (Mn-SOD)	98 (e)	Up	6.2
51	AY246754-56	Matrix metalloproteinase-1 (MMP-1)	99 (e)	Up	8.4
52	AY246757	Serum amyloid A protein (SAA)	91 (b)	Up	3.1
53	AY246760	Tumor rejection antigen (gp96)	95 (h)	Up	2.9
		Hypothetical proteins			
54	AY246761	Hypothetical protein, similar to DET1	89 (h)	Up	2.6
55	AY246762	KIAA0185 hypothetical protein, RRP5 protein homolog	89 (h)	Down	-2.5
56	AY246763	KIAA1053 hypothetical protein	87 (h)	Up	2.6
57	AY246764	PTD016 hypothetical protein	88 (h)	Up	2.4

Species Homology Key: b = bovine, c = canine, e = equine, h = human, m = murine, p = porcine, r = rabbit

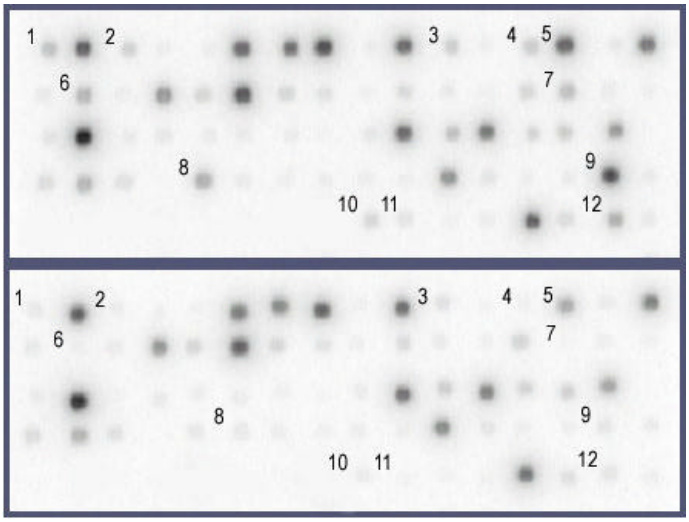

Figure 5.2 - cDNA array analysis of forward and reverse subtracted library probes.

Upper panel: Synovium forward subtracted labeled probe ('SF'), Bottom panel: Synovium reverse subtracted labeled probe ('SR') hybridized to 72 equine cDNA targets not derived by SSH-PCR. Numbered targets correspond to cDNAs increased > 2-fold ('SF'/'SR'): 1= ferritin, 2= decorin, 3= capping protein actin filament, 4= biglycan, 5= β-actin, 6= IL-1β, 7= GCP2, 8= RPL5, 9= MMP-3, 10= ZNP-9, 11= ubiquitin, 12= TIMP-1.

RT-PCR

Increased expression levels for six of the twelve genes detected by array analysis corresponded to increases in mRNA levels detected by RT-PCR: IL-1β (+ 1.4-fold), TIMP-1 (+ 3.3-fold), MMP-3 (+ 5.6-fold), biglycan (+ 1.8-fold), ferritin (+ 1.3-fold) and β-actin (+ 1.2-fold). In addition, up-regulated transcription of the MMP-1 clone identified using SSH-PCR was verified (+ 2.0-fold).

5.E. Discussion

The primary objective of this study to profile the transcriptome associated with an EqIL-1β induced acute synovitis was met. Combined results indicate an *in-vivo* EqIL-1β stimulation of synovium to result in altered steady state mRNA levels corresponding to genes involved in various biological processes **(Figure 5.3)**, and SSH-PCR to be an effective method for identifying a subset of differentially expressed genes. Results may apply to existing or novel anti-IL-1 therapies targeted to minimizing synovial inflammation, and may assist in the further understanding of the role of the synovium in the progression of joint disease.

Messenger RNA levels for twelve genes increased > 2-fold in response to an intra-articular injection of EqIL-1β exposure were detected using the customized cDNA array analysis, but were not isolated using SSH-PCR. These results might suggest practical limitations of the technology to detect differentially expressed transcripts, possibly due to suboptimal efficiencies associated with the cloning and differential hybridization screening steps. A recent paper mathematically modeling SSH-PCR on second order hybridization kinetics reported effective enrichment of differential genes to require target mRNAs to represent at least 0.01% of the total mRNA population and be present at a differential of > 5-fold concentrations (Ji, *et al.*, 2002). Therefore, we acknowledge that our results might represent the most differentially expressed subset of cDNAs. Further, we suggest the combination of SSH-PCR and cDNA array

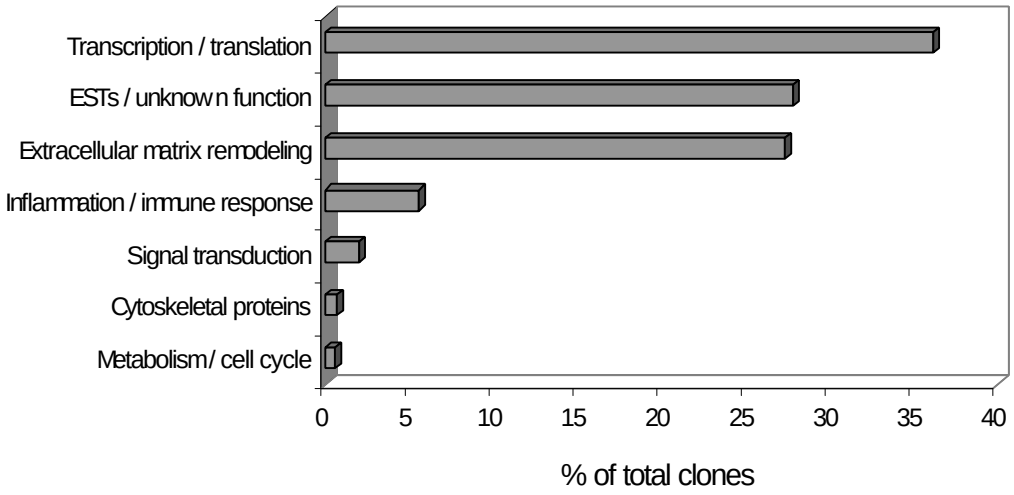

Figure 5.3 - Data distributed by categories of biological function.

hybridization to yield more comprehensive results, and RT-PCR to be an effective means to verify altered expression levels.

The clones derived by SSH-PCR were distributed into broad categories of biological function: 1) cellular growth and metabolism, 2) intracellular signaling, 3) transcription and translation, 4) cytoskeletal regulation, 5) extracellular matrix metabolism, and 6) inflammation / immunology **(Figure 5.3)**. This categorical system was adopted in this study as a means to organize the discussion of the results and to classify the retrieved clones for further use in cDNA array manufacture and analysis. Such an attempt to group these results is decidedly subjective, as many of the described cDNAs likely span multiple categories of biological function.

1. Growth and metabolism

Results suggest an EqIL-1β induced synovitis to involve FGF-1 mediated fibroblast proliferation by way of increased FGF receptor expression levels. Increased lactate dehydrogenase B (LDHB) transcript levels correlate with reports of increased LDHB expression in rheumatoid arthritic synoviocytes and suggestions for use of this enzyme as a detection marker for synovial membrane inflammation (Rejno, 1976; Masuda, *et al.*, 2002). Increased mRNA levels for ferritin are consistent with previous observations of synovium from patients with rheumatoid arthritis and support evidence for regulatory loops between IL-1 induced nitric oxide production and iron metabolism (Heller, *et al.*, 1997; Konttinen, *et al.*, 2000; Zanders, *et al.*, 2000).

2. Intracellular signaling

Results suggest an experimentally induced acute synovitis to involve alterations of basal mRNA levels corresponding to guanine nucleotide binding proteins, serine-threonine kinases, protein kinase C, stress activated kinases, and phosphatidylinositol degradative pathways. Altered expression levels detected for seven in absentia-2 (Siah-2), Grb-2 associated binder protein-1 (Gab-1), and an endothelial cell derived growth

factor receptor type III tyrosine-kinase (KIDR), suggest a complex regulation of tyrosine kinase mediated signaling. Abnormal tyrosine kinase activity has been implicated in cytokine-mediated fibroblast phenotype transformation observed in inflammatory joint disease, possibly through dimerization of tyrosine kinase membrane associated receptors (Williams, *et al.*, 1992).

3. Transcription and translation

The majority of SSH-PCR identified differentially expressed cDNAs were designated to this category **(Figure 5.3)**. Altered transcripts levels of these transcription factors / co-activators may contribute to induced transcription, mRNA processing, and cell-cycling processes associated with an EqIL-1β induced model of synovitis. Results suggest the involvement of two novel bromodomain containing proteins, possibly through chromatin-mediated mechanisms (Dyson, *et al.*, 2001). The altered transcript levels of ten distinct ribosomal proteins corresponding to both 60S and 40S subunits may imply an overall heightened degree of protein synthesis.

4. Cytoskeletal regulation

Synovial fibroblast cytoskeletal remodeling is described in cellular proliferation, differentiation, and chemotaxis (Konttinen, *et al.*, 2000). Altered transcript levels of β-actin, actin-filament capping protein, thymosin β4, gelsolin, and a microtubule-associated motor protein kinesin-like protein suggest the involvement of actin-modulating mechanisms and increased microfibril / intermediate filament structural fluidity in an EqIL-1β induced synovial inflammation. Increased mRNA levels for syntenin and calpactin I (annexin II ligand) suggest the roles of these membrane-associated proteins in synoviocyte cytoskeletal and extracellular matrix adhesion during an early synovitis response.

5. Extracellular matrix metabolism

Activated synoviocytes are a primary source of Zn-dependent MMPs, which degrade collagen and proteoglycan structures of the articular cartilage (Evans, 1992; Konttinen, *et al.*, 2000). Increased matrix metalloproteinase-1 (MMP-1), stromelysin (MMP-3), and matrix metalloproteinase-13 (MMP-13) transcript levels agree with reports of elevated transcription of these proteases in synovial fibroblasts following IL-1 stimulation and in diseased states (Dayer, *et al.*, 1986; Hutchinson, *et al.*, 1992; Heller, *et al.*, 1997; Zanders, *et al.*, 2000) (DiBattista, *et al.*, 1995a). The synovium ECM modulates important biomechanical, proliferative, migratory, and differentiative functions of embedded synoviocytes and infiltrating inflammatory cells (Konttinen, *et al.*, 2000). Increased biglycan and decorin expression levels may further implicate these small non-aggregating proteoglycans in collagen binding, adhesion, differentiation, migration, and fibrillogenesis in EqIL-1β induced inflammation (Todhunter, 1996). Altered proteoglycan 4, laminin B1, and tenascin C mRNA levels may support the involvement of these proteins in synovium lubrication, synovial fibroblast ECM interactions, and cytoprotection in inflammatory joint disease (Scott, *et al.*, 1984; McCachren and Lightner, 1992; Rinaldi, *et al.*, 1995).

6. Inflammatory / immunological responses

Increased steady state levels of mRNA for granulocyte chemotactic protein-2 support proposed chemokine-mediated neutrophilic migration into the synovium following an EqIL-1β stimulation (Van Damme, *et al.*, 1989). Altered transforming growth factor beta receptor II transcript levels further support the roles of this growth factor in regulation of inflammatory processes in the synovium (Taketazu, *et al.*, 1994). Results may implicate increased serum amyloid A transcription in inflammation-mediated ECM metabolic feedback mechanisms, by inducing collagenase production and as a novel substrate for MMP-1 and MMP-3 (Mitchell, *et al.*, 1993). Beta-2 microglobulin increased mRNA levels support reports of heightened protein detection in

diseased synovium, further implicating its roles in amyloidogenic deposition and fibrillogenesis associated with inflammation (Ohashi, 2001). Steady state mRNA levels of two antioxidative proteins were altered by EqIL-1β stimulation: manganese superoxide dismutase (Mn-SOD) and plasma selenoenzyme glutathione peroxidase (GPx). Mn-SOD treatment of an experimental arthritis model reduced joint swelling and serum globulin elevation; SOD activity was correlated with severity and type of joint disease (Parizada, *et al.*, 1991; Sumii, *et al.*, 1996). Decreased mRNA levels of GPx activity may indicate a possible regulation of the ECM degradative effects associated with this antioxidative pathway (Chaudiere, 1986).

Summary

An *in-vivo* EqIL-1β induced model for acute synovitis has been described. Results indicate intra-articular injection of EqIL-1β to induce a number of effects at the level of gene expression during an acute inflammation of the synovium. Results likely reflect responses of heterogenous synoviocyte and infiltrating inflammatory cell populations. Distinct differentially expressed transcripts with proposed relation to cellular metabolism, signaling, transcription, cytoskeletal modulation, neutrophil chemotaxis, inflammation, and synovial fibroblast / ECM biology are identified. These results agree with previous reports of modulated levels of particular transcripts in synovial cells following IL-1 stimulation or in diseased synovial tissue and present additional novel cDNAs of potential function in joint biology. This information contributes to our understanding of IL-1 mediated synovitis and may point to transcription-based strategies for anti-IL-1 treatment strategies.

5.F. Acknowledgments

The authors thank Dr. Dean W. Richardson, University of Pennsylvania School of Veterinary Medicine, Kennett Square, PA for the generous donation of the equine cDNA clones for MMP-3, TIMP-1, biglycan, and decorin and Dr. David Horohov, Louisiana State Univeristy, College of Veterinary Medicine, Baton Rouge, LA for donating the equine cDNA clone for β-actin.

CHAPTER VI: Significance and Future Directions

An important focus of osteoarthritis (OA) research is elucidating the roles of specific inflammatory-related cytokines, soluble mediators, and growth factors to disease etiology, pathogenesis, and severity. This dissertation was designed to study proximal effects of equine IL-1 (EqIL-1) on non-diseased articular cartilage, chondrocytes, and synovium in the experimental modeling of early OA and an acute synovitis. Results add to the current understanding of EqIL-1 induced effects in the joint and possible contributions to inflammatory cascades and extracellular matrix (ECM) catabolic processes. Our results agree with the limited number of reports of EqIL-1β to increase proteoglycan and prostaglandin E_2 release in equine articular cartilage (Fenton, *et al.*, 2002; Tung, *et al.*, 2002b), and to increase matrix metalloproteinase (MMP) mRNA levels in isolated chondrocytes (Tung, *et al.*, 2002a; Tung, *et al.*, 2002b). Our model for synovitis is the first to evaluate species-specific EqIL-1β effects on steady state mRNA levels in equine synovium. In addition, these exploratory investigations into IL-1 altered gene expression levels in equine chondrocytes and synovium are the first of their kind to date; similar studies of the effects of IL-1 on equine chondrocytes have examined hypothesis-driven changes in a select number of MMPs and cartilage-matrix related transcripts at a time (Caron, *et al.*, 1996; Richardson and Dodge, 2000; Tung, *et al.*, 2002b; Richardson and Dodge, 2003). Combined results demonstrate the potent bioactivity of our EqIL-1 proteins and establish culture conditions and experimental techniques that may be used for further studies of IL-1 / joint disease pathobiology.

Experimental models of OA

A primary objective of this research was to develop culture models for the controlled evaluation of EqIL-1 effects on articular cartilage and chondrocytes. These systems enabled the quantitative assessment of exogenous EqIL-1 induction of

chondrocytic ECM remodeling, prostaglandin E_2 production, and steady state mRNA levels over various protein concentrations and time points. Such observations would have been more difficult to experimentally design and achieve in *in-vivo* conditions. It must be acknowledged that these observations represent biological activity of tissues and cells removed from underlying bone, synovium, blood supply, and biomechanical loading forces, and thus may not be indicative of EqIL-1 induced effects in a biologically functional joint.

Additional studies might evaluate combinations of similar concentrations of exogenous EqIL-1 with other cytokines and growth factors in the attempt to elucidate possible associations of inflammatory networks to joint disease pathogenesis. Further studies might be directed toward testing the appropriateness of these articular cartilage and chondrocyte culturing methods for modeling IL-1 imbalances during a naturally occurring joint disease. Specifically, the presented results may be compared to the study of similar EqIL-1 induced effects on proteoglycan metabolism in OA diseased equine cartilage and gene expression levels in primary cultured OA chondrocytes. In addition, results from the adherent chondrocyte gene expression studies could be evaluated for how well they represent those of differentiated chondrocytes by three-dimensional / suspension culturing to re-establish chondrocyte phenotypes (Aulthouse, *et al.*, 1989; Cook, *et al.*, 2000).

Experimental model of synovitis

The synovium is important to biomechanical and immuno-inflammatory processes in the joint; changes in synovial fibroblast morphology and phenotype may contribute to destruction of articular cartilage and deformities of joints in human rheumatoid arthritis (Konttinen, *et al.*, 2000). An intra-articular injected model of acute synovitis was used to study EqIL-1β modulated changes in mRNA steady state levels. Unlike the two *in-vitro* systems, this approach was taken to evaluate exogenous IL-1 treatment effects on tissues in functional joints from a living animal. Potential for

erroneous conclusions due to genetic variability was minimized by comparisons of untreated and EqIL-1 treated synovium from the same horse; however, conclusions made in this study were limited to observations from only one animal.

Although this synovitis model best represents responses of biologically interactive tissues in joints, results drawn from this study likely correspond to a heterogeneous cellular population of resident synoviocytes and infiltrating leukocytes. Additional studies might involve similar EqIL-1β *in-vitro* treatments of synovium from multiple horses, to begin to distinguish the unique contributions of synovial fibroblasts, and not infiltrating inflammatory cells, to the observed transcript level responses. Further, it would be of interest to profile mRNA changes in articular cartilage during a similar EqIL-1β induced synovitis, to begin to understand the relationships between articular cartilage and synovium in early OA pathobiological mechanisms. Finally, to evaluate the best model for naturally occurring synovitis (and OA) in horses, these results could be compared to similar investigations of other experimentally instigated arthritides (i.e. surgical / trauma induced, collagen / adjuvant / fibronectin / cartilage fragment injected).

Transcriptome analysis

The cDNA array and subtractive hybridization techniques are effective in detecting modulated steady state mRNA levels in cultured chondrocytes and synovial tissues. The low-density customized cDNA array analysis enables the parallel study of a more manageable number of genes than a microarray analysis involving thousands of genes. Although the potential exists to miss interesting effects using this targeted approach, use of these smaller cDNA arrays likely lowers possibilities for cross-hybridization signal noise, subsequent inaccurate conclusions for significant effects (type I errors), and erroneous detection of co-regulated patterns in gene expression. Subtractive hybridization was able to identify a number of altered transcripts of potentially the greatest biological significance, but was unable to account for less dramatic effects detected by our cDNA array analysis. Both approaches are limited to the

identification of relative, and not absolute mRNA levels, that would be of the most biological interest. Moreover, the techniques are most accurate of transcriptome level effects and are not able to distinguish mRNA splice variants. Finally, although these techniques may reflect transcript levels, such generated information may not directly correlate with translated and mature protein levels; thus, direct postulations of applications of results to biological processes must be carefully guarded.

Clinical applications

Evaluations of steady state mRNA levels in both articular cartilage and synovial tissues suggest MMPs (-1, -3, and –13), ferritin, and serum amyloid A as potential transcriptional markers for elevated EqIL-1 levels possibly related to local intra-articular joint inflammation. Results also indicate exogenous EqIL-1 to induce mRNA levels corresponding to transforming growth factor beta and bone morphogenetic protein-4, and two antioxidative enzymes (manganese superoxide dismutase and glutathione peroxidase). These observations may reflect biological attempts of normal chondrocytes and synoviocytes to counter EqIL-1 initiated inflammatory cascades and production of reactive oxygen species, and may be promising targets for anti-inflammatory directed therapies. Future studies are required to relate these findings to proteomics-based analysis and / or assessment of protein activity (e.g. MMP zymography, activation of latent MMPs) of various stages of diseased cartilage, synovium, and synovial effusions, to ultimately establish validity as diagnostic markers and therapies for OA.

These results may also apply to approaches for existing treatment strategies for clinical OA. Our findings of increased MMP mRNA levels in response to EqIL-1β stimulation may support the use of synthetic MMP inhibitors (currently entering clinical trials in humans), and gene therapy targeted to regulating cartilage ECM remodeling (e.g. MMPs and tissue inhibitors of MMPs (TIMPs)). Results also appear to support other OA therapies currently under investigation, including glycosaminoglycan and hyaluronic acid injections, and gene therapies intended to sustain endogenous levels of anti-inflammatory

cytokines, growth factors, and IL-1 receptor antagonist (IL-1ra). Intra-articular IL-1ra gene therapy has been shown to result in sustained levels of IL-1ra protein levels and improved clinical and histological assessments of an experimental OA in horses (Frisbie and McIlwraith, 2000; Frisbie, *et al.*, 2002). Successful viral-mediated IL-1ra delivery into osteoarthritic chondrocytes and synovial cells has been described (Baragi, *et al.*, 1995; Fernandes, *et al.*, 2000).

Summary

Development of *in-vitro* and *in-vivo* models is essential to clarify the complex roles of IL-1 in early cytokine imbalance and inflammation in the equine joint. Our data support the hypothesis that IL-1 may stimulate cartilage ECM catabolism and contribute to early inflammatory cascades linked to initiation and propagation of pathophysiologic mechanisms of joint disease in horses. These generated cDNA arrays are an invaluable resource for future investigations where cytokine and matrix biology, or the gene expression profiling of stages of a naturally occurring OA, are of interest. This documentation adds to the current understanding of equine IL-1 induced effects in equine articular cartilage chondrocytes and synovium, and may lay a foundation for possible inflammatory mediated joint disease research in humans.

LITERATURE CITED

ABRAMSON, S. B. & AMIN, A. (2002). Blocking the effects of IL-1 in rheumatoid arthritis protects bone and cartilage. *Rheumatology (Oxford)* **41,** 972-80.

AIGNER, T., ZIEN, A., GEHRSITZ, A., GEBHARD, P. M. & MCKENNA, L. (2001). Anabolic and catabolic gene expression pattern analysis in normal versus osteoarthritic cartilage using complementary DNA-array technology. *Arthritis Rheum* **44,** 2777-89.

AIGNER, T., ZIEN, A., HANISCH, D. & ZIMMER, R. (2003). Gene expression in chondrocytes assessed with use of microarrays. *J Bone Joint Surg Am* **85-A Suppl 2,** 117-23.

AL-HUMIDAN, A., RALSTON, S. H., HUGHES, D. E., CHAPMAN, K., AARDEN, L., RUSSELL, R. G. & GOWEN, M. (1991). Interleukin-6 does not stimulate bone resorption in neonatal mouse calvariae. *J Bone Miner Res* **6,** 3-8.

ALWAN, W. H., CARTER, S. D., DIXON, J. B., BENNETT, D., MAY, S. A. & EDWARDS, G. B. (1991). Interleukin-1-like activity in synovial fluids and sera of horses with arthritis. *Res Vet Sci* **51,** 72-7.

AREND, W. P., WELGUS, H. G., THOMPSON, R. C. & EISENBERG, S. P. (1990). Biological properties of recombinant human monocyte-derived interleukin 1 receptor antagonist. *J Clin Invest* **85,** 1694-7.

ARNER, E. C. (1994). Effect of animal age and chronicity of interleukin-1 exposure on cartilage proteoglycan depletion in vivo. *J Orthop Res* **12,** 321-30.

ATTUR, M. G., DAVE, M., CIPOLLETTA, C., KANG, P., GOLDRING, M. B., PATEL, I. R., ABRAMSON, S. B. & AMIN, A. R. (2000). Reversal of autocrine and paracrine effects of interleukin 1 (IL-1) in human arthritis by type II IL-1 decoy receptor. Potential for pharmacological intervention. *J Biol Chem* **275,** 40307-15.

ATTUR, M. G., PATEL, R. N., ABRAMSON, S. B. & AMIN, A. R. (1997). Interleukin-17 up-regulation of nitric oxide production in human osteoarthritis cartilage. *Arthritis Rheum* **40,** 1050-3.

AULTHOUSE, A. L., BECK, M., GRIFFEY, E., SANFORD, J., ARDEN, K., MACHADO, M. A. & HORTON, W. A. (1989). Expression of the human chondrocyte phenotype in vitro. *In Vitro Cell Dev Biol* **25,** 659-68.

BARAGI, V. M., RENKIEWICZ, R. R., JORDAN, H., BONADIO, J., HARTMAN, J. W. & ROESSLER, B. J. (1995). Transplantation of transduced chondrocytes protects articular cartilage from interleukin 1-induced extracellular matrix degradation. *J Clin Invest* **96,** 2454-60.

BENDER, S., HAUBECK, H. D., VAN DE LEUR, E., DUFHUES, G., SCHIEL, X., LAUWERIJNS, J., GREILING, H. & HEINRICH, P. C. (1990). Interleukin-1 beta induces synthesis and secretion of interleukin-6 in human chondrocytes. *FEBS Lett* **263,** 321-4.

BENDRUPS, A., HILTON, A., MEAGER, A. & HAMILTON, J. A. (1993). Reduction of tumor necrosis factor alpha and interleukin-1 beta levels in human synovial tissue by interleukin-4 and glucocorticoid. *Rheumatol Int* **12,** 217-20.

BENYA, P. D., PADILLA, S. R. & NIMNI, M. E. (1978). Independent regulation of collagen types by chondrocytes during the loss of differentiated function in culture. *Cell* **15,** 1313-21.

BENYA, P. D. & SHAFFER, J. D. (1982). Dedifferentiated chondrocytes reexpress the differentiated collagen phenotype when cultured in agarose gels. *Cell* **30,** 215-24.

BHAUMICK, B. & BALA, R. M. (1991). Differential effects of insulin-like growth factors I and II on growth, differentiation and glucoregulation in differentiating chondrocyte cells in culture. *Acta Endocrinol (Copenh)* **125,** 201-11.

BINETTE, F., MCQUAID, D. P., HAUDENSCHILD, D. R., YAEGER, P. C., MCPHERSON, J. M. & TUBO, R. (1998). Expression of a stable articular cartilage phenotype without evidence of hypertrophy by adult human articular chondrocytes in vitro. *J Orthop Res* **16,** 207-16.

BIRKEDAL-HANSEN, H., MOORE, W. G., BODDEN, M. K., WINDSOR, L. J., BIRKEDAL-HANSEN, B., DECARLO, A. & ENGLER, J. A. (1993). Matrix metalloproteinases: a review. *Crit Rev Oral Biol Med* **4,** 197-250.

BLANCO, F. J., GUITIAN, R., VAZQUEZ-MARTUL, E., DE TORO, F. J. & GALDO, F. (1998). Osteoarthritis chondrocytes die by apoptosis. A possible pathway for osteoarthritis pathology. *Arthritis Rheum* **41,** 284-9.

BLANCO, F. J., OCHS, R. L., SCHWARZ, H. & LOTZ, M. (1995). Chondrocyte apoptosis induced by nitric oxide. *Am J Pathol* **146,** 75-85.

BOCK, H. C., MICHAELI, P., BODE, C., SCHULTZ, W., KRESSE, H., HERKEN, R. & MIOSGE, N. (2001). The small proteoglycans decorin and biglycan in human articular cartilage of late-stage osteoarthritis. *Osteoarthritis Cartilage* **9,** 654-63.

BORASCHI, D., VILLA, L., VOLPINI, G., BOSSU, P., CENSINI, S., GHIARA, P., SCAPIGLIAT, G., NENCIONI, L., BARTALINI, M., MATTEUCCI, G. & ET AL. (1990). Differential activity of interleukin 1 alpha and interleukin 1 beta in the stimulation of the immune response in vivo. *Eur J Immunol* **20,** 317-21.

BRADFORD, M. M. (1976). A rapid and sensitive method for the quantitation of microgram quantities of protein utilizing the principle of protein-dye binding. *Anal Biochem* **72,** 248-54.

BROWN, M. P., WEST, L. A., MERRITT, K. A. & PLAAS, A. H. (1998). Changes in sulfation patterns of chondroitin sulfate in equine articular cartilage and synovial fluid in response to aging and osteoarthritis. *Am J Vet Res* **59,** 786-91.

BUNNING, R. A., CRAWFORD, A., RICHARDSON, H. J., OPDENAKKER, G., VAN DAMME, J. & RUSSELL, R. G. (1987). Interleukin 1 preferentially stimulates the production of tissue-type plasminogen activator by human articular chondrocytes. *Biochim Biophys Acta* **924,** 473-82.

CAMPBELL, I. K., GOLDS, E. E., MORT, J. S. & ROUGHLEY, P. J. (1986). Human articular cartilage secretes characteristic metal dependent proteinases upon stimulation by mononuclear cell factor. *J Rheumatol* **13,** 20-7.

CAMPBELL, I. K., PICCOLI, D. S., BUTLER, D. M., SINGLETON, D. K. & HAMILTON, J. A. (1988). Recombinant human interleukin-1 stimulates human articular cartilage to undergo resorption and human chondrocytes to produce both tissue- and urokinase-type plasminogen activator. *Biochim Biophys Acta* **967,** 183-94.

CAMPBELL, I. K., PICCOLI, D. S. & HAMILTON, J. A. (1990). Stimulation of human chondrocyte prostaglandin E2 production by recombinant human interleukin-1 and tumour necrosis factor. *Biochim Biophys Acta* **1051,** 310-8.

CANALIS, E., CENTRELLA, M. & MCCARTHY, T. (1988). Effects of basic fibroblast growth factor on bone formation in vitro. *J Clin Invest* **81,** 1572-7.

CARON, J. P., TARDIF, G., MARTEL-PELLETIER, J., DIBATTISTA, J. A., GENG, C. & PELLETIER, J. P. (1996). Modulation of matrix metalloprotease 13 (collagenase 3) gene expression in equine chondrocytes by interleukin 1 and corticosteroids. *Am J Vet Res* **57,** 1631-4.

CASTAGNOLA, P., DOZIN, B., MORO, G. & CANCEDDA, R. (1988). Changes in the expression of collagen genes show two stages in chondrocyte differentiation in vitro. *J Cell Biol* **106,** 461-7.

CATTERALL, J. B., CARRERE, S., KOSHY, P. J., DEGNAN, B. A., SHINGLETON, W. D., BRINCKERHOFF, C. E., RUTTER, J., CAWSTON, T. E. & ROWAN, A. D. (2001). Synergistic induction of matrix metalloproteinase 1 by interleukin-1alpha and oncostatin M in human chondrocytes involves signal transducer and activator of transcription and activator protein 1 transcription factors via a novel mechanism. *Arthritis Rheum* **44,** 2296-310.

CHANDRASEKHAR, S., HARVEY, A. K. & HRUBEY, P. S. (1992). Intra-articular administration of interleukin-1 causes prolonged suppression of cartilage proteoglycan synthesis in rats. *Matrix* **12,** 1-10.

CHANG, J., GILMAN, S. C. & LEWIS, A. J. (1986). Interleukin 1 activates phospholipase A2 in rabbit chondrocytes: a possible signal for IL 1 action. *J Immunol* **136,** 1283-7.

CHAUDIERE, J. (1986). [Possible role of glutathione peroxidase in the regulation of collagenase activity]. *Ann Biol Clin (Paris)* **44,** 181-7.

CHIN, J. E., HATFIELD, C. A., KRZESICKI, R. F. & HERBLIN, W. F. (1991). Interactions between interleukin-1 and basic fibroblast growth factor on articular chondrocytes. Effects on cell growth, prostanoid production, and receptor modulation. *Arthritis Rheum* **34,** 314-24.

CHIN, J. E. & LIN, Y. A. (1988). Effects of recombinant human interleukin-1 beta on rabbit articular chondrocytes. Stimulation of prostanoid release and inhibition of cell growth. *Arthritis Rheum* **31,** 1290-6.

CHRISMAN, O. D. (1969). Biochemical aspects of degenerative joint disease. *Clin Orthop* **64,** 77-86.

CHU, T. M., WEIR, B. & WOLFINGER, R. (2002). A systematic statistical linear modeling approach to oligonucleotide array experiments. *Math Biosci* **176,** 35-51.

CHUNG, J. Y., PARK, Y. C., YE, H. & WU, H. (2002). All TRAFs are not created equal: common and distinct molecular mechanisms of TRAF-mediated signal transduction. *J Cell Sci* **115,** 679-88.

CIMPEAN, A., CALOIANU, M., ALEXANDRU, D., EFIMOV, N. & BUZGARIU, W. (2000). Effect of the interleukin-1b on gelatinolytic activity and cell morphology of human osteoarthritic chondrocytes in culture. *J Med Biochem* **4,** 113-29.

CLEGG, P. D. & CARTER, S. D. (1999). Matrix metalloproteinase-2 and -9 are activated in joint diseases. *Equine Vet J* **31,** 324-30.

CLEGG, P. D., COUGHLAN, A. R., RIGGS, C. M. & CARTER, S. D. (1997). Matrix metalloproteinases 2 and 9 in equine synovial fluids. *Equine Vet J* **29,** 343-8.

COOK, J. L., ANDERSON, C. C., KREEGER, J. M. & TOMLINSON, J. L. (2000). Effects of human recombinant interleukin-1beta on canine articular chondrocytes in three-dimensional culture. *Am J Vet Res* **61,** 766-70.

CRABB, I. D., O'KEEFE, R. J., PUZAS, J. E. & ROSIER, R. N. (1990). Synergistic effect of transforming growth factor beta and fibroblast growth factor on DNA synthesis in chick growth plate chondrocytes. *J Bone Miner Res* **5,** 1105-12.

DAVIES, U. M., JONES, J., REEVE, J., CAMACHO-HUBNER, C., CHARLETT, A., ANSELL, B. M., PREECE, M. A. & WOO, P. M. (1997). Juvenile rheumatoid arthritis. Effects of disease activity and recombinant human growth hormone on insulin-like growth factor 1, insulin-like growth factor binding proteins 1 and 3, and osteocalcin. *Arthritis Rheum* **40,** 332-40.

DAYER, J. M., DE ROCHEMONTEIX, B., BURRUS, B., DEMCZUK, S. & DINARELLO, C. A. (1986). Human recombinant interleukin 1 stimulates collagenase and prostaglandin E2 production by human synovial cells. *J Clin Invest* **77,** 645-8.

DEAN, D. D., MARTEL-PELLETIER, J., PELLETIER, J. P., HOWELL, D. S. & WOESSNER, J. F., JR. (1989). Evidence for metalloproteinase and metalloproteinase inhibitor imbalance in human osteoarthritic cartilage. *J Clin Invest* **84,** 678-85.

DERISI, J., PENLAND, L., BROWN, P. O., BITTNER, M. L., MELTZER, P. S., RAY, M., CHEN, Y., SU, Y. A. & TRENT, J. M. (1996). Use of a cDNA microarray to analyse gene expression patterns in human cancer. *Nat Genet* **14,** 457-60.

DIATCHENKO, L., LAU, Y. F., CAMPBELL, A. P., CHENCHIK, A., MOQADAM, F., HUANG, B., LUKYANOV, S., LUKYANOV, K., GURSKAYA, N., SVERDLOV, E. D. & SIEBERT, P. D. (1996). Suppression subtractive hybridization: a method for generating differentially regulated or tissue-specific cDNA probes and libraries. *Proc Natl Acad Sci U S A* **93,** 6025-30.

DIBATTISTA, J. A., MARTEL-PELLETIER, J., MORIN, N., JOLICOEUR, F. C. & PELLETIER, J. P. (1994). Transcriptional regulation of plasminogen activator inhibitor-1 expression in human synovial fibroblasts by prostaglandin E2: mediation by protein kinase A and role of interleukin-1. *Mol Cell Endocrinol* **103,** 139-48.

DIBATTISTA, J. A., PELLETIER, J. P., ZAFARULLAH, M., FUJIMOTO, N., OBATA, K. & MARTEL-PELLETIER, J. (1995a). Coordinate regulation of

matrix metalloproteases and tissue inhibitor of metalloproteinase expression in human synovial fibroblasts. *J Rheumatol Suppl* **43,** 123-8.

DIBATTISTA, J. A., PELLETIER, J. P., ZAFARULLAH, M., IWATA, K. & MARTEL-PELLETIER, J. (1995b). Interleukin-1 beta induction of tissue inhibitor of metalloproteinase (TIMP-1) is functionally antagonized by prostaglandin E2 in human synovial fibroblasts. *J Cell Biochem* **57,** 619-29.

DINARELLO, C. A. (1994a). The interleukin-1 family: 10 years of discovery. *Faseb J* **8,** 1314-25.

DINARELLO, C. A. (1994b). The biological properties of interleukin-1. *Eur Cytokine Netw* **5,** 517-31.

DINARELLO, C. A. (1996). Biologic basis for interleukin-1 in disease. *Blood* **87,** 2095-147.

D'LIMA, D. D., HASHIMOTO, S., CHEN, P. C., COLWELL, C. W., JR. & LOTZ, M. K. (2001). Human chondrocyte apoptosis in response to mechanical injury. *Osteoarthritis Cartilage* **9,** 712-9.

DREZNER, M. K., NEELON, F. A. & LEBOVITZ, H. E. (1976). Stimulation of cartilage macromolecule synthesis by adenosine 3',5'-monophosphate. *Biochim Biophys Acta* **425,** 521-31.

DRIPPS, D. J., BRANDHUBER, B. J., THOMPSON, R. C. & EISENBERG, S. P. (1991). Interleukin-1 (IL-1) receptor antagonist binds to the 80-kDa IL-1 receptor but does not initiate IL-1 signal transduction. *J Biol Chem* **266,** 10331-6.

DYSON, M. H., ROSE, S. & MAHADEVAN, L. C. (2001). Acetyllysine-binding and function of bromodomain-containing proteins in chromatin. *Front Biosci* **6,** D853-65.

EVANS, C. H. (1992). Response of synovium to mechanical injury. In *Biology and biomechanics of the traumatized synovial joint*, ed. G. Finerman & F. Noyes, pp. 17-26. American Academy of Orthopedic Surgery.

FARNDALE, R. W., SAYERS, C. A. & BARRETT, A. J. (1982). A direct spectrophotometric microassay for sulfated glycosaminoglycans in cartilage cultures. *Connect Tissue Res* **9,** 247-8.

FENTON, J. I., CHLEBEK-BROWN, K. A., CARON, J. P. & ORTH, M. W. (2002). Effect of glucosamine on interleukin-1-conditioned articular cartilage. *Equine Vet J Suppl,* 219-23.

FERNANDES, J. C., MARTEL-PELLETIER, J. & PELLETIER, J. P. (2002). The role of cytokines in osteoarthritis pathophysiology. *Biorheology* **39,** 237-46.

FERNANDES, J. C., MARTEL-PELLETIER, J. & PELLETIER, J. P. (2000). Gene therapy for osteoarthritis: new perspectives for the twenty-first century. *Clin Orthop,* S262-72.

FLANNERY, C. R., LITTLE, C. B., CATERSON, B. & HUGHES, C. E. (1999a). Effects of culture conditions and exposure to catabolic stimulators (IL-1 and retinoic acid) on the expression of matrix metalloproteinases (MMPs) and disintegrin metalloproteinases (ADAMs) by articular cartilage chondrocytes. *Matrix Biol* **18,** 225-37.

FLANNERY, C. R., LITTLE, C. B., HUGHES, C. E. & CATERSON, B. (1999b). Expression of ADAMTS homologues in articular cartilage. *Biochem Biophys Res Commun* **260,** 318-22.

FREAN, S. P., GETTINBY, G., MAY, S. A. & LEES, P. (2000). Influence of interleukin-1beta and hyaluronan on proteoglycan release from equine navicular hyaline cartilage and fibrocartilage. *J Vet Pharmacol Ther* **23,** 67-72.

FRISBIE, D. D., GHIVIZZANI, S. C., ROBBINS, P. D., EVANS, C. H. & MCILWRAITH, C. W. (2002). Treatment of experimental equine osteoarthritis by in vivo delivery of the equine interleukin-1 receptor antagonist gene. *Gene Ther* **9,** 12-20.

FRISBIE, D. D. & MCILWRAITH, C. W. (2000). Evaluation of gene therapy as a treatment for equine traumatic arthritis and osteoarthritis. *Clin Orthop***,** S273-87.

FRISBIE, D. D. & NIXON, A. J. (1997). Insulin-like growth factor 1 and corticosteroid modulation of chondrocyte metabolic and mitogenic activities in interleukin 1-conditioned equine cartilage. *Am J Vet Res* **58,** 524-30.

FUKUDA, K., KUMANO, F., TAKAYAMA, M., SAITO, M., OTANI, K. & TANAKA, S. (1995). Zonal differences in nitric oxide synthesis by bovine chondrocytes exposed to interleukin-1. *Inflamm Res* **44,** 434-7.

GOLDRING, M. B., BIRKHEAD, J., SANDELL, L. J., KIMURA, T. & KRANE, S. M. (1988). Interleukin 1 suppresses expression of cartilage-specific types II and IX collagens and increases types I and III collagens in human chondrocytes. *J Clin Invest* **82,** 2026-37.

GOLDRING, M. B., BIRKHEAD, J. R., SUEN, L. F., YAMIN, R., MIZUNO, S., GLOWACKI, J., ARBISER, J. L. & APPERLEY, J. F. (1994). Interleukin-1 beta-modulated gene expression in immortalized human chondrocytes. *J Clin Invest* **94,** 2307-16.

GOWEN, M., WOOD, D. D., IHRIE, E. J., MEATS, J. E. & RUSSELL, R. G. (1984). Stimulation by human interleukin 1 of cartilage breakdown and production of collagenase and proteoglycanase by human chondrocytes but not by human osteoblasts in vitro. *Biochim Biophys Acta* **797,** 186-93.

GUERNE, P. A., CARSON, D. A. & LOTZ, M. (1990). IL-6 production by human articular chondrocytes. Modulation of its synthesis by cytokines, growth factors, and hormones in vitro. *J Immunol* **144,** 499-505.

GUERNE, P. A., SUBLET, A. & LOTZ, M. (1994). Growth factor responsiveness of human articular chondrocytes: distinct profiles in primary chondrocytes, subcultured chondrocytes, and fibroblasts. *J Cell Physiol* **158,** 476-84.

GURSKAYA, N. G., DIATCHENKO, L., CHENCHIK, A., SIEBERT, P. D., KHASPEKOV, G. L., LUKYANOV, K. A., VAGNER, L. L., ERMOLAEVA, O. D., LUKYANOV, S. A. & SVERDLOV, E. D. (1996). Equalizing cDNA subtraction based on selective suppression of polymerase chain reaction: cloning of Jurkat cell transcripts induced by phytohemaglutinin and phorbol 12-myristate 13-acetate. *Anal Biochem* **240,** 90-7.

HAMERMAN, D. (1993). Aging and osteoarthritis: basic mechanisms. *J Am Geriatr Soc* **41,** 760-70.

HAMILTON, J. A., HART, P. H., LEIZER, T., VITTI, G. F. & CAMPBELL, I. K. (1991). Regulation of plasminogen activator activity in arthritic joints. *J Rheumatol Suppl* **27,** 106-9.

HARDY, J., BERTONE, A. L. & MALEMUD, C. J. (1998a). Effect of synovial membrane infection in vitro on equine synoviocytes and chondrocytes. *Am J Vet Res* **59,** 293-9.

HARDY, J., BERTONE, A. L., WEISBRODE, S. E., MUIR, W. W., O'DORISIO, T. M. & MASTY, J. (1998b). Cell trafficking, mediator release, and articular metabolism in acute inflammation of innervated or denervated isolated equine joints. *Am J Vet Res* **59,** 88-100.

HART, P. H., AHERN, M. J., SMITH, M. D. & FINLAY-JONES, J. J. (1995). Comparison of the suppressive effects of interleukin-10 and interleukin-4 on synovial fluid macrophages and blood monocytes from patients with inflammatory arthritis. *Immunology* **84,** 536-42.

HEEMSKERK, V. H., DAEMEN, M. A. & BUURMAN, W. A. (1999). Insulin-like growth factor-1 (IGF-1) and growth hormone (GH) in immunity and inflammation. *Cytokine Growth Factor Rev* **10,** 5-14.

HELLER, R. A., SCHENA, M., CHAI, A., SHALON, D., BEDILION, T., GILMORE, J., WOOLLEY, D. E. & DAVIS, R. W. (1997). Discovery and analysis of inflammatory disease-related genes using cDNA microarrays. *Proc Natl Acad Sci U S A* **94,** 2150-5.

HILL, D. J. (1992). Peptide growth factor interactions in embryonic and fetal growth. *Horm Res* **38,** 197-202.

HIRAKI, Y., INOUE, H., SHIGENO, C., SANMA, Y., BENTZ, H., ROSEN, D. M., ASADA, A. & SUZUKI, F. (1991). Bone morphogenetic proteins (BMP-2 and BMP-3) promote growth and expression of the differentiated phenotype of rabbit chondrocytes and osteoblastic MC3T3-E1 cells in vitro. *J Bone Miner Res* **6,** 1373-85.

HOMANDBERG, G. A. (1999). Potential regulation of cartilage metabolism in osteoarthritis by fibronectin fragments. *Front Biosci* **4,** D713-30.

HOPKINS, S. J. & HUMPHREYS, M. (1989). Simple, sensitive and specific bioassay of interleukin-1. *J Immunol Methods* **120,** 271-6.

HOWARD, R. (1997). Cloning, Sequence, and Prokaryotic Expression of the cDNAs for equine Interleukin-1, Colorado State University, PhD dissertation.

HOWARD, R. D., MCILWRAITH, C. W., TROTTER, G. W. & NYBORG, J. K. (1998a). Cloning of equine interleukin 1 alpha and equine interleukin 1 beta and determination of their full-length cDNA sequences. *Am J Vet Res* **59,** 704-11.

HOWARD, R. D., MCILWRAITH, C. W., TROTTER, G. W. & NYBORG, J. K. (1998b). Cloning of equine interleukin 1 receptor antagonist and determination of its full-length cDNA sequence. *Am J Vet Res* **59,** 712-6.

HOWELL, D. S. & PELLETIER, J. P. (1993). Etiopathogenesis of osteoarthritis. In *Arthritis and Allied Conditions, 12th ed.*, ed. D. J. McCarthy & W. J. Koopman, pp. 1723. Lea & Febiger.

HUTCHINSON, N. I., LARK, M. W., MACNAUL, K. L., HARPER, C., HOERRNER, L. A., MCDONNELL, J., DONATELLI, S., MOORE, V. & BAYNE, E. K. (1992). In vivo expression of stromelysin in synovium and cartilage of rabbits injected intraarticularly with interleukin-1 beta. *Arthritis Rheum* **35,** 1227-33.

IKEBE, T., HIRATA, M. & KOGA, T. (1986). Human recombinant interleukin 1-mediated suppression of glycosaminoglycan synthesis in cultured rat costal chondrocytes. *Biochem Biophys Res Commun* **140,** 386-91.

IMAI, K., OHTA, S., MATSUMOTO, T., FUJIMOTO, N., SATO, H., SEIKI, M. & OKADA, Y. (1997). Expression of membrane-type 1 matrix metalloproteinase and activation of progelatinase A in human osteoarthritic cartilage. *Am J Pathol* **151,** 245-56.

ISHIMI, Y., MIYAURA, C., JIN, C. H., AKATSU, T., ABE, E., NAKAMURA, Y., YAMAGUCHI, A., YOSHIKI, S., MATSUDA, T., HIRANO, T. & ET AL. (1990). IL-6 is produced by osteoblasts and induces bone resorption. *J Immunol* **145,** 3297-303.

JEFFCOTT, L. B., ROSSDALE, P. D., FREESTONE, J., FRANK, C. J. & TOWERS-CLARK, P. F. (1982). An assessment of wastage in thoroughbred racing from conception to 4 years of age. *Equine Vet J* **14,** 185-98.

JI, W., WRIGHT, M. B., CAI, L., FLAMENT, A. & LINDPAINTNER, K. (2002). Efficacy of SSH PCR in isolating differentially expressed genes. *BMC Genomics* **3,** 12.

JOVANOVIC, D., PELLETIER, J. P., ALAAEDDINE, N., MINEAU, F., GENG, C., RANGER, P. & MARTEL-PELLETIER, J. (1998a). Effect of IL-13 on cytokines, cytokine receptors and inhibitors on human osteoarthritis synovium and synovial fibroblasts. *Osteoarthritis Cartilage* **6,** 40-9.

JOVANOVIC, D. V., DI BATTISTA, J. A., MARTEL-PELLETIER, J., JOLICOEUR, F. C., HE, Y., ZHANG, M., MINEAU, F. & PELLETIER, J. P. (1998b). IL-17 stimulates the production and expression of proinflammatory cytokines, IL-beta and TNF-alpha, by human macrophages. *J Immunol* **160,** 3513-21.

KATO, H., OHASHI, T., NAKAMURA, N., NISHIMURA, Y., WATARI, T., GOITSUKA, R., TSUJIMOTO, H. & HASEGAWA, A. (1995). Molecular cloning of equine interleukin-1 alpha and -beta cDNAs. *Vet Immunol Immunopathol* **48,** 221-31.

KAWCAK, C. E., TROTTER, G. W., FRISBIE, D. D. & MCILWRAITH, C. W. (1996). Maintenance of equine articular cartilage explants in serum-free and serum-supplemented media, compared with that in a commercial supplemented medium. *Am J Vet Res* **57,** 1261-5.

KIKUCHI, H., TANAKA, S. & MATSUO, O. (1987). Plasminogen activator in synovial fluid from patients with rheumatoid arthritis. *J Rheumatol* **14,** 439-45.

KIM, Y.-J., SAH, R., DOONG, J.-Y. & GRODZINSKY, A. (1998). Fluorometric assay of DNA in cartilage explants using Hoechst 33258. *Anal Biochem* **174,** 168-76.

KO, Y. (1995). Reverse transcriptase-polymerase chain reaction (RT-PCR): a sensitive method to examine basic fibroblast growth factor-induced expression of the early

growth response gene-1 (egr-1) in human umbilical arterial endothelial cells. *Molecular and Cellular Probes* **9,** 215-22.

KOLESNICK, R. N., HAIMOVITZ-FRIEDMAN, A. & FUKS, Z. (1994). The sphingomyelin signal transduction pathway mediates apoptosis for tumor necrosis factor, Fas, and ionizing radiation. *Biochem Cell Biol* **72,** 471-4.

KONTTINEN, Y. T., LI, T. F., HUKKANEN, M., MA, J., XU, J. W. & VIRTANEN, I. (2000). Fibroblast biology. Signals targeting the synovial fibroblast in arthritis. *Arthritis Res* **2,** 348-55.

KRONENBERG, H. M., LEE, K., LANSKE, B. & SEGRE, G. V. (1997). Parathyroid hormone-related protein and Indian hedgehog control the pace of cartilage differentiation. *J Endocrinol* **154 Suppl,** S39-45.

KUHN, K., HASHIMOTO, S. & LOTZ, M. (2000). IL-1 beta protects human chondrocytes from CD95-induced apoptosis. *J Immunol* **164,** 2233-9.

LEDERER, J. A. & CZUPRYNSKI, C. J. (1989). Species preference of bovine thymocytes and fibroblasts for bovine interleukin 1. *Vet Immunol Immunopathol* **23,** 213-22.

LEE, Z. H., LEE, S. E., KIM, C. W., LEE, S. H., KIM, S. W., KWACK, K., WALSH, K. & KIM, H. H. (2002). IL-1alpha stimulation of osteoclast survival through the PI 3-kinase/Akt and ERK pathways. *J Biochem (Tokyo)* **131,** 161-6.

LEFEBVRE, V., PEETERS-JORIS, C. & VAES, G. (1990a). Modulation by interleukin 1 and tumor necrosis factor alpha of production of collagenase, tissue inhibitor of metalloproteinases and collagen types in differentiated and dedifferentiated articular chondrocytes. *Biochim Biophys Acta* **1052,** 366-78.

LEFEBVRE, V., PEETERS-JORIS, C. & VAES, G. (1990b). Production of collagens, collagenase and collagenase inhibitor during the dedifferentiation of articular chondrocytes by serial subcultures. *Biochim Biophys Acta* **1051,** 266-75.

LI, X., COMMANE, M., JIANG, Z. & STARK, G. R. (2001). IL-1-induced NFkappa B and c-Jun N-terminal kinase (JNK) activation diverge at IL-1 receptor-associated kinase (IRAK). *Proc Natl Acad Sci U S A* **98,** 4461-5.

LODISH, H., BERK, A., ZIPURSKY, S., MATSUDAIRA, P., BALTIMORE, D. & DARNELL, J. (1999). *Molecular Cell Biology*, 4th edition edn. W.H. Freeman and Company.

LOESER, R. F. & SHANKER, G. (2000). Autocrine stimulation by insulin-like growth factor 1 and insulin-like growth factor 2 mediates chondrocyte survival in vitro. *Arthritis Rheum* **43,** 1552-9.

LOTZ, M. (2001). Cytokines in cartilage injury and repair. *Clin Orthop***,** S108-15.

LOTZ, M., BLANCO, F. J., VON KEMPIS, J., DUDLER, J., MAIER, R., VILLIGER, P. M. & GENG, Y. (1995). Cytokine regulation of chondrocyte functions. *J Rheumatol Suppl* **43,** 104-8.

LOTZ, M. & GUERNE, P. A. (1991). Interleukin-6 induces the synthesis of tissue inhibitor of metalloproteinases-1/erythroid potentiating activity (TIMP-1/EPA). *J Biol Chem* **266,** 2017-20.

LOTZ, M., MOATS, T. & VILLIGER, P. M. (1992a). Leukemia inhibitory factor is expressed in cartilage and synovium and can contribute to the pathogenesis of arthritis. *J Clin Invest* **90,** 888-96.

LOTZ, M., TERKELTAUB, R. & VILLIGER, P. M. (1992b). Cartilage and joint inflammation. Regulation of IL-8 expression by human articular chondrocytes. *J Immunol* **148,** 466-73.

LUYTEN, F. P., CHEN, P., PARALKAR, V. & REDDI, A. H. (1994). Recombinant bone morphogenetic protein-4, transforming growth factor-beta 1, and activin A enhance the cartilage phenotype of articular chondrocytes in vitro. *Exp Cell Res* **210,** 224-9.

LYONS-GIORDANO, B., DAVIS, G. L., GALBRAITH, W., PRATTA, M. A. & ARNER, E. C. (1989). Interleukin-1 beta stimulates phospholipase A2 mRNA synthesis in rabbit articular chondrocytes. *Biochem Biophys Res Commun* **164,** 488-95.

MACDONALD, M. H., STOVER, S. M., WILLITS, N. H. & BENTON, H. P. (1992). Regulation of matrix metabolism in equine cartilage explant cultures by interleukin 1. *Am J Vet Res* **53,** 2278-85.

MACDONALD, M. H., STOVER, S. M., WILLITS, N. H. & BENTON, H. P. (1994). Effect of bacterial lipopolysaccharides on sulfated glycosaminoglycan metabolism and prostaglandin E2 synthesis in equine cartilage explant cultures. *Am J Vet Res* **55,** 1127-38.

MALEMUD, C. J. (1993). Markers of osteoarthritis and cartilage research in animal models. *Curr Opin Rheumatol* **5,** 494-502.

MALEMUD, C. J. & SOKOLOFF, L. (1977). The effect of prostaglandins of cultured lapine articular chondrocytes. *Prostaglandins* **13,** 845-60.

MALLEIN-GERIN, F., GARRONE, R. & VAN DER REST, M. (1991). Proteoglycan and collagen synthesis are correlated with actin organization in dedifferentiating chondrocytes. *Eur J Cell Biol* **56,** 364-73.

MARGERIE, D., FLECHTENMACHER, J., BUTTNER, F. H., KARBOWSKI, A., PUHL, W., SCHLEYERBACH, R. & BARTNIK, E. (1997). Complexity of IL-1 beta induced gene expression pattern in human articular chondrocytes. *Osteoarthritis Cartilage* **5,** 129-38.

MARTEL-PELLETIER, J., DI BATTISTA, J. A., LAJEUNESSE, D. & PELLETIER, J. P. (1998). IGF/IGFBP axis in cartilage and bone in osteoarthritis pathogenesis. *Inflamm Res* **47,** 90-100.

MARTEL-PELLETIER, J., MCCOLLUM, R., FUJIMOTO, N., OBATA, K., CLOUTIER, J. M. & PELLETIER, J. P. (1994). Excess of metalloproteases over tissue inhibitor of metalloprotease may contribute to cartilage degradation in osteoarthritis and rheumatoid arthritis. *Lab Invest* **70,** 807-15.

MASUDA, K., MASUDA, R., NEIDHART, M., SIMMEN, B. R., MICHEL, B. A., MULLER-LADNER, U., GAY, R. E. & GAY, S. (2002). Molecular profile of synovial fibroblasts in rheumatoid arthritis depends on the stage of proliferation. *Arthritis Res* **4,** R8.

MAY, S. A., HOOKE, R. E. & LEES, P. (1992a). Interleukin-1 stimulation of equine articular cells. *Res Vet Sci* **52,** 342-8.
MAY, S. A., HOOKE, R. E. & LEES, P. (1992b). Species restrictions demonstrated by the stimulation of equine cells with recombinant human interleukin-1. *Vet Immunol Immunopathol* **30,** 373-84.
MAY, S. A., HOOKE, R. E. & LEES, P. (1992c). Inhibition of interleukin-1 activity by equine synovial fluid. *Equine Vet J* **24,** 99-102.
MAY, S. A., HOOKE, R. E. & LEES, P. (1989). Identity of the E-series prostaglandin produced by equine chondrocytes and synovial cells in response to a variety of stimuli. *Res Vet Sci* **46,** 54-7.
MCCACHREN, S. S. & LIGHTNER, V. A. (1992). Expression of human tenascin in synovitis and its regulation by interleukin-1. *Arthritis Rheum* **35,** 1185-96.
MCCARTHY, T. L., CENTRELLA, M. & CANALIS, E. (1989). Insulin-like growth factor (IGF) and bone. *Connect Tissue Res* **20,** 277-82.
MCILWRAITH, C. W. (1987). Diseases of joints, tendons, ligaments, and related structures. In *Lameness in Horses, 4th ed*, ed. T. Stashak, pp. 339-485. Lea & Febiger.
MCILWRAITH, C. W. (1996). General pathobiology of the joint and response to injury. In *Joint Disease in the Horse*, ed. C. W. McIlwraith & G. W. Trotter, pp. 41-70. W.B. Saunders Company.
MENGSHOL, J. A., VINCENTI, M. P. & BRINCKERHOFF, C. E. (2001). IL-1 induces collagenase-3 (MMP-13) promoter activity in stably transfected chondrocytic cells: requirement for Runx-2 and activation by p38 MAPK and JNK pathways. *Nucleic Acids Res* **29,** 4361-72.
MENGSHOL, J. A., VINCENTI, M. P., COON, C. I., BARCHOWSKY, A. & BRINCKERHOFF, C. E. (2000). Interleukin-1 induction of collagenase 3 (matrix metalloproteinase 13) gene expression in chondrocytes requires p38, c-Jun N-terminal kinase, and nuclear factor kappaB: differential regulation of collagenase 1 and collagenase 3. *Arthritis Rheum* **43,** 801-11.
MITCHELL, T. I., JEFFREY, J. J., PALMITER, R. D. & BRINCKERHOFF, C. E. (1993). The acute phase reactant serum amyloid A (SAA3) is a novel substrate for degradation by the metalloproteinases collagenase and stromelysin. *Biochim Biophys Acta* **1156,** 245-54.
MOLDOVAN, F., PELLETIER, J. P., HAMBOR, J., CLOUTIER, J. M. & MARTEL-PELLETIER, J. (1997). Collagenase-3 (matrix metalloprotease 13) is preferentially localized in the deep layer of human arthritic cartilage in situ: in vitro mimicking effect by transforming growth factor beta. *Arthritis Rheum* **40,** 1653-61.
MORRIS, E. A., MCDONALD, B. S., WEBB, A. C. & ROSENWASSER, L. J. (1990). Identification of interleukin-1 in equine osteoarthritic joint effusions. *Am J Vet Res* **51,** 59-64.
MORRIS, E. A. & TREADWELL, B. V. (1994). Effect of interleukin 1 on articular cartilage from young and aged horses and comparison with metabolism of osteoarthritic cartilage. *Am J Vet Res* **55,** 138-46.

MURAKAMI, S., LEFEBVRE, V. & DE CROMBRUGGHE, B. (2000). Potent inhibition of the master chondrogenic factor Sox9 gene by interleukin-1 and tumor necrosis factor-alpha. *J Biol Chem* **275,** 3687-92.

MURATA, M., TRAHAN, C., HIRAHASHI, J., MANKIN, H. J. & TOWLE, C. A. (2003). Intracellular interleukin-1 receptor antagonist in osteoarthritis chondrocytes. *Clin Orthop***,** 285-95.

NEIDEL, J., SCHULZE, M. & SOVA, L. (1994). Insulin-like growth factor I accelerates recovery of articular cartilage proteoglycan synthesis in culture after inhibition by interleukin 1. *Arch Orthop Trauma Surg* **114,** 43-8.

NGUYEN, C., ROCHA, D., GRANJEAUD, S., BALDIT, M., BERNARD, K., NAQUET, P. & JORDAN, B. R. (1995). Differential gene expression in the murine thymus assayed by quantitative hybridization of arrayed cDNA clones. *Genomics* **29,** 207-16.

NIETFELD, J. J., WILBRINK, B., HELLE, M., VAN ROY, J. L., DEN OTTER, W., SWAAK, A. J. & HUBER-BRUNING, O. (1990). Interleukin-1-induced interleukin-6 is required for the inhibition of proteoglycan synthesis by interleukin-1 in human articular cartilage. *Arthritis Rheum* **33,** 1695-701.

NIXON, A. J., LUST, G. & VERNIER-SINGER, M. (1992). Isolation, propagation, and cryopreservation of equine articular chondrocytes. *Am J Vet Res* **53,** 2364-70.

OHASHI, K. (2001). Pathogenesis of beta2-microglobulin amyloidosis. *Pathol Int* **51,** 1-10.

OLEE, T., HASHIMOTO, S., QUACH, J. & LOTZ, M. (1999). IL-18 is produced by articular chondrocytes and induces proinflammatory and catabolic responses. *J Immunol* **162,** 1096-100.

OLNEY, R. C., ANHALT, H., NEELY, E. K. & WILSON, D. M. (1995). A quantitative assay for IGF-I and IGF binding protein mRNAs: expression in malignant melanoma cells. *Mol Cell Endocrinol* **110,** 213-23.

O'NEILL, L. A. (1995). Towards an understanding of the signal transduction pathways for interleukin 1. *Biochim Biophys Acta* **1266,** 31-44.

OSBORN, K. D., TRIPPEL, S. B. & MANKIN, H. J. (1989). Growth factor stimulation of adult articular cartilage. *J Orthop Res* **7,** 35-42.

PALMER, R. M., HICKERY, M. S., CHARLES, I. G., MONCADA, S. & BAYLISS, M. T. (1993). Induction of nitric oxide synthase in human chondrocytes. *Biochem Biophys Res Commun* **193,** 398-405.

PARIZADA, B., WERBER, M. M. & NIMROD, A. (1991). Protective effects of human recombinant MnSOD in adjuvant arthritis and bleomycin-induced lung fibrosis. *Free Radic Res Commun* **15,** 297-301.

PASTERNAK, R. D., HUBBS, S. J., CACCESE, R. G., MARKS, R. L., CONATY, J. M. & DIPASQUALE, G. (1986). Interleukin-1 stimulates the secretion of proteoglycan- and collagen-degrading proteases by rabbit articular chondrocytes. *Clin Immunol Immunopathol* **41,** 351-67.

PELLETIER, J. P., MARTEL-PELLETIER, J., HOWELL, D. S., GHANDUR-MNAYMNEH, L., ENIS, J. E. & WOESSNER, J. F., JR. (1983). Collagenase and collagenolytic activity in human osteoarthritic cartilage. *Arthritis Rheum* **26,** 63-8.

PETTIPHER, E. R., HIGGS, G. A. & HENDERSON, B. (1986). Interleukin 1 induces leukocyte infiltration and cartilage proteoglycan degradation in the synovial joint. *Proc Natl Acad Sci U S A* **83,** 8749-53.

PLATT, D. (1996). Articular cartilage homeostasis and the role of growth factors and cytokines in regulating matrix composition. In *Joint Disease in the Horse*, ed. C. W. McIlwraith & G. W. Trotter, pp. 29-40. W.B. Saunders Company.

PLATT, D. & BAYLISS, M. T. (1994). An investigation of the proteoglycan metabolism of mature equine articular cartilage and its regulation by interleukin-1. *Equine Vet J* **26,** 297-303.

POTTS, J. R. & CAMPBELL, I. D. (1996). Structure and function of fibronectin modules. *Matrix Biol* **15,** 313-20; discussion 21.

PRUZANSKI, W., BOGOCH, E., WLOCH, M. & VADAS, P. (1991). The role of phospholipase A2 in the physiopathology of osteoarthritis. *J Rheumatol Suppl* **27,** 117-9.

REBOUL, P., PELLETIER, J. P., TARDIF, G., CLOUTIER, J. M. & MARTEL-PELLETIER, J. (1996). The new collagenase, collagenase-3, is expressed and synthesized by human chondrocytes but not by synoviocytes. A role in osteoarthritis. *J Clin Invest* **97,** 2011-9.

RECKLIES, A. D., BAILLARGEON, L. & WHITE, C. (1998). Regulation of cartilage oligomeric matrix protein synthesis in human synovial cells and articular chondrocytes. *Arthritis Rheum* **41,** 997-1006.

REDISKE, J. J., KOEHNE, C. F., ZHANG, B. & LOTZ, M. (1994). The inducible production of nitric oxide by articular cell types. *Osteoarthritis Cartilage* **2,** 199-206.

REGINATO, A. M., IOZZO, R. V. & JIMENEZ, S. A. (1994). Formation of nodular structures resembling mature articular cartilage in long-term primary cultures of human fetal epiphyseal chondrocytes on a hydrogel substrate. *Arthritis Rheum* **37,** 1338-49.

REJNO, S. (1976). LDH and LDH isoenzymes of synovial fluid in the horse. *Acta Vet Scand* **17,** 178-89.

RICHARDSON, D. W. & DODGE, G. R. (2000). Effects of interleukin-1beta and tumor necrosis factor-alpha on expression of matrix-related genes by cultured equine articular chondrocytes. *Am J Vet Res* **61,** 624-30.

RICHARDSON, D. W. & DODGE, G. R. (1998). Molecular characteristics of equine stromelysin and the tissue inhibitor of metalloproteinase 1. *Am J Vet Res* **59,** 1557-62.

RICHARDSON, D. W. & DODGE, G. R. (2003). Dose-dependent effects of corticosteroids on the expression of matrix-related genes in normal and cytokine-treated articular chondrocytes. *Inflamm Res* **52,** 39-49.

RINALDI, N., BARTH, T., LEPPELMANN-JANSEN, P., GANSAUGE, S., WILLHAUCK, M., BERGHOF, R. & SCHWARZ-EYWILL, M. (1995). [Normal synoviocytes and synoviocytes from osteoarthritis and rheumatoid arthritis bind extracellular matrix proteins differently]. *Immun Infekt* **23,** 62-4.

RONZIERE, M. C., RICARD-BLUM, S., TIOLLIER, J., HARTMANN, D. J., GARRONE, R. & HERBAGE, D. (1990). Comparative analysis of collagens solubilized from human foetal, and normal and osteoarthritic adult articular cartilage, with emphasis on type VI collagen. *Biochim Biophys Acta* **1038,** 222-30.

RUCKLIDGE, G. J., MILNE, G. & ROBINS, S. P. (1996). Collagen type X: a component of the surface of normal human, pig, and rat articular cartilage. *Biochem Biophys Res Commun* **224,** 297-302.

RUPP, E. A., CAMERON, P. M., RANAWAT, C. S., SCHMIDT, J. A. & BAYNE, E. K. (1986). Specific bioactivities of monocyte-derived interleukin 1 alpha and interleukin 1 beta are similar to each other on cultured murine thymocytes and on cultured human connective tissue cells. *J Clin Invest* **78,** 836-9.

SAIKI, R. K., GELFAND, D. H., STOFFEL, S., SCHARF, S. J., HIGUCHI, R., HORN, G. T., MULLIS, K. B. & ERLICH, H. A. (1988). Primer-directed enzymatic amplification of DNA with a thermostable DNA polymerase. *Science* **239,** 487-91.

SANGER, F., NICKLEN, S. & COULSON, A. R. (1977). DNA sequencing with chain-terminating inhibitors. *Proc Natl Acad Sci U S A* **74,** 5463-7.

SCHENA, M. (2003). *Microarray Analysis.* John Wiley & Sons, Inc.

SCHENA, M., HELLER, R. A., THERIAULT, T. P., KONRAD, K., LACHENMEIER, E. & DAVIS, R. W. (1998). Microarrays: biotechnology's discovery platform for functional genomics. *Trends Biotechnol* **16,** 301-6.

SCHENA, M., SHALON, D., HELLER, R., CHAI, A., BROWN, P. O. & DAVIS, R. W. (1996). Parallel human genome analysis: microarray-based expression monitoring of 1000 genes. *Proc Natl Acad Sci U S A* **93,** 10614-9.

SCHENA, M. E. (1999). *DNA microarrays: a practical approach*. Oxford University Press.

SCHERLE, P. A., PRATTA, M. A., FEESER, W. S., TANCULA, E. J. & ARNER, E. C. (1997). The effects of IL-1 on mitogen-activated protein kinases in rabbit articular chondrocytes. *Biochem Biophys Res Commun* **230,** 573-7.

SCHNYDER, J., PAYNE, T. & DINARELLO, C. A. (1987). Human monocyte or recombinant interleukin 1's are specific for the secretion of a metalloproteinase from chondrocytes. *J Immunol* **138,** 496-503.

SCOTT, D. L., SALMON, M., MORRIS, C. J., WAINWRIGHT, A. C. & WALTON, K. W. (1984). Laminin and vascular proliferation in rheumatoid arthritis. *Ann Rheum Dis* **43,** 551-5.

SHUKUNAMI, C., AKIYAMA, H., NAKAMURA, T. & HIRAKI, Y. (2000). Requirement of autocrine signaling by bone morphogenetic protein-4 for chondrogenic differentiation of ATDC5 cells. *FEBS Lett* **469,** 83-7.

STOKES, D. G., LIU, G., COIMBRA, I. B., PIERA-VELAZQUEZ, S., CROWL, R. M. & JIMENEZ, S. A. (2002). Assessment of the gene expression profile of differentiated and dedifferentiated human fetal chondrocytes by microarray analysis. *Arthritis Rheum* **46,** 404-19.

SUDA, T., KOBAYASHI, K., JIMI, E., UDAGAWA, N. & TAKAHASHI, N. (2001). The molecular basis of osteoclast differentiation and activation. *Novartis Found Symp* **232,** 235-47; discussion 47-50.

SUMII, H., INOUE, H., ONOUE, J., MORI, A., ODA, T. & TSUBOKURA, T. (1996). Superoxide dismutase activity in arthropathy: its role and measurement in the joints. *Hiroshima J Med Sci* **45,** 51-5.

SUNIC, D., MCNEIL, J. D., RAYNER, T. E., ANDRESS, D. L. & BELFORD, D. A. (1998). Regulation of insulin-like growth factor-binding protein-5 by insulin-like growth factor I and interleukin-1alpha in ovine articular chondrocytes. *Endocrinology* **139,** 2356-62.

SVOBODA, K. K. (1998). Chondrocyte-matrix attachment complexes mediate survival and differentiation. *Microsc Res Tech* **43,** 111-22.

TAKAFUJI, V. A., MCILWRAITH, C. W. & HOWARD, R. D. (2002). Effects of equine recombinant interleukin-1alpha and interleukin-1beta on proteoglycan metabolism and prostaglandin E2 synthesis in equine articular cartilage explants. *Am J Vet Res* **63,** 551-8.

TAKETAZU, F., KATO, M., GOBL, A., ICHIJO, H., TEN DIJKE, P., ITOH, J., KYOGOKU, M., RONNELID, J., MIYAZONO, K., HELDIN, C. H. & ET AL. (1994). Enhanced expression of transforming growth factor-beta s and transforming growth factor-beta type II receptor in the synovial tissues of patients with rheumatoid arthritis. *Lab Invest* **70,** 620-30.

TANI-ISHII, N., TSUNODA, A., TERANAKA, T. & UMEMOTO, T. (1999). Autocrine regulation of osteoclast formation and bone resorption by IL-1 alpha and TNF alpha. *J Dent Res* **78,** 1617-23.

TARDIF, G., PELLETIER, J. P., DUPUIS, M., GENG, C., CLOUTIER, J. M. & MARTEL-PELLETIER, J. (1999). Collagenase 3 production by human osteoarthritic chondrocytes in response to growth factors and cytokines is a function of the physiologic state of the cells. *Arthritis Rheum* **42,** 1147-58.

TASKIRAN, D., STEFANOVIC-RACIC, M., GEORGESCU, H. & EVANS, C. (1994). Nitric oxide mediates suppression of cartilage proteoglycan synthesis by interleukin-1. *Biochem Biophys Res Commun* **200,** 142-8.

THOMPSON, R. C., DRIPPS, D. J. & EISENBERG, S. P. (1992). Interleukin-1 receptor antagonist (IL-1ra) as a probe and as a treatment for IL-1 mediated disease. *Int J Immunopharmacol* **14,** 475-80.

TIMM, N. (2002). *Applied multivariate analysis.* Springer Verlag.

TKATCHENKO, A. V., LE CAM, G., LEGER, J. J. & DECHESNE, C. A. (2000). Large-scale analysis of differential gene expression in the hindlimb muscles and diaphragm of mdx mouse. *Biochim Biophys Acta* **1500,** 17-30.

TODHUNTER, P. G., KINCAID, S. A., TODHUNTER, R. J., KAMMERMANN, J. R., JOHNSTONE, B., BAIRD, A. N., HANSON, R. R., WRIGHT, J. M., LIN, H. C. & PUROHIT, R. C. (1996). Immunohistochemical analysis of an equine model of synovitis-induced arthritis. *Am J Vet Res* **57,** 1080-93.

TODHUNTER, R. J. (1996). Anatomy and physiology of synovial joints. In *Joint Disease in the Horse*, ed. C. W. McIlwraith & G. W. Trotter, pp. 1-28. W.B. Saunders Company.

TODHUNTER, R. J., WOOTTON, J. A., LUST, G. & MINOR, R. R. (1994). Structure of equine type I and type II collagens. *Am J Vet Res* **55,** 425-31.

TOKUKODA, Y., TAKATA, S., KAJI, H., KITAZAWA, R., SUGIMOTO, T. & CHIHARA, K. (2001). Interleukin-1beta stimulates transendothelial mobilization of human peripheral blood mononuclear cells with a potential to differentiate into osteoclasts in the presence of osteoblasts. *Endocr J* **48,** 443-52.

TOWLE, C. A., TRICE, M. E., OLLIVIERRE, F., AWBREY, B. J. & TREADWELL, B. V. (1987). Regulation of cartilage remodeling by IL-1: evidence for autocrine synthesis of IL-1 by chondrocytes. *J Rheumatol* **14 Spec No,** 11-3.

TUNG, J. T., ARNOLD, C. E., ALEXANDER, L. H., YUZBASIYAN-GURKAN, V., VENTA, P. J., RICHARDSON, D. W. & CARON, J. P. (2002a). Evaluation of the influence of prostaglandin E2 on recombinant equine interleukin-1beta-stimulated matrix metalloproteinases 1, 3, and 13 and tissue inhibitor of matrix metalloproteinase 1 expression in equine chondrocyte cultures. *Am J Vet Res* **63,** 987-93.

TUNG, J. T., FENTON, J. I., ARNOLD, C., ALEXANDER, L., YUZBASIYAN-GURKAN, V., VENTA, P. J., PETERS, T. L., ORTH, M. W., RICHARDSON, D. W. & CARON, J. P. (2002b). Recombinant equine interleukin-1beta induces putative mediators of articular cartilage degradation in equine chondrocytes. *Can J Vet Res* **66,** 19-25.

TYLER, J., BIRD, J. & GILLER, T. (1990). Interleukin-1 inhibits the production of types II, IX, and XI procollagen mRNA in cartilage. *Ann N Y Acad Sci* **580,** 512-17.

TYLER, J. A. (1985). Chondrocyte-mediated depletion of articular cartilage proteoglycans in vitro. *Biochem J* **225,** 493-507.

TYLER, J. A. & BENTON, H. P. (1988). Synthesis of type II collagen is decreased in cartilage cultured with interleukin 1 while the rate of intracellular degradation remains unchanged. *Coll Relat Res* **8,** 393-405.

VAN BEUNINGEN, H. M., VAN DER KRAAN, P. M., ARNTZ, O. J. & VAN DEN BERG, W. B. (1993). Protection from interleukin 1 induced destruction of articular cartilage by transforming growth factor beta: studies in anatomically intact cartilage in vitro and in vivo. *Ann Rheum Dis* **52,** 185-91.

VAN DAMME, J., DECOCK, B., CONINGS, R., LENAERTS, J. P., OPDENAKKER, G. & BILLIAU, A. (1989). The chemotactic activity for granulocytes produced by virally infected fibroblasts is identical to monocyte-derived interleukin 8. *Eur J Immunol* **19,** 1189-94.

VAN DE LOO, F. A., ARNTZ, O. J. & VAN DEN BERG, W. B. (1997). Effect of interleukin 1 and leukaemia inhibitory factor on chondrocyte metabolism in articular cartilage from normal and interleukin-6-deficient mice: role of nitric oxide and IL-6 in the suppression of proteoglycan synthesis. *Cytokine* **9,** 453-62.

VAN DEN BERG, W. B., JOOSTEN, L. A. & VAN DE LOO, F. A. (1999). TNF alpha and IL-1 beta are separate targets in chronic arthritis. *Clin Exp Rheumatol* **17,** S105-14.

VAN HAL, N. L., VORST, O., VAN HOUWELINGEN, A. M., KOK, E. J., PEIJNENBURG, A., AHARONI, A., VAN TUNEN, A. J. & KEIJER, J. (2000). The application of DNA microarrays in gene expression analysis. *J Biotechnol* **78,** 271-80.

VILLIGER, P. M. & LOTZ, M. (1992). Differential expression of TGF beta isoforms by human articular chondrocytes in response to growth factors. *J Cell Physiol* **151,** 318-25.

VINCENTI, M. P. & BRINCKERHOFF, C. E. (2001). Early response genes induced in chondrocytes stimulated with the inflammatory cytokine interleukin-1beta. *Arthritis Res* **3,** 381-8.

WILLIAMS, W. V., VONFELDT, J. M., RAMANUJAM, T. & WEINER, D. B. (1992). Tyrosine kinase signal transduction in rheumatoid synovitis. *Semin Arthritis Rheum* **21,** 317-29.

WODICKA, L., DONG, H., MITTMANN, M., HO, M. H. & LOCKHART, D. J. (1997). Genome-wide expression monitoring in Saccharomyces cerevisiae. *Nat Biotechnol* **15,** 1359-67.

WOLFINGER, R. D., GIBSON, G., WOLFINGER, E. D., BENNETT, L., HAMADEH, H., BUSHEL, P., AFSHARI, C. & PAULES, R. S. (2001). Assessing gene significance from cDNA microarray expression data via mixed models. *J Comput Biol* **8,** 625-37.

WOOD, D. D., IHRIE, E. J. & HAMERMAN, D. (1985). Release of interleukin-1 from human synovial tissue in vitro. *Arthritis Rheum* **28,** 853-62.

ZAFARULLAH, M., SU, S., MARTEL-PELLETIER, J., DIBATTISTA, J. A., COSTELLO, B. G., STETLER-STEVENSON, W. G. & PELLETIER, J. P. (1996). Tissue inhibitor of metalloproteinase-2 (TIMP-2) mRNA is constitutively expressed in bovine, human normal, and osteoarthritic articular chondrocytes. *J Cell Biochem* **60,** 211-7.

ZANDERS, E. D., GOULDEN, M. G., KENNEDY, T. C. & KEMPSELL, K. E. (2000). Analysis of immune system gene expression in small rheumatoid arthritis biopsies using a combination of subtractive hybridization and high-density cDNA arrays. *J Immunol Methods* **233,** 131-40.

ZIELENIEWSKI, W., ZIELENIEWSKI, J. & STEPIEN, H. (1995a). Effect of interleukin-1a, IL-1b and IL-1 receptor antibody on the proliferation and steroidogenesis of regenerating rat adrenal cortex. *Exp Clin Endocrinol Diabetes* **103,** 373-7.

ZIELENIEWSKI, W., ZIELENIEWSKI, J. & STEPIEN, H. (1995b). Interleukin-1 beta, but not IL-1 alpha, stimulates cell proliferation in the adrenal cortex. *Cytobios* **84,** 199-204.

APPENDIX I: Recombinant equine interleukin-1

A. Interleukin-1 constructs

Expression constructs of the putative mature forms of recombinant equine interleukin-1 alpha (EqIL-1α), beta (EqIL-1β), and receptor antagonist (EqIL-1ra) were generated by polymerase chain reaction (PCR) **(Figure A1)** (Howard, 1997 #16;Howard, 1998 #15;Howard, 1998 #16). Templates used for PCR reactions were the full-length cDNAs for EqIL-1α (pBluescript/EqIL-1α), EqIL-1β (pBluescript/EqIL-1β), and EqIL-1ra (pBluescript/EqIL-1ra). Synthetic primers were designed to produce *BamH1* and *HindIII* restriction enzyme sites bracketing the predicted mature forms of the proteins: S-113 to F-270 for EqIL-1α, A-116 to A-268 for EqIL-1β, and H-26 to Q-177 for EqIL-1ra. A pentapeptide enterokinase nucleotide cleavage site (D_4K) was placed 5' to the amino terminus of the mature proteins. Amplification products were cloned into pQE-30 encoding a hexahistadyl peptide at the amino terminus of the translated fusion proteins and transformed into competent pM15[pRep] host cells (Qiagen Inc, Chatsworth, CA).

B. Protein expression

(Modified from 'The QIAexpress System', Qiagen Inc, Chatsworth, CA)

Starter cultures of M15[pRep] transformed cells were used to inoculate luria bertani broth cultures (1 L) supplemented with ampicillin (100 ug/ml) and kanamycin (25 ug/ml). Cultures were incubated at 37°C with shaking (150 rpm) until log growth was achieved after 4-5 hours (A_{600} = 0.5). Expression of recombinant proteins was induced by the addition of isopropyl β-D-thiogalactopyranoside (2 U/L). The cultures were incubated at 37°C, 150 rpm, for 4-5 hours until A_{600} = 1.0. Cells were pelleted by centrifugation at 4,000 x g, for 20 minutes (4°C), weighed, resuspended in a sonication buffer (50 mM $NaPO_4$, 300 mM NaCl, pH 8.0) (3 ml buffer / 1 gram pellet), and frozen at -20°C. Cell solutions were thawed and subjected to alternating bursts of sonication and incubation on ice (1 min burst (200-300 Watt) / 1 min cooling), until turbidity was visibly

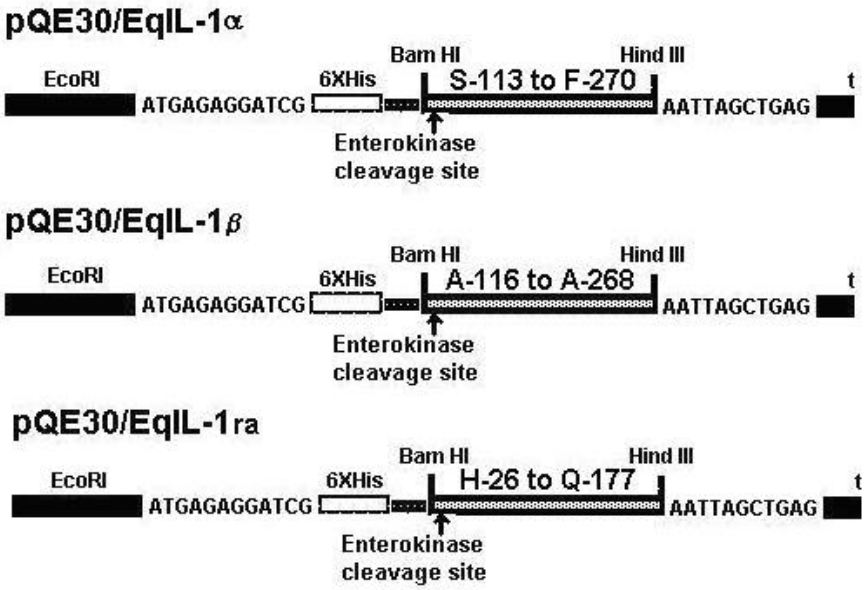

Figure A1 - EqIL-1 expression constructs.

decreased (A_{600} = 0.3). Cell lysates were drawn through a 20-gauge needle and centrifuged at 10,000 x g for 20 minutes at 4°C.

C. Protein purification and storage

Crude cell lysates were loaded onto 1.6 cm diameter columns containing 50% nickel nitrilo-triacetic acid resin (8 ml) and incubated with gentle rocking at 4°C for 2 hours. The effluent was removed by gravity filtration and the columns were washed with a sonication buffer containing aprotinin (2 ug/ml), leuprotinin (2 ug/ml), and phenylmethylsulfonyl fluoride (100 ug/ml) at a flow rate of 1 ml/min at 4°C for 70 minutes. Columns were washed (50 mM $NaPO_4$, 300 mM NaCl, 10% glycerol, pH 6.0) at a flow rate of 1 ml/min for 70 minutes. The proteins were eluted with 0.3 M imidazole in wash buffer, pooled, and dialyzed overnight against an enterokinase digestion buffer (50 mM Tris-HCl pH 8.0, 10 mM $CaCl_2$, 0.1% Tween-20). Fusion proteins were subjected to an enterokinase digestion (7 U/ml) for 24 hours at 4°C with gentle rocking (EnterokinaseMAX™, Invitrogen Corporation, Carlsbad CA). Digested protein solutions were dialyzed overnight against two changes of phosphate buffered saline (PBS) at 4°C. Protein solutions (~ 5 ml volumes) were subjected to size exclusion fast protein liquid chromatography at 4°C using a PBS running buffer and were collected in 2 ml volumes (0.75 ml/min flow rate) (High-load 16/60 Superdex 75 column, Pharmacia Biotech Inc, Uppsala, Sweden). Protein solutions were incubated with an endotoxin removal protein-linked resin at 4°C for 24 hours and separated by centrifugation, 1200 x g at 4°C for 2 minutes. Proteins without a carrier protein (EqIL-1α and EqIL-1β) and with 0.1 % bovine serum albumin (EqIL-1ra) were aliquotted and stored at –70°C.

D. Protein characterization

Proteins were evaluated by sodium dodecyl-sulfate polyacrylamide gel electrophoresis (SDS-PAGE). Fractions migrating as single protein bands consistent with the predicted molecular mass of the mature forms of EqIL-1 (18.147 kDa for IL-1α, 17.3 kDa for IL-1β, and 17.423 kDa for IL-1ra) were pooled and re-analyzed by SDS-

PAGE **(Figure A2)**. Purity was verified by single peak protein detection at appropriate molecular weights using high-pressure reversed phase liquid chromatography and a trifluoroacetic acid gradient mobile phase (1.0 ml/min flow rate, 2500 psi, 25°C) **(Figure A3)**. Endotoxin levels were determined using a limulus amebocyte lysate assay (< 0.01 ng/ug) (Associates of Cape Cod, Inc, Falmouth MA). Protein concentrations were determined using a Bradford spectrophotometric assay (Sigma Chemical Co, St Louis MO): EqIL-1α = 4.24 ug/ml, EqIL-1β = 70.75 ug/ml, and EqIL-1ra = 34.0 ug/ml.

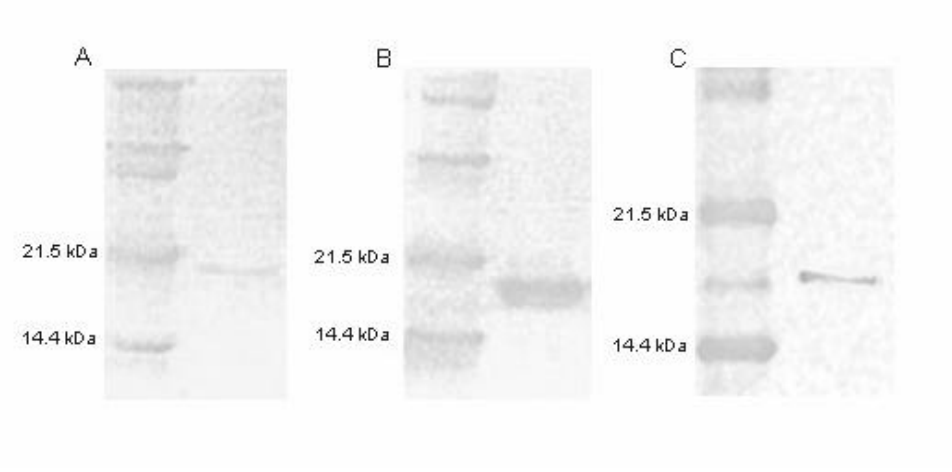

Figure A2 - IL-1 protein SDS-PAGE results.

A= EqIL-1α, B= EqIL-1β, C= EqIL-1ra.

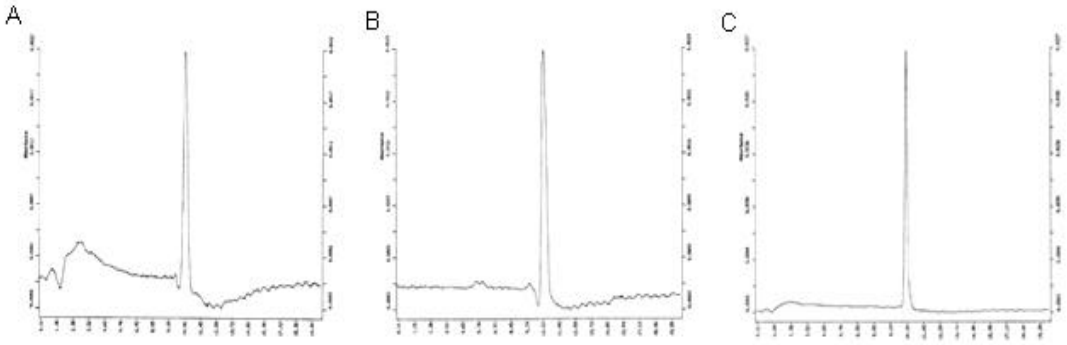

Figure A3 - IL-1 protein HPLC results.

A= EqIL-1α, B= EqIL-1β, C= EqIL-1ra.

APPENDIX II: Approaches to cDNA array development

A. Target clone compilation

1. Donation

Thirty-nine equine clones were donated from multiple sources **(Table AI)**: 1) Dr. Rick Howard, Colorado State University, Fort Collins, CO, 2) Dr. Dean Richardson, University of Pennsylvania School of Veterinary Medicine, Kennett Square, PA, 3) Dr. Nobushige Ishida, Laboratory of Molecular and Cellular Biology, Equine Research Institute, Tokami-Cho, Utsunomiya, Tochigi, Japan, 4) Dr. David Horohov, Department of Veterinary Science, University of Kentucky, Lexington, KY, 5) Dr. Jim Belknap, Auburn University, Large Animal Surgery / Medicine, Auburn, AL, and 6) Dr. Peter Clegg, Department of Veterinary Clinical Science and Animal Husbandry, University Teaching Hospital, University of Liverpool, Leahurst, Neston, UK.

Seven non-equine cDNA probes were donated by: 1) Dr. Victor Han, MRC Group in Fetal and Neonatal Health and Development, University of Western Ontario, Ontario Canada, 2) Dr. Joshua Vanhouten, Yale University School of Medicine, New Haven, CT, 3) Dr. Eric Smith, Division of Endocrinology, Children's Hospital Medical Center, Cincinnati, OH, and 4) Dr. Russel Hovey, National Institutes of Health, Molecular and Cellular Endocrinology Section, Bethesda MD.

Table AI - Donated cDNA clones.

Gene	*Species*	*Donator*	*Genbank*	*Category **	*Length (bp)*
Constitutively expressed nitric oxide synthase (c-NOS)	Equine	Belknap	X	6	416
Endothelin	Equine	Belknap	X	5	354
Tissue factor (TF)	Equine	Belknap	X	5	449
Insulin-like growth factor binding protein-1 (IGF BP-1)	Ovine	Han	X	1	500
Insulin-like growth factor binding protein-2 (IGFBP-2)	Ovine	Han	S44612	1	690
Insulin-like growth factor binding protein-3 (IGFBP-3)	Rat	Smith	X	1	440
Insulin-like growth factor binding protein-5 (IGFBP-5)	Porcine	Berry	X	1	317
Keratinocyte growth factor (KGF)	Ovine	Hovey	X	1	622
Parathyroid hormone receptor (PtHR)	Murine	Van Houten	X	1	283
Parathyroid hormone related protein (PThrP)	Murine	Van Houten	X	1	467
Insulin-like growth factor 1 receptor (IGF-1R)	Equine	Clegg	X	1	589
Lysysl oxidase (LO)	Equine	Clegg	X	5	2603
Matrix metalloproteinase-2 (MMP-2)	Equine	Clegg	X	5	396
TNF*? converting enzyme (TACE)*	Equine	Clegg	X	6	1058
Tissue inhibitor of matrix metalloproteinase-2 (TIMP-2)	Equine	Clegg	X	5	313
? -Actin	Equine	Horohov	AF035774	4	1128
Interleukin-10 (IL-10)	Equine	Horohov	U38200	6	739
Interleukin-2 (IL-2)	Equine	Horohov	L06009	6	447
Interleukin-4 (IL-4)	Equine	Horohov	L06010	6	396
Interleukin-5 (IL-5)	Equine	Horohov	U91947	6	405
Interleukin-6 (IL-6)	Equine	Horohov	U64794	6	745
Interleukin-1alpha (IL-1*?)*	Equine	Howard	U92480	6	1728
Interleukin-1 beta (IL-1*?)*	Equine	Howard	U92481	6	1473
Interleukin-1 receptor antagonist (IL-1ra)	Equine	Howard	U92482	6	1614
Cartilage oligomeric protein (COMP)	Equine	Ishida	AB040453	5	309
Cyclooxygenase-1 (COX-1)	Equine	Ishida	AB039865	6	385
Cyclooxygenase-2 (COX-2)	Equine	Ishida	AB041771	6	1267
Inducible nitric oxide synthase (I-NOS)	Equine	Ishida	AB039864	6	412
Tumor necrosis factor alpha (TNF*?)*	Equine	Ishida	AB035735	6	791
Insulin-like growth factor-1 (IGF-1)	Equine	Richardson	X	1	407
Link protein	Equine	Richardson	X	5	2603
Matrix metalloproteinase-13 (MMP-13)	Equine	Richardson	AF034087	5	2727
Matrix metalloproteinase-3 (MMP-3)	Equine	Richardson	U62529	5	1804
Tissue inhibitor of matrix metalloproteinase-1 (TIMP-1)	Equine	Richardson	U95039	5	742
Type II Collagen	Equine	Richardson	U62528	5	3778
Type X Collagen	Equine	Richardson	X	5	3180
Biglycan	Equine	Richardson	AF035934	5	2294
Decorin	Equine	Richardson	AF038127	5	1348
Aggrecan	Equine	Richardson	X	5	1937

*Category Code

1=Growth/metabolism, 2=Intracellular signaling, 3=Transcription/translation, 4=Cell adhesion/cytoskeletal regulation, 5=Extracellular matrix metabolism, 6=Inflammation/immunological response

2. Library screening / reverse-transcriptase-PCR (RT-PCR)

A subset of the remaining equine-specific cDNA probes was obtained by screening an LPS-stimulated equine monocyte cDNA library using traditional plaque hybridization techniques (Howard, 1997) **(Table AII)**. Standard RT-PCR amplification techniques were employed using RNA material isolated from injected EqIL-1β (10 ng/ml) carpal joint synovium and articular cartilage tissues to retrieve additional equine cDNAs. Primers were designed to complement partial coding regions of reported equine nucleotide sequences (PrimerSelect, DNASTAR Inc, Madison WI) **(Table AII)**. Degenerate primers were designed for the partial coding region of plasminogen activating inhibitor-1 (PAI-1) based on alignments of human, murine, rat, pig, and bovine sequences (AF508034) (Megalign, DNASTAR Inc, Madison WI).

Briefly, 2.5 ul aliquots of oligo d(T) or random primed reverse transcribed RNA (4 ug) (Universal RiboClone^{TM} cDNA synthesis system, Promega Corporation, Madison WI) were added to PCR reactions consisting of gene-specific primers (0.4 uM), 50 mM KCl, 10 mM Tris-HCl, 0.2 mM dNTPs, and 2.5 U Taq polymerase (Promega Corporation, Madison WI) (50 ul volumes). Aliquots of amplification reactions producing amplicons of the expected length were cloned into pCR2.1 (Invitrogen Corporation, Carlsbad CA) and introduced into TOP10 *E.Coli* cells. Transformants were selected by ampicillin resistance (100 ug/ml). Single colonies were grown in terrific broth starter cultures at 37°C for 16 hours for plasmid isolation and cDNA sequence analysis.

Table AII - Equine clones.

Clone	Genbank	Length (bp)	RT-PCR primers
Aggrecanase-1 (AGG-1) (**)	AF368321	576	UPP: 5'ATGGCTGATGTGGGCACTGT3' LOW: 5'CCAACCACCAGCCTGTG3'
Capping protein, actin-filament, 3'UTR (*)	AF506976	422	
Collagen I (type I) (**)	AF034691	617	UPP: 5'CCCCACCCCAGCCGCAAAGA3' LOW: 5'GGGGGCCAGGGAGACCACGAG3'
Cullin 4A (CUL4A), partial cds (*)	AF508033	736	
Cullin 4B (CUL4B), partial cds (*)	AF513243	438	
Ferritin, heavy chain, complete cds (*)	AY112742	914	
Glyeraldehyde dehydrogenase 3-phosphatase (GADPH) (*)	AF157626		
Galactocerebrosidase (GALC), partial cds and 3'UTR (*)	AF506974	705	
Glucose-regulated protein (GRP94) (TRA1) (*)	AF508791	553	
Granulocyte chemotactic protein-2 (GCP2), complete cds (*)	AY114351	636	
Granulocyte colony stimulating factor (G-CSF), complete cds (*)	AF503365	1361	
Interleukin-1 converting enzyme (ICE) (**)	AF090119	692	UPP: 5'CACACGGCTTGCGCTCATTAT3' LOW: 5'CTCTTTCGGCAGTGGGCATCT3'
Interferon gamma (IFN-g)? (**)	D28520	431	UPP: 5'GTGTGCGATTTTGGGTTCTTCTAC3' LOW: 5'GACTCCTCTTCCGCTTCCTCAG3'
IL-1 receptor (type I), partial cds (**)	AB020338	461	UPP: 5'AAAACCCTTCCCTCAAAA3' LOW: 5'GTCTTCCCCAACATAGTCATC3'
IL-1 receptor (type II), partial cds (**)	AB033415	1079	UPP: 5'TGTTCCCGCCTTCACCATTCAGC3' LOW: 5'TGCGCATCCATATTCCTCCCAAAACC3'
Leukocyte common antigen (LCA), partial cds (*)	AY114350	465	
LPS-induced TNFa factor (LITAF), complete cds (*)	AF503366	1579	
Monocyte chemotactic protein-2 (mcp-2), complete cds (*)	AF506972	828	
Plasminogen activating inhibitor-1 (PAI-1), partial cds (**)	AF508034	844	UPP: 5'GGG(CG)CC(GA)TGGAACAA(GA)GATGAGAT3' LOW: 5'TGCCG(CGA)ACCAC(GA)AA(GC)AG3'
Plasminogen activating inhibitor-2 (PAI-2), 3'UTR (*)	AF508790	510	
Phosphoinositol-3-kinase related kinase (PI-3-K), 3'UTR (*)	AF506975	979	
Phosphoprotein (C8FW), partial cds (*)	AF506971	492	
Ras GTPase-activating protein (NGAP), partial cds and 3'UTR (*)	AY113683	1221	
Ribosomal protein L5 (RPL5), complete cds (*)	AY113682	987	
Small inducible cytokine A5 (RANTES), complete cds (*)	AF506970	773	
Special AT-rich binding protein-1 (SATB1), partial cds (*)	AF508032	505	
Transforming growth factor beta-1 (TGF-b1) (**)	AF175709	623	UPP: 5'AGTGCCCGATCCCATGCTGCTCTCC3' LOW: 5'ACGCGCCCGGGTTGTGCTGGTTGTA3'
Thymosin beta 10, complete cds (*)	AF506973	465	
Ubiquitin, complete cds (*)	AF506969	1157	
Zinc finger binding protein-9 (ZNF9), partial 3'UTR (*)	AF513861	587	

* Derived by plaque hybridization screening of a LPS-stimulated monocyte cDNA library

** Derived by reverse transcriptase polymerase chain reaction (RT-PCR)

Bolded Genbank accessions refer to cDNAs submitted by our laboratory

3. Suppression subtractive hybridization-PCR

Equine cDNA clones corresponding to known and unknown sequences (expressed sequence tags, (ESTs)) were obtained using a suppressive subtraction hybridization-PCR (SSH-PCR) strategy and synovial tissues stimulated with EqIL-1β (*Chapter V*). In some instances, multiple non-overlapping clones corresponding to the same gene were identified (SeqMan, DNASTAR Inc, Madison WI) and are denoted by different nucleotide sequence lengths **(Table AIII)**. The remaining equine clones were retrieved using SSH-PCR to identify: 1) Differentially expressed genes in lung tissue biopsied from horses in remission and those with an induced chronic obstructive pulmonary condition, and 2) Differentially expressed genes in normal small intestinal tissue and reperfused tissue following a surgically induced mucosal ischemia (K. Seat[1], V. Takafuji[2], R. Howard[2], M. Crisman[1], A. Blikslager[3], Molecular Diagnostics Laboratory[1] and Orthopedic Research Laboratory[2], Large Animal Clinical Sciences, VA-MD Regional College of Veterinary Medicine and College of Veterinary Medicine, North Carolina State University, Raleigh NC[3]) **(Table AIV)** (data not published).

4. Commercial purchase

Murine cDNAs were purchased from American Tissue Culture Collection, Manassas VA and Incyte Genomic Inc, La Jolla CA as plasmid constructs **(Table AV)**. Clones were received as bacterial slants and grown in culture for plasmid isolation as described below. Sequence identity was verified using single-pass sequencing and alignment to public databases as described below. Nucleotide cDNA lengths were verified by restriction enzyme digestion and agarose gel electrophoresis / ethidium bromide visualization analysis.

Table AIII - Equine clones derived by SSH-PCR (Chapter V).

cDNA	*Genbank Accession*	*Length (bp)*	*Category **
Acidic ribosomal protein P2 (RPP2)	AY246717	384	3
Associated binder-1 protein (Grb-2)	AY246706	192	2
b-2 microglobulin (b2M)	AY246748	401	6
Bromodomain containing 1 nuclear protein (BDNF)	AY246718	95	3
Bromodomain transcription factor (BPTF)	AY246719	190	3
Calpactin I light chain (p11)	AY246740	117	4
Cartilage leucine-rich protein, chondroadherin (CHO)	AY343542	394	5
Complement C1s (CC1s)	AY246749	223	6
Cytochrome c oxidase subunit IV isoform (COXIV)	AY246701	109	6
Elongation factor 1A (EF1A)	AY246720	246	3
Basic fibroblast growth factor receptor 1 (FGFRI)	AY246707	148	1
G-beta like protein, guanine nucleotide binding protein	AY246708	452	2
Gelsolin	AY246741	249	4
Glutathione peroxidase, plasma isoform (GPx-3)	AY246750	126	6
Growth factor receptor tyrosine kinase (KIDR)	AY246709	236	2
Heterogenous ribonucleoprotein D-like (hnRNPD)	AY246721	358, 734	3
Histone H3.3B (His3B)	AY246722	198	3
HnRNP core protein A1 (HCP-1)	AY246723	184	3
Hypothetical protein, similar to DET1 (DET1)	AY246761	338	7
KIAA0185 hypothetical protein	AY246762	737	7
KIAA1053 hypothetical protein	AY246763	352	7
Kinesin, heavy chain-like protein (KHCHP)	AY246742	337	4
Lactate dehydrogenase B (LDHB)	AY246702	431	1
Laminin, *β1 (Lamb1)*	AY246744	112	5
Manganese superoxide dismutase (Mn-SOD)	AY246751 - AY246753	526, 241	6
Metalloproteinase-1 (MMP-1)	AY246754 - AY246756	372, 126, 333	6
N-myc / STAT interactor	AY246724	535	3
Nucleolin (NCL)	AY246725	379	3
PCTAIRE protein kinase 1	AY246710	71	2
Pleckstrin (p47)	AY246711	743	2
Proliferation-associated protein 2G4 (Pa2g4)	AY246703	79	1
Protein phosphatase 1 (PPP1), catalytic subunit	AY246712	263	2
Proteoglycan 4 (PRG4)	AY246745	190	5
PTD016 hypothetical protein	AY246764	267	7
Retinoblastoma related protein-1	AY246704	362	1
Ribosomal protein L17 (RPL17)	AY246726	246	3
Ribosomal protein L18 (RPL18)	AY343541	107	3
Ribosomal protein L19 (RPL19)	AY246727	243	3
Ribosomal protein L35a related pseudogene (RPL35a)	AY246728	165	3
Ribosomal protein L41 (RPL41)	AY246729	201	3
Ribosomal protein L7 (RPL7)	AY246730	182	3
Ribosomal protein S12 (RPS12)	AY246731	154	3
Ribosomal protein S26 (RPS26)	AY246732	278	3
Ribosomal protein S9 (RPS9)	AY246733	331	3
Ring finger protein (RFP)	AY246734	104	3
RNA binding protein, ewing sarcoma (EWS)	AY246735	223	3
Serine-threonine kinase (STE20)	AY246713, AY246714	395, 340	2
Serum amyloid A (SAA)	AY246757	362	6
Seven in absentia homolog (Siah2)	AY246715	418	2
Signal transducer and activator of transcription (STAT3)	AY246736	227	3
Suppressor of RNA polymerase B homolog (SRB7)	AY246737	304	3

*Category Code

1=Growth/metabolism, 2=Intracellular signaling, 3=Transcription/translation, 4=Cell adhesion/cytoskeletal regulation, 5=Extracellular matrix metabolism, 6=Inflammation/immunological response, 7=unknown function

Table AIII (Cont.) - Equine clones derived by SSH-PCR (Chapter V)

cDNA	*Genbank Accession*	*Length (bp)*	*Category **
Superoxide dismutase-2 (SOD-2)	AY246758, AY246759	50, 332, 402	6
Syntenin, syndecan binding protein	AY246746	498	5
Tenascin C (hexabrachion)	AY246747	123	5
Thymosin b4 (Thy b4)	AY246743	152	4
Transforming growth factor beta receptor 2 (TGFbR2)	AY246716	85	6
Transketolase (TKT)	AY343543	627	1
Tumor rejection antigen (gp96)	AY246760	138	6
Ubiquitin-like ribosomal protein (fau)	AY246705	355	1
WW domain binding protein 11 (SNP70)	AY246738	390	3
Zinc finger protein (ZFP)	AY246739	308	3
Est1	AY246765	229	7
Est2	AY246766	279	7
Est3	AY246767	161	7
Est4	AY246768	190	7
Est5	AY246769	350	7
Est6	AY246770	412	7
Est7	AY246771	250	7
Est8	AY246772	227	7
Est9	AY246773	437	7
Est10	AY246774	226	7
Est11	AY246775	304	7
Est12	AY246776	399	7
Est13	AY246777	282	7
Est14	AY246778	771	7
Est15	AY246779	505	7
Est16	AY246780	277	7
Est17	AY246781	163	7
Est18	AY246782	327	7
Est19	AY246783	515	7
Est20	AY246784	704	7
Est21	AY246785	654	7
Est22	AY246786	629	7
Est23	AY246787	308	7
Est24	AY246788	122	7
Est25	AY246789	139	7
Est26	AY246790	277	7
Est27	AY246791	715	7
Est28	AY246792	193	7
Est29	AY246793	74	7
Est30	AY246794	515	7
Est31	AY246795	648	7
Est32	AY246796	67	7
Est33	AY246797	216	7
Est34	AY246798	110	7
Est35	AY246799	303	7
Est36	AY246800	549	7
Est37	AY246801	194	7
Est38	AY246802	212	7
Est39	AY246803	410	7
Est40	AY246804	263	7
Est41	AY246805	235	7

*Category Code
1=Growth/metabolism, 2=Intracellular signaling, 3=Transcription/translation, 4=Cell adhesion/cytoskeletal regulation, 5=Extracellular matrix metabolism, 6=Inflammation/immunological response, 7=unknown function

Table AIII (Cont.) - Equine clones derived by SSH-PCR (Chapter V)

cDNA	*Genbank Accession*	*Length (bp)*	*Category **
Est42	AY246806	652	7
Est43	AY246807	553	7
Est44	AY246808	654	7
Est45	AY246809	344	7
Est46	AY246810	285	7
Est47	AY246811	427	7
Est48	AY246812	322	7
Est49	AY246813	265	7
Est50	AY246814	499	7
Est51	AY246815	620	7
Est52	AY246816	574	7
Est53	AY246817	324	7
Est54	AY246818	534	7
Est55	AY246819	304	7
Est56	AY246820	140	7
Est57	AY246821	268	7
Est58	AY246822	256	7
Est59	AY246823	285	7
Est60	AY246824	349	7
Est61	AY246825	640	7
Est62	AY246826	379	7
Est63	AY246827	417	7
Est64	AY246828	194	7
Est65	AY246829	241	7
Est66	AY246830	214	7
Est67	AY246831	535	7
Est68	AY246832	167	7
Est69	AY246833	153	7
Est70	AY246834	114	7
Est71	AY246835	241	7
Est72	AY246836	700	7
Est73	AY246837	209	7
Est74	AY343544	448	7
Est75	AY343545	493	7
Est76	AY246838	941	7
Est77	AY246839	761	7
Est78	AY246840	620	7
Est79	AY246841	684	7
Est80	AY246842	704	7
Est81	AY246843	765	7
Est82	AY246844	270	7
Est83	AY246845	836	7
Est84	AY246846	104	7
Est85	AY246847	519	7
Est86	AY246848	535	7
Est87	AY246849	873	7
Est88	AY246850	700	7
Est89	AY246851	476	7
Est90	AY246852	687	7
Est91	AY246853	573	7
Est92	AY246854	679	7
Est93	AY246855	503	7

*Category Code

1=Growth/metabolism, 2=Intracellular signaling, 3=Transcription/translation, 4=Cell adhesion/cytoskeletal regulation, 5=Extracellular matrix metabolism, 6=Inflammation/immunological response, 7=unknown function

Table AIV - Additional equine clones derived by SSH-PCR.

(K. Seat[1], V. Takafuji[2], R. Howard[2], M. Crisman[1], A. Blikslager[3], Molecular Diagnostics Laboratory[1] and Orthopedic Research Laboratory[2], Large Animal Clinical Sciences, VA-MD Regional College of Veterinary Medicine and College of Veterinary Medicine, North Carolina State University, College of Veterinary Medicine, Raleigh NC[3])

cDNA	*PCR product length estimate (bp)*	*Category**
EST #1 [APOD]	400	7
Ras homolog gene family, member A (A-ras)	750	2
BTAF1 RNA polymerase II	500	3
Cadherin 1, E-cadherin	700	4
EST #2 [Calcineurin A]	450	7
28S rRNA [CACY]	600	1
EST #3 [Calnexin]	400	7
Cdk1/cdc2	650	1
Collagen type III, alpha 1 chain (COLIIIA1)	500	5
Collagen type IV	350	5
Cytokeratin 20 (KRT20)	650	5
Deoxyribonuclease I-like 1 (DNASE1L1)	1000	3
Dermatopontin (DPT)	500	5
Dipeptidase	650	1
Eukaryotic translation initiation factor 3, subunit 7 (EIF3s7)	400	3
Glia maturation factor B (GMFB)	1000	7
G-protein pathway suppressor	375	2
Heat shock protein 90 (Hsp90)	450	6
Immunodominant MHC-assoc peptides	800	6
Liprin	475	2
Lumican	450	5
Lysosomal associated membrane protein-2 (LAMP-2)	800	6
Matrix Gla protein	1000	5
Meprin A, beta (MEP1B)	500	6
Major histocompatibility complex class II (MHCII)	490	6
Mucin / cadherin-like (MUCDHL)	600	4
Nucleosome assembly protein 1-like 4 (NAPIL4)	450	3
NCK-1 associated protein	300	1
Neuropilin-1	1500	7
Nucleolar protein GU2 (GU2)	1000	3
Osteoclast stimulating factor (OSF)	400	7
Platelet activating factor acetylhydrolase (PAFA)	700	6
Phosphatidic acid phosphatase type 2A (PAP2A)	800	2
Protein phosphatase type IB, beta isoform (PP1B)	700	2
Pre-mRNA processing 8 (Prp8)	475	3
Proteosome subunit, alpha type 4 (PSMA4)	500	1
Selenoprotein P (SEPP1)	850	1
Sialomucin (CD164)	650	4
Similar to serine / threonine kinase (STK)	800	2
Splicing factor 3b, subunit 1 (SF3b)	450	3
Supervillin (SVIL)	800	4
Terminal deoxynucleotidyl transferase (TdT)	450	3
Transcription factor YY1 (YY1)	600	3
Transmembrane protein (TMP)	600	4
Tumor associated calcium signal transducer (CST)	550	2
Type I collagen, alpha 2 chain (COLIA2)	475	5
Vesicle associated membrane protein, A (VAMPA)	800	1
Zinc finger protein 216 (ZNP216)	1000	3

*Category Code

1=Growth/metabolism, 2=Intracellular signaling, 3=Transcription/translation, 4=Cell adhesion/cytoskeletal regulation, 5=Extracellular matrix metabolism, 6=Inflammation/immunological response, 7=unknown function

Table AV - Purchased cDNA clones.

Gene	*IMAGE #*	*ATCC #*	*Incyte #*	*Genbank #*	*Category **
AA3	573265	731673	148439	AA119121	4
AA4	693045	261454	148440	AA397114	4
AA5	426546	883660	148441	AA002439	4
AA6	876698	249577	148442	AA499296	4
AA7	681168	239295	148443	AA242060	4
Api2	599072	757480		AA172848	1
BAD	3367405	9565960		BF117194	1
BAK	1432180	1699621		AA986402	1
BAX	1348860	1616301		AA981864	1
bcl2l	478723	935817	171537	AI401297	1
BID	2332217	3523937		AW259335	1
BMP-4	873328		171539	AA473799	1
BMP-5	737934		148446	AA270991	1
c-abl	2101588		171535	AW209918	2
Cad2	671834	240243	148452	AA242226	4
Cad3	329780	586893	148453	W12889	4
Calm3	571789	730197	171540	AA109041	1
Casp11	1365932	1633373		AI0212244	1
Casp12	1511485	3130597		AI1786517	1
Casp14	608722		171541	AI448765	1
Casp-2	639403	797811	148449	AA200808	1
Casp6	1314468	1581909		AA914450	1
Casp7	1498931	1765988		AI131763	1
Casp8	2136335	3334583		AI1957073	1
Casp9	1477823	1744880		AI155822	1
CcnB1	751977		148455	AA396324	1
CcnD2	424433	881547	148456	W98440	1
CcnG	523713	980827	148457	AA067318	1
cdc2a	468792	925906	148450	AA035888	1
cf11	350344	807458	148454	W40725	6
c-fos	426070	883184R		AA602910	2
c-jun	975691	1231045		AA572155	2
CREB	1039340	1294694	171543	AA624941	2
c-rel	1846617	1855169		AI247359	2
Cytochrome C	481959		171544	AA059641	6
DHFR	1327568	1595009		AA920415	1
E2f1	751755		148458	AA396123	3
EGF	1970574	1979126		AI648855	1
EGFR	493277	940371		AA061578	1
Egr-1	1313961	1581402		AA914501	2
Egr-2	1209893	1477334		AA727313	2
ep-1	990752	1246106		X	6
ep2	1400942	1668383		AI463444	6
ERK-1	1248312	1515753		AA789576	2
ERK-2	687970	256379		AA235927	2
FGF-1	720400	288809	148459	AA261582	1
Fibronectin	748123			AA275041	5
Fol1	580643	739051		AA139715	1
Fol2	468045	925159		AA015571	1
GAS	493391	950485		AA087048	1
GAS-2	820540	1081270	148461	AA423395	1
GAS-5	1327920	1595361		AA915397	1
GDF-1	386194	843308	148462	W65054	1
GH	330360	587476		W14555	1
GST	421833	878947	148460	W91402	1
GzmB	636781	795189	148463	AA183327	6
Gzmf	456459	913573	148464	AA023418	6

*Category Code

1=Growth/metabolism, 2=Intracellular signaling, 3=Transcription/translation, 4=Cell adhesion/cytoskeletal regulation, 5=Extracellular matrix metabolism, 6=Inflammation/immunological response

Table AV (Cont.) - Purchased cDNA clones

Gene	*IMAGE #*	*ATCC #*	*Incyte #*	*Genbank #*	*Category **
Histone 3a	776614		171546	AA275906	3
Ia1	1149832	1417273		AA795625	4
Ia5	440295	897408		AA016695	4
Ia6	2372672	3569768		AW318623	4
Ib1	670661	239070		AA23903	4
Ib2	808785			AA467489	4
IER-2	472605	929719	148465	AA038052	2
IGF-2	482009	939103		AA059967	1
Ihh	699460	267869		AA245525	1
IKBa	641058	799466	148466	AA204405	2
IL-12-35	1379220	1646661		AI050362	6
IL-12-40	720765	289174R		AA267353	6
IL-15	1263853	1531294		AA862763	6
IL-16	2803347		171549	AW761753	6
IL-9R	557898	716306	171548	AA106013	6
Jak-2	621226	779634	148467	AA178495	2
Jak-3	457114	914228	148468	AA023670	2
mdm-2	2803092		171551	AW822859	1
Mekk	621032	621032	148469	AA178632	3
MIP-1a	533862	990976	171552	AI326603	1
MMP-9	1969661		171553	AI574470	5
NFKB-1	777643	1046053		AA276822	3
NFKB-2	482952	940046		AI385509	3
Nos-3	620940	620940	148471	AA177420	6
p21	1153742	1421183		AA792520	1
p21/H-ras-1	1398160	1665601		AI116111	1
p53	1279021	1546462		AA896672	1
PDGFA	2227972	3420076		AI583995	1
PDGFB	343320	800434		AA162467	1
PGDS	571621	730029		AI323558	6
PIAS-1	1435826	1703267		AA937577	1
Pkacb	478265	935379	148473	AA049744	2
PKCa	371215		171556	AI894239	2
PKCd	1067015	1332353		AA616214	2
Rb1	832714	1089220	148474	AA427019	1
RhoA	578550	736958		AA162923	2
RhoC	670886	239295	148444	AA221997	2
R-ras	807845	1070111		AA432641	2
Rxra	676526	244935	148475	AA209592	2
SMAD3	456861	913975	148476	AA023641	2
SOCS-1	819829	1080559		AA437930	3
STAT-1	760885	1029295		AA386678	6
TGF-b2	524678	981792		AI323791	6
TGF-b3	554266	712674		AA103431	2
TRAF-1	636225		171559	AA183167	2
TRAF2A	614108	772516		AA165848	2
TRAF5	616797	775205		AA170423	2
wee-1	539548	996662		AA123301	1

*Category Code

1=Growth/metabolism, 2=Intracellular signaling, 3=Transcription/translation, 4=Cell adhesion/cytoskeletal regulation, 5=Extracellular matrix metabolism, 6=Inflammation/immunological response

5. Clone processing, electrotransformation, sequencing

Clones received as agar slant cultures were grown in terrific broth starter cultures with ampicillin (100 ug/ml) overnight at 37°C. Clones received as plasmid aliquots were transformed into electrocompetent *E.Coli BMH 71-18* mutant cells (CLONTECH Laboratories, cat. K1600-1, Palo Alto, CA) at a 1.25 kV/cm field strength for approximate 5 millisecond pulses (Electroporator 2510, Eppendorf Scientific Inc, Westbury NY). Cuvettes, cell solutions (40 ul), and DNA solutions were chilled on ice prior to electroporation (0-4°C). Single clone transformants were grown at 37°C for 16 hours in terrific broth starter cultures (10 ml) with ampicillin (100 ug/ml). Clones obtained by donation, plaque hybridization screening, and SSH-PCR were verified for identity using bi-directional automated DNA sequencing on an ABI 377 automated DNA Sequencer or an ABI 3100 capillary sequencer and using Applied Biosystems BigDye (version 3.0) Terminator chemistry (Core Laboratory Facility, Virginia Bioinformatics Institute, Blacksburg VA). Cycle sequencing reactions were performed using 400 ng plasmid templates (10ng / 100bp for PCR products) and 3.2 pmol vector-specific primers in 15 ul reaction volumes. Cycling parameters were: 30 cycles of 95°C for 30 seconds, 50°C for 15 seconds, 60°C for 4minutes. Reactions were purified using Multiscreen^{TM} plates (Millipore, Bedford, MA), dried, and re-suspended as per manufacturer's protocols for loading on the automated sequencer. Chromatogram results were viewed and edited using Editview software (DNASTAR Inc, Madison WI) and aligned to public nucleotide databases (BLAST, National Center for Biotechnology Information, NIH, Bethesda MD). Nucleotide probe lengths were verified by restriction enzymatic digestion and agarose gel electrophoresis / ethidium bromide visualization. Glycerol stocks (1 ml volume) (15 %) were stored at -70°C.

6. Plasmid isolation

Starter cultures were used to seed terrific broth cultures (500 ml) grown at 37°C, 180 rpm, for 16 hours (A_{600} = 1.0) with ampicillin (100 ug/ml). Bacterial cells were

pelleted at 6000 rpm for 15 minutes at 4°C and resuspended in a buffer of 500 mM glucose, 10 mM EDTA, 25 mM Tris-HCl, pH 8.0. Cells were lysed with a 0.2 N NaOH, 1% SDS solution on ice for 10 minutes. Cellular debris was removed by precipitation with a 3M potassium acetate solution (pH 5.2) and centrifugation at 10,000 rpm for 15 minutes. Supernatants were filtered through sterile gauze and treated with RNAase (0.2 mg / ml supernatant) at 37°C for 40 minutes. Protein was extracted with the serial addition of three volumes of chloroform (1:1) and centrifugation at 6000 rpm for 15 minutes. DNA was precipitated with isopropanol (1:1 volume), centrifuged at 6000 rpm for 15 minutes at 25°C, re-suspended in distilled water, and re-precipitated with NaCl and polyethylene glycol on ice for 60 minutes. Solutions were centrifuged at 10,000 rpm at 4°C for 15 minutes and DNA pellets were washed with 70% ethanol, vortexed, and centrifuged at 10,000 rpm at 4°C for 15 minutes. DNA pellets were air-dried and resuspended in appropriate volumes of TE buffer (10 mM Tris-HCl, 1 mM EDTA, pH 7.5).

B. Array construction

1. 169-element cDNA array (Chapter III) (Table AVI)

This array consisted of: 102 equine clones (33 genes and 9 ESTs from suppression subtractive hybridization-PCR project), 67 murine, 3 ovine, 1 porcine, 1 rat; 4 house-keeping controls (equine and murine glyceraldehyde-3-phosphatase dehydrogenase (GAPDH) and β-actin), 3 positive hybridization controls (cDNA from chondrocytes, synovium, cartilage), and 1 negative hybridization control (plasmid DNA). Duplicate spots were printed on duplicate membranes (quadruplicate data points total).

2. 380-element cDNA array (Chapter IV) (Table AVII)

This array consisted of: 265 equine clones (63 genes and 93 ESTs from suppression subtractive hybridization project), 108 murine, 3 ovine, 1 porcine, 1 rat; 2 house-keeping controls (equine glyceraldehyde-3-phosphatase dehydrogenase (GAPDH) and β-actin), 1 positive hybridization control (chondrocyte cDNA), 1 positive labeling control (poly A oligo), 1 negative hybridization control (plasmid DNA), and 1 negative printing control (printing solution alone). Single spots were printed on duplicate membranes (duplicate data points total).

Table AVI - 169-element cDNA array (Chapter III).

EST #1	IL-4	TIMP-1	mdm-2
AGG-1	IL-5	TIMP-2	Mekk
Aggrecan	IL-6	TNFa	MIP-1a
EQ b-Actin	I-NOS	Transketolase	MMP-9
Biglycan	KGH	EST #9	NFKB-1
b2-microglobulin	KIAA1053	Tubulin	NFKB-2
BPTF	LCA	Type II Collagen	Nos-3
C8FW	Link protein	Type X Collagen	p21
Actin-filament	LITAF	Ubiquitin	p53
EST #2	LO	ZNP9	PDGFA
c-NOS	mcp-2	Mu*β*-actin	PDGFB
COL1A1	MHCI	BAD	PGDS
COMP	MMP-1	BAX	PKB
COX-1	MMP-13	bcl2l	PKCa
COX-2	MMP-2	BMP-4	PKCd
Cullin 4A	MMP-3	BMP-5	R-ras
Cullin 4B	Mn-SOD	Calm3	SMAD3
COXIV	EST #4	Casp-2	SOCS-1
Decorin	EST #5	Casp-9	STAT-1
EF1A	NF *yθ*	cf11	STAT3
Endothelin	NGAP	c-fos	TGF-b2
EWS	N-myc / STAT	c-jun	TGF-b3
Fau	Nucleolin	CREB	TRAF-1
Ferritin	PAI-1	E2f1	TRAF2A
EST #3	PAI-2	EGF	TRAF5
GALC	EST #6	EGFR	wee-1
EQ GAPDH	PI-3-K	EstR	Positive control (Syn sscDNA)
G-beta like protein	Pleckstrin	FGF-1	Positive control (Cart sscDNA)
GCP2	EST #7	Fibronectin	Positive control (Ch sscDNA)
Gelsolin	PTD016	Fol1	Printing control (solution alone)
GM-CSF	PtHR	Fol2	
GPx	PThrP	Mu GAPDH	
Gab-1	RANTES	GAS	
hnRNP	EST #8	GH	
ICE	RPL18	Ib1	
IFNg	RPL19	Ib5	
IGF BP-1	RPL5	Ib6	
IGF BP-2	RPL7	Ib1	
IGF BP-3	RPP2	Ib2	
IGF BP-5	RPS9	IGF-2	
IGF-1	SATB1	Ihh	
IGF-1R	SRB7	IKBa	
IL-10	STE20	IL-12-35	
IL-1a	TACE	IL-12-40	
IL-1b	Tenascin	IL-15	
IL-1ra	TF	IL-16	
IL-1RI	TGF-b1	IL-9R	
IL-1RII	TGFbR2	Jak-2	
IL-2	Thymosin b10	Jak-3	

Table AVII - 380-element cDNA array (Chapter IV).

AGG-1	MMP-3	CcnD2	MIP-1a	KIAA0185	28S rRNA (CACY)	Est57
Aggrecan	MRP Rnase	CcnG	MMP-9	KIAA1053	Cdk1/cdc2	Est58
b-Actin	NF yβ	cdc2a	NFKB-1	KHCHP	COLIIIa1	Est59
Biglycan	NGAP	cf11	NFKB-2	LDHB	COLIV	Est60
C8FW	PAI-1	c-fos	Nos-3	Lamb1	Cyto c	Est61
Actin filament	PAI-2	c-jun	p21	Mn-SOD	KRT20	Est62
c-NOS	PI-3-K	CREB	p21/H-ras-1	MMP-1	DNASE1L1	Est63
COL1A1	PtHR	c-rel	p53	N-myc / STAT	DPT	Est64
COMP	PThrP	DHFR	PDGFA	Nucleolin	Dipeptidase	Est65
COX-1	RANTES	E2f1	PDGFB	PCTAIRE-1	GMFB	Est66
COX-2	RPL5	EGF	PGDS	Pleckstrin	G-suppressor	Est67
Cullin 4A	SATB1	EGFR	PIAS-1	Pa2g4	G-regulator	Est68
Cullin 4B	TACE	Egr-1	PKB	PPP1	Hsp90	Est69
Decorin	TF	Egr-2	PKCa	PRG4	MHC peptides	Est70
Endothelin	TGF-b1	ep-1	PKCd	PTD016	Liprin	Est71
Ferritin	Thy b10	ep2	Rb1	Rb protein-1	Lumican	Est72
GALC	TIMP-1	ERK-1	RhoA	RPL17	LAMP-2	Est73
GAPDH	TIMP-2	ERK-2	RhoC	RPL18	Matrix Gla	Est74
GCP2	TNFa	FGF-1	R-ras	RPL19	Meprin A, beta	Est75
GM-CSF	COLII	Fibronectin	Rxya	RPL35a	MHCII	Est76
ICE	COLX	Fol1	SMAD3	RPL41	MUCDHL	Est77
IFNg	Ubiquitin	Fol2	SOCS-1	RPL7	NCK-1	Est78
IGF BP-1	ZNP9	GAS	STAT-1	RPS12	Neuropilin-1	Est79
IGF BP-2	AA3	GAS-2	ZNP216	RPS26	GU2	Est80
IGF BP-3	AA4	GAS-5	TGF-b2	RPS9	OSF	Est81
IGF BP-5	AA5	GDF-1	TGF-b3	RFP	PAFA	Est82
IGF-1	AA6	GH	TRAF-1	EWS	PAP2A	Est83
IGF-1R	AA7	GST	TRAF2A	STE20	PP1B	Est84
IL-10	Api2	Gzmf	TRAF5	SAA	Prp8	Est85
IL-1a	BAD	GznB	wee-1	Siah2	PSMA4	Est86
IL-1b	BAK	Histone 3a	RPP2	STAT3	TMP	Est87
IL-1ra	BAX	Ib1	Gab-1	SRB7	SEPP1	Est88
IL-1RI	bcl2l	Ib5	b-2M	SOD-2	Sialomucin	Est89
IL-1RII	BID	Ib6	BDNF	Syntenin	STK	Est90
IL-2	BMP-4	Ib1	BPTF	Tenascin C	EIF3s7	Est91
IL-4	BMP-5	Ib2	CalpI (p11)	Thymosin b4	SF3b	Est92
IL-5	c-abl	IER-2	CHO	TGFbR2	SVIL	Est93
IL-6	Cad2	IGF-2	CC1s	TKT	TdT	Printing control (solution alone)
I-NOS	Cad3	Ihh	COXIV	Tubulin	YY1	Negative control (plasmid DNA)
KGH	Calm3	IKBa	EF1?	Gp96	CST	Positive control (sscDNA)
LCA	Casp11	IL-12-35	FGFRI	Fau	COLIA2	Positive control (polyA oligo)
Link protein	Casp12	IL-12-40	G-b protein	SNP70	VAMPA	
LITAF	Casp14	IL-15	Gelsolin	ZFP	Est1	
LO	Casp-2	IL-16	GPx-3	EST #1 [APOD]	Est2	
mcp-2	Casp6	IL-9R	KIDR	A-ras	Est3	
MHCI	Casp7	Jak-2	hnRNPD	BTAF1	Est4	
NAPIL4	Casp8	Jak-3	His3B	Cadherin 1	Est5	
MMP-13	Casp9	mdm-2	HCP-1	EST #2 [CalcA]	Est6	
MMP-2	CcnB1	Mekk	DET1	EST#3 [CALN]	Est7	

3. Array printing

Fifty microliters of purified PCR products diluted in TE buffer (5.0 ng/ul) (~15-50 nM target solutions) were pipetted into four 96-well 'source' PCR-plates after determining the desired printing order on the membrane (i.e. using the 2 x 2 spacing on the plate orienter will result in a 384-array). Two microliter volumes of a 0.125 % bromophenol blue dye solution (0.005 % final concentration) were added to the side of each tube using a multi-channel pipetter and spun down into solution (500 x g for 30 seconds). DNA was denatured by heating the plates to 95°C for 10 minutes followed by quenching in an ice water bath (5 minutes). The plates were thoroughly blotted on paper towels, spun down (500 x g for 30 seconds at 0°C), and placed into a chilled 96-well plate cooler (Eppendorf Scientific Inc, Westbury NY) at 0°C during the printing procedure.

The 96-fixed pin library replicator was washed with a dilute acid solution and ethanol according to the manufacturer's instructions (V&P Scientific, San Diego CA). Pins were carefully placed into the first source PCR-plate and slowly pumped up and down through the fluid surface at least three times to ensure fluid entry into the pin slots. The replicator was slowly and evenly lifted out of the solution and positioned using the orienter for the desired printing location (2 x 2 array membrane). The replicator was evenly touched across all 96 pins to positively charged nylon membranes (Hybond^{TM}-XL, Amersham NJ) pre-cut to the dimensions of plastic Omni^{TM} trays (~ 8.5 x 10 cm) to allow capillary transfer. The replicator was evenly tapped several times to ensure all fluid was dispensed (0.5 ul volume) and washed between printing additional source plates, as previously described. Arrays were allowed to dry in the dark overnight in the covered trays, fixed by cross-linking (70,000 uJ/cm^2), and stored between protective sheets at room temperature in the dark.

Printing 'pointers':

1. *The speed at which the pins break and leave the fluid surface may affect the reproducibility of good prints. Make sure the same practiced person does the printing for a complete batch of membranes for an experiment. The dye solution itself can be used to practice and conserve DNA material.*
2. *Make sure no traces of water remain on the plate directly following quenching in the ice water bath (after heat denaturation) since it will cause the solution to freeze and affect the capillary action properties of some of the pins.*
3. *The first several prints using a freshly cleaned replicator may be problematic. Allow for several 'tester' membranes not included in the final membrane count.*
4. *Single target prints that do not transfer can be manually printed using a pipettor (0.5 ul), but do not use membranes missing more than one print in the efforts for quality control. Make a note of which membranes have been manually printed and track these prints during analysis for contribution to data outliers.*
5. *Change plate coolers when temperature of block increases (>0°C) to keep solutions denatured during the entire printing process. (Keep one cooler in the freezer while using another cooler at room temperature).*
6. *Do not let pins dry out since this will affect surface tension and capillary action of the pin slots and result in irregular and inconsistent printing. Leave replicator sitting in DNA solution between printing membranes from one source plate.*
7. *Handle the membranes with clean forceps and gloved hands at all times.*
8. *Use canned air to remove noticeable dust and dirt on membranes.*
9. *If printing a large number of membranes at a time (~100), it is advisable to have two people involved (one to position the Omni trays for the second to print).*
10. *If fewer than ten arrays are printed, consider using 'multi-print' orienters (V&P Scientific) taped to uncut membrane rolls. This will avoid the problem of cut membranes curling, not evenly lie in the trays, and resulting in skewed prints.*

C. Array hybridization

1. RNA isolation

Chondrocyte monolayers were solubilized in Trizol™ reagent (Invitrogen Corporation, Carlsbad CA) (1 ml / 60-mm culture dish) and transferred to 1.5 ml microcentrifuge tubes for storage at –70°C. Following thaw at room temperature, the samples were vortexed and allowed to further incubate at room temperature for 5-15 minutes. For each 1.0 ml Trizol™ volume, 0.2 ml chloroform was added, mixed by manual shaking, and incubated at room temperature for 5 minutes. Trilayer separation

was accomplished with centrifugation at 10,000 rpm for 15 minutes at 4°C. The top aqueous layer was carefully removed and transferred to a new 1.5ml centrifuge tube. RNA was precipitated with the addition of an equal volume of isopropanol (0.5 ml) and incubation at room temperature for 20 minutes. The precipitate was collected by centrifugation at 10,000 rpm for 15 minutes at 4°C, and washed with 70% ethanol in DEPC-treated/nuclease-free water (1.0 ml) followed by centrifugation at 8,000 rpm for 5 minutes at 4°C. The RNA was allowed to air dry (5-10 minutes) before reconstitution in an appropriate volume of nuclease-free water for downstream applications.

Notes:

1. *Use RNAse-free plasticware (i.e. filter pipette tips, microcentrifuge tubes) for all steps downstream of the Trizol steps. Remove RNAses from the working benchtop area and gloves prior to handling the samples to ensure optimal integrity of the RNA.*
2. *Longer incubations of thawed Trizol fractions at room temperature (for longer than 5 minutes) were determined to yield greater RNA yields.*
3. *Save all ethanol precipitation and wash supernatants until the procedure is completed in case the RNA pellet has been accidentally lost during pipetting during these steps. Spin these fractions again to recover lost material.*
4. *If possible, store RNA in ethanol wash at –70°C rather than in reconstituted form. RNA can be stored up to one year in 70% ethanol at –70°C.*

2. RNA quantification

Accurate RNA quantification was critical to ensure equal loading of starting material to reverse transcription reactions for direct comparison of transcript levels between samples. Typically, spectrophotometric absorbance measurements at A_{260nm} are used to estimate concentrations; however DNA, salt, and protein contaminates can skew results. A more sensitive and accurate means for quantification was utilized, involving the generation of a ribosomal RNA standard curve and Ribogreen fluorescent dye binding (RiboGreen™ RNA quantification reagent, Molecular Probes Inc, Eugene OR). The dye specifically binds to the phosphate groups of the RNA backbone; quantitation of as little as 1 ng/ml RNA is possible. However, the dye will also bind to DNA, so if there is concern of residual DNA in the sample, a DNAse I step may be necessary.

Ribosomal 18S RNA standards were diluted to 2.0 ug/ml in TE buffer (10 mM Tris-HCl, 1 mM EDTA, pH 7.5). The concentration was verified using triplicate absorbance readings at a 1 cm path length (A_{260nm} = 0.05). Standards were serially diluted in black 96-well microtiter plates (0 - 100 ug / 100 ul). A 1 ul aliquot of each sample was added to 99 ul TE (1:100 dilution). Samples with high RNA yields were further diluted ten-fold prior to measurement to ensure readings on the linear range of the standard curve. The RiboGreen™ dye concentrate was diluted in TE buffer (1:40), added to both standard and sample wells (100 ul), and gently mixed by shaking. After adding the dye component, the plate was allowed to incubate at room temperature for 5-10 minutes protected from light; fluorescence was read at 485 nm excitation / 535 nm emission (Genios plate reader, Tecan US Inc, Durham NC). All raw data were corrected by fluorescence values of wells containing reagent alone. Final mean concentration values for duplicate or triplicate readings were calculated by factoring for dilution (1000X).

3. cDNA synthesis and radioactive labeling

(Modified from Powerscript™ reverse transcriptase protocol PT3396-2, CLONTECH Laboratories Inc, Palo Alto CA)

Annealing

1. Add the following to a 0.5 ml microcentrifuge tube:

Total RNA (10 ug)	up to 6ul
oligo d(T) primer (2 ug)	4 ul (500 ug/ml working stock)
Nuclease-free H_20	qs to 10ul

2. Incubate in thermocycler at 70°C for 10 minutes.
3. Quench on ice for 2 minutes.
4. Spin down and place on ice.

cDNA synthesis

1. Add the following to the tube on ice (30 ul total volume):

5X first strand buffer	6.0 ul
DTT (0.1 M)	1.0 ul (3.3 mM)
dNTPs (20 mM)	1.5 ul (1.0 mM)
Powerscript^{TM} RT (200 U/ul)	1.5 ul (300 U)
H_20	qs to 20 ul

2. Pipet gently / flick tube to mix.
3. Add 20 uCi [α-^{32}P]-dATP (~ 3000 Ci/mmol) in radioactive designated use area. Flick briefly to mix.
4. Incubate in thermocycler at 37°C for 90 min.

Probe clean-up / labeling efficiency calculations

1. Run volume through 'post-reaction purification column' (Sigma Chemical Co, St. Louis, MO) for 4 minutes at 750 x g, 25°C.
2. Collect 1 ul from each sample before and after running through column and dispense into scintillation tubes filled with 2.5 ml scintillation fluid ('unincorporated' and 'incorporated' counts, respectively).
3. Read tubes on beta-scintillation counter (LS window 0-800).
4. Denature in 0.5 ml microcentrifuge tubes (95°C, 5 min).
5. Quench immediately on ice and add to fluid at the bottom of hybridization tubes being careful not to apply directly to membranes.

% incorporation =
[incorporated counts / incorporated counts + unincorporated counts] X 100
(Typical range = 20-60%)

First strand cDNA yield:
4 (nmol dNTP/ul) x rxn vol (ul) x % first strand incorporation / 100 = nmol dNTP incorporated

nmol dNTP incorporated x 330 ng/nmol =
ng cDNA synthesized

ng cDNA synthesized / ng mRNA in reaction (approx 500 ng) x 100 =
% mRNA converted to cDNA
Minimum QC levels = 12%
(Typical range = 20-50%)

4. Array hybridization

Prepared membranes were briefly moistened in double-distilled water and carefully placed lengthwise into 35 mm x 150 mm glass Pyrex tubes (VWR International Inc, West Chester PA), avoiding air bubbles between membranes and the sides of the tubes. Arrays were pre-hybridized in a heated modified Church buffer (15 ml) (0.5M sodium phosphate, 7% SDS, 10mM EDTA, 100 ug/ml herring sperm DNA) at 65°C for at least 1 hour. Overnight hybridizations were conducted at 65°C, 8-10 rpm / min. Membranes were washed in increasing stringency and temperature: 2X SSC / 0.1% SDS (2X 5 min, 25°C), 1X SSC / 0.1% SDS (1X 15 min, 42°C), and 0.1X SSC / 0.1% SDS (2X 10 min, 65°C). Membranes were briefly air-dried and exposed to a blanked phosphorimaging screen (2 hours). Data were digitally scanned using a Storm 820 phosphorimager and analyzed using ImageQuant™ software (Amersham Pharmacia Biotech, Piscataway NJ). Hybridization signals were manually designated with equal sized ellipses on arrays. No background subtraction calculations were conducted since background values appeared even across membranes.

Hybridization 'tips':

1. *These methods have been optimized for two membranes per tube. Do not hybridize more than two membranes at a time without considering using a hybridization mesh and possibly increasing hybridization buffer volumes.*
2. *It is very important to heat the hybridization buffer prior to aliquotting to the hybridization tubes (either in an incubator or a water bath at 37°C). The SDS easily precipitates out of solution at room temperature and will result in unwanted background problems.*
3. *Conduct all washes in Tupperware boxes with volumes at least 50 mls / membrane. Carefully and slowly pour off the wash into proper radioactive liquid waste receptacles. Individually handle membranes using forceps during washes to avoid sticking of membranes and uneven exposure to the wash. Try not to pour the next wash directly on the membrane to avoid uneven washing. All washes should be conducted using complete immersion and constant but gentle movement of liquid.*
4. *Do not let washed membranes completely dry out. Drying will irreversibly fix the probe and make efficient stripping difficult. Alternately, membranes may be set aside to allow radioactivity to go through at least two half-lives. Always test membranes by exposing to a phosphorimaging screen for 1-2 hours before re-using arrays to ensure*

no radioactivity remains which could affect downstream results. (In our hands, complete removal of probe from Hybond XL membranes was problematic and membranes were not re-used).

5. Membrane stripping

Membranes were placed into a rinse solution of 2 X SSC in a Tupperware container. A stripping solution of 0.1X SSC, 0.5 % SDS was brought to a boil in a 2 L flask with constant stirring and poured into a second Tupperware container. The rinsed membranes were individually placed into the boiling solution (400 mls / 20 membranes), gently shaked, and allowed to sit for 15 minutes. The stripping solution was poured off and a second stripping step was repeated as described. Membranes were briefly rinsed in 2 X SSC and air-dried on paper towels.

6. Differential expression results validation

Altered expression of select genes identified in the chondrocyte experiments *(Chapters III, IV)* and the cDNA array analysis involved in the SSH-PCR project *(Chapter V)* were validated by reverse-transcriptase PCR (RT-PCR) methods. Primers were designed to partial coding regions of the reported equine nucleotide sequences (PrimerSelect, DNASTAR Inc, Madison WI) (Integrated DNA Technologies, Coralville IA) **(Table AVIII)**.

Table AVIII - Optimized RT-PCR conditions.

Gene	*Length*	*Primer sequence*	*Length*	*Mg2+*	*Anneal temp*	*Optimal cycles*
b-actin	22-mer	5' CGACGAGGCCCAGAGCAAGAGG 3'	501 bp	1.5 mM	61	30
	21-mer	5' TCCAGGGCGACATAGCAGAGC 3'				
BMP-4	17-mer	5' AGCTCCGGCCCCTCCTG 3'	426 bp	1.5 mM	61	32
	24-mer	5' AGCGGCACCCACATCCCTCTACTA 3'				
BPTF	17-mer	5' GAACCGGGGCTGGATTT 3'	180 bp	1.5 mM	50	30
	19-mer	5' CTATGGGGTCAAGTGTAAC 3'				
GAPDH	24-mer	5' AGGGTGGAGCCAAAAGGGTCATCA 3'	418 bp	1.5 mM	61	28
	23-mer	5' GCTTTCTCCAGGCGGCAGGTCAG 3'				
IGF-2	19-mer	5' GCCCGCAAGCCGCATCAAC 3'	169 bp	1.5 mM	61	26
	22-mer	5' CACGGGGTATCTGGGGGAGTCG 3'				
IL-6	23-mer	5' GCTGCTCCTGGTGATGGCTACTG 3'	533 bp	1.5 mM	61	23
	23-mer	5' CAAGGCTTCGAAGGATGAGGTGA 3'				
MHCI	23-mer	5' AGCCGCCTCCTCAGTCCACCATC 3'	430 bp	1.5 mM	61	28
	18-mer	5' CCCGCCCAGCCCCACCTC 3'				
Biglycan	22-mer	5' ATGTCGCCCGCCTCACTTCTGC 3'	477 bp	1.5 mM	61	28
	24-mer	5' TTGCTCAAAACTCCCGCCACTCTA 3'				
COL1A2	21-mer	5' CGCGGCCGAGGTACTTGTTTT 3'	316 bp	2.5 mM	50	26
	24-mer	5' ATTTAATTTTTCTGCTTGTCTGAG 3'				
COLII	24-mer	5' GAAGAGCGGAGACTACTGGATTGA 3'	501 bp	1.5 mM	62	34
	20-mer	5' AGGCGCGAGGTCTTCTGTGA 3'				
Ferritin	24-mer	5' CAGCCCTCCTTCACCTCCTCACAG 3'	404 bp	1.5 mM	61	28
	24-mer	5' TTCAGCCCATTCTCCCAGTCATCC 3'				
MMP-1	28-mer	5' TTTGCAGAATGAGATATAAATAAGATTA 3'	305 bp	1.5 mM	50	28
	22-mer	5' ATCCCAAAATGATAGCAGATGA 3'				
MMP-13	24-mer	5' GGGGAGCATATGGTAGCCTTACAC 3'	400 bp	1.5 mM	50	30
	24-mer	5' TGCCGTGGTCTTAGATCATTTTGA 3'				
MMP-3	22-mer	5' AGATGCGGAGTTCCTGATGTCG 3'	470 bp	1.5 mM	57	25
	21-mer	5' GCCGGGCCTTTGAGTGTATTG 3'				
OSF	18-mer	5' CCGCCCGGGCAGATACAT 3'	294 bp	2.0 mM	50	32
	24-mer	5' ACCAGCAAAGAGTGATACCAGAAA 3'				
TIMP-1	24-mer	5' CCTGGTCTCCGGCATTCTGTTGTT 3'	419 bp	1.5 mM	61	31
	20-mer	5' CGGCGGCGTAGGTCTTGGTG 3'				
IL-1b	23-mer	5' AAGATACCCGTTCCCTGCTCACA 3'	542 bp	1.5 mM	57	30
	22-mer	5' CGGCCGCCTCTGGTATTTCCTA 3'				

D. Customized macroarray characterization

1. Signal sensitivity / saturation assessment

The range of signal intensity in our newly described array system was evaluated. Seven separate cDNAs of similar length (1000-1200 bp) and low homology (10-24 %) were amplified, processed, and printed to membranes as previously described for array construction. The cDNAs (100 ng each template) were used to generate radiolabeled probes using a hot asymmetric PCR (50 ul volume reactions): T7 primer (0.6 uM), 50 mM KCl, 10 mM Tris-HCl, 1.5 mM $MgCl_2$, 0.2 mM dCTP, dGTP, dTTP and 0.024 mM dATP, 2.5 U Taq polymerase (Promega Corporation, Madison WI), and 40 uCi [α-^{32}P]-dATP (Amersham Pharmacia Biotech, Piscataway NJ). Cycling involved an initial denaturation at 95°C for 5 minutes and 40 cycles of: 95°C for 45 seconds, 50°C for 45 seconds, and 72°C for 4 minutes, and a final extension at 72°C for 10 minutes. Unincorporated dNTPs were removed and probes were quantified by calculating percent incorporation of [α-^{32}P]-dATP, specific activity, and actual labeled yields. A range in mass (0 - 5.0 ng) of the seven different labeled DNA probes was used to generate one complex probe which was denatured (95°C for 5 minutes), quenched on ice, and added to the hybridization of duplicate membranes using the methods previously described. The results indicated the dynamic linear range of signal intensities spanning 2 - 3 orders of magnitude; sensitivity fell between 0.001 - 0.01 ng labeled probe and saturation was defined between 1.0 - 5.0 ng labeled probe **(Figure A4)**. These values were calculated to correspond to a 15 x 10^{-6} to 15 x 10^{-3} pmol range of labeled probe concentrations, with detection of as low as 1 - 10 transcripts. It must be acknowledged that these results are estimations and cannot be directly applied to the quantification of absolute mRNA levels in the cDNA array generated data due to the differences in probe amplification and methods of primed labeling.

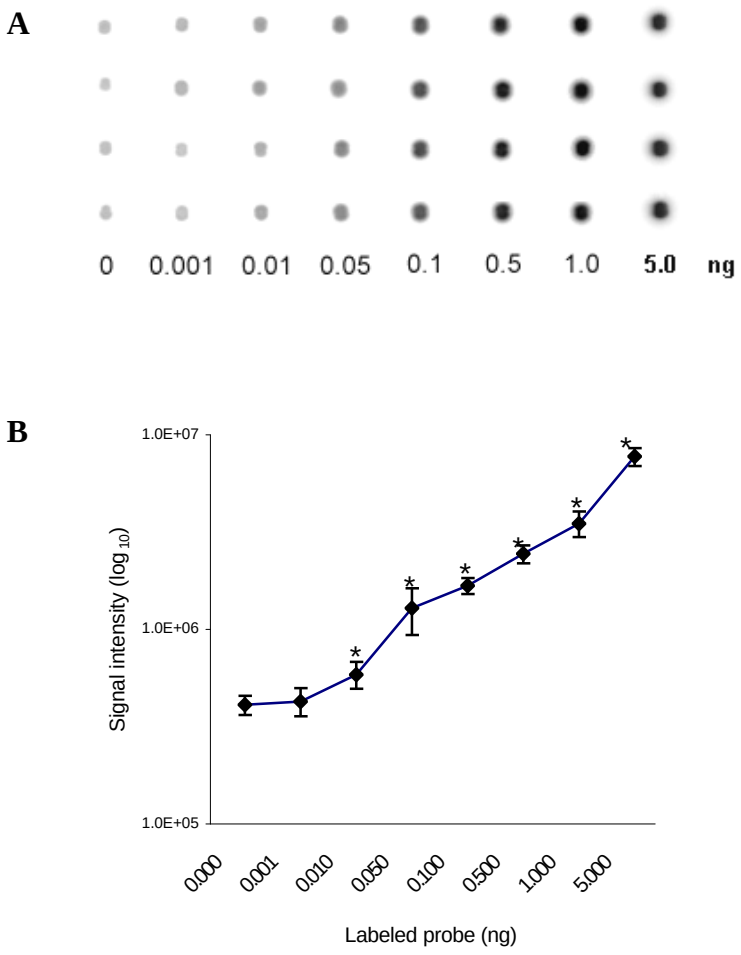

Figure A4 - Sensitivity and saturation assessment of cDNA hybridization system.

Data represent the mean and standard error values from two separate hybridizations.
* Significance relative to unlabeled probe ('0'), $p<0.05$.

2. Bias assessment

Preliminary evaluation of the 169-element cDNA array (Chapter III) indicated the intriguing possibility of a spatial bias in the media treated control generated data, as the signal intensities for array B were consistently lower than those for array A across all genes analyzed in duplicate on the same membrane **(Figure A5a)**. In addition, the signal values of the membrane placed on top during the hybridizations (membrane 2) were consistently higher than the bottom membrane (membrane 1), suggesting the competition of the quadruplicate target probes for potentially limiting labeled probe (perhaps reflecting more rarely expressed transcripts) **(Figure A5b)**. Since the combination of these potential biases appeared systemic, that is, not remarkably gene specific or related to localization on the membrane, means of the two array values were calculated and used in further analysis; correcting the values to either of the arrays was deemed unjustified. The unavoidable result of this averaging was increased noise in the data for the controls, as the variation associated with each mean gene signal was greater than if a correction method to one of the arrays had been employed. The identification of this potential bias further emphasized the importance of valid statistical analyses undertaken to pick out true differential effects using this set of arrays.

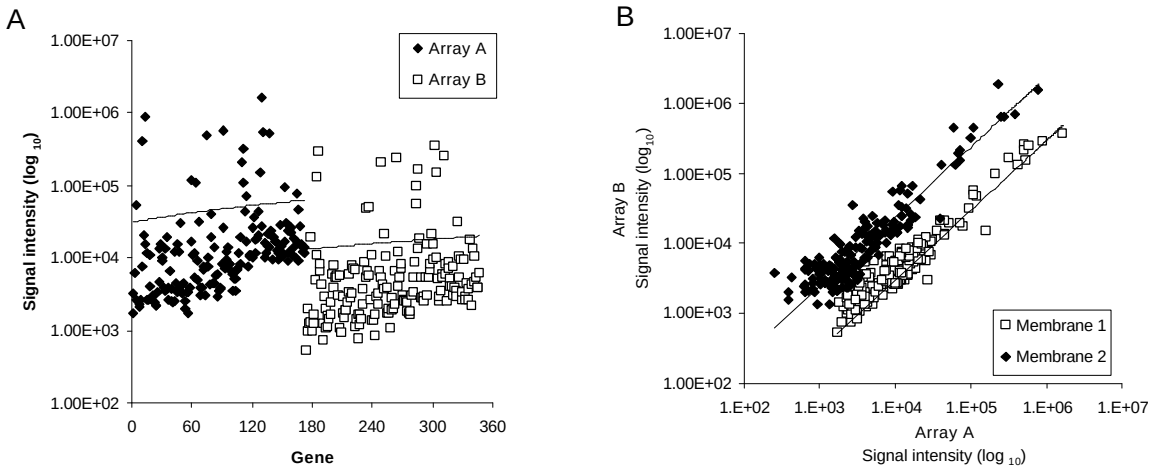

Figure A5 - Graphic depiction of signal bias of 169-element cDNA array.

A= Plot of duplicate signals on a single membrane hybridized with a media control labeled probe; note the overall higher signal values for 'array A' (oriented toward bottom of tube). B= Plot of quadruplicate hybridization signals from two membranes hybridized with a media control labeled probe in the same tube; note the overall higher signal values for 'membrane 2' (placed on top in the hybridization tube).

Further investigation into this potential bias was provided during the preliminary evaluation of the 380-element cDNA array (Chapter IV) media treated control generated data, in which single instead of duplicate printing on each membrane was conducted. Interestingly, the signal intensities of the right side of the membrane were consistently lower than the left, but were more similar across the duplicate membranes than the first array **(Figure A6)**. This indicated that the hybridization of duplicate (2 x 2.5 ng) rather than quadruplicate (4 x 2.5 ng) target probes was better suited for this system, correlating with the labeled probe saturation levels previously defined in the signal calibration assessment (1.0-5.0 ng target probe). Additionally, these results suggested this recurrent bias was not due to spatial printing concerns, but rather to inadequate hybridization fluidics, since the right half was always placed at the top of the tube and the left half toward the tube bottom where the labeled probe was added to the hybridization buffer. Although the fluid appeared to be evenly moved throughout the length of the tube during hybridization, it was possible that the hybridization oven was not completely effective in rotating the fluid, thus resulting in the bias of greater signals on the left half of the arrays. This realization highlighted the importance of placing membranes to be hybridized in the same orientation in tubes during an experiment for proper comparative analysis.

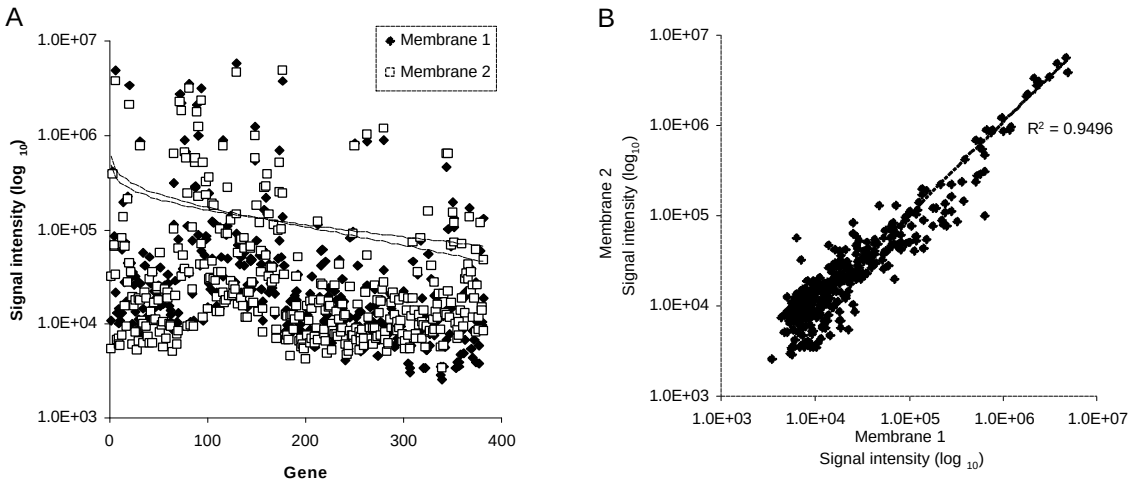

Figure A6 - Graphic depiction of signal bias of 380-element cDNA array.

A= Plot of duplicate signals from two membranes hybridized with a media control labeled probe; note the left half of the membrane signal intensities (oriented toward the bottom of the tube) to be slightly greater than the right half, but similar between the two membranes. B= Correlation of duplicate data points from two membranes in the same tube hybridized with a media control labeled probe.

APPENDIX III: DNA quantification

Chondrocyte monolayer cellular densities were evaluated in the attempt to detect possible differences between media controls and EqIL-1 treatments which may have contributed to the expression level changes observed in the cDNA array analyses (*refer to Chapters III and IV*). Genomic DNA concentrations were measured using an AT-rich double-stranded DNA dye-binding system (Hoechst 33258 reagent, Molecular Probes Inc, Eugene OR). Fifty microliter aliquots of genomic DNA precipitated from the protein interface and phenol layers of Trizol^{TM} fractions were added to 50 ul TE buffer (1:2 dilution) (10mM Tris, 1 mM EDTA, pH 7.5). A concentrated dye solution (1 mg/ml) was diluted 1:1600 in TE buffer and 100 ul volumes were added to wells of black 96-well microtiter plates (200 ul total volume). Fluorescence was read at excitation 360 nm / emission 465 nm (Genios plate reader, Tecan US Inc, Durham NC), following an incubation at room temperature protected from light (5-10 minutes). Calf thymus DNA standard curves were generated by dilution in TE buffer (0-100 ug/ml). Mean values of duplicate measurements corresponding to media controls and EqIL-1 treatments were compared using Student's t-tests. Similar DNA levels were indicated in both studies across the three horses and treatment conditions relative to controls ($p>0.05$) (ranging from 4.0-6.5 ug DNA/ monolayer). These results assure similar cellular contents across horses and treatment conditions compared by the cDNA array analyses.

Vita
Vivian Ann Takafuji

Date of birth

September 9, 1975

Education

The University of Virginia, Charlottesville, VA 22904
Bachelor of Arts, Biology, May 1996

Laboratory experience

August 1998-
Present

Research Assistant
Veterinary Medical Sciences
Orthopedic Research Laboratory
Molecular Diagnostics Laboratory
VA-MD Regional College of Veterinary Medicine
Large Animal Clinical Sciences
Virginia Polytechnic Institute and State University
Duckpond Drive, Blacksburg, VA 24061-0442

May 1996-
August 1998

Laboratory Specialist
University of Virginia, Health Sciences Center
Internal Medicine, Department of Gastroenterology
MR4 Building, Charlottesville, VA 22908

Publications

Takafuji VA, McIlwraith CW, Howard RD. Effects of equine recombinant interleukin-1α and interleukin-1β on proteoglycan metabolism and prostaglandin E_2 synthesis in equine articular cartilage explants. *Am J Vet Res*. 2002 Apr; 63(4): 551-8.

Takafuji VA, Evans A, Lynch KR, Roche JK. PGE_2 receptors and synthesis in human gastric mucosa: perturbation in cancer. *Prostaglandins Leukot Essent Fatty Acids*. 2002Jan; 66(1): 71-81.

Takafuji V, Lublin D, Lynch K, Roche JK. Mucosal prostanoid receptors and synthesis in familial adenomatous polyposis. *Histochem Cell Biol*. 2001 Aug; 116(2): 171-81.

Takafuji V, Cosme R, Lublin D, Lynch K, Roche JK. Prostanoid receptors in intestinal epithelium: selective expression, function, and change with inflammation. *Prostaglandins Leukot Essent Fatty Acids*. 2000 Oct; 63(4): 223-35.

Cosme R, Lublin D, **Takafuji V**, Lynch K, Roche JK. Prostanoids in human colonic mucosa: effects of inflammation on PGE_2 receptor expression. *Hum Immunol*. 2000 Jul; 61(7): 684-96.

Planchon S, Fiocchi C, **Takafuji V**, Roche JK. Transforming growth factor-beta1 preserves epithelial barrier function: identification of receptors, biochemical intermediates, and cytokine antagonists. *J Cell Physiol*. 1999 Oct; 181(1): 55-66.

Vita
Vivian Ann Takafuji

Nucleotide Accessions

Equus caballus granulocyte chemotactic protein 2 (GCP2) mRNA, complete cds; gi|21747886|gb|AY114351.1|[21747886]
Equus caballus leukocyte common antigen mRNA, partial cds; gi|21747884|gb|AY114350.1|[21747884]
Equus caballus Ras GTPase-activating protein (NGAP) mRNA, partial cds; gi|21483853|gb|AY113683.1|[21483853]
Equus caballus ribosomal protein L5 (RPL5) mRNA, complete cds; gi|21483851|gb|AY113682.1|[21483851]
Equus caballus ferritin heavy chain mRNA, complete cds; gi|21435815|gb|AY112742.1|[21435815]
Equus caballus zinc finger-binding protein (ZNF9) mRNA, 3' UTR; gi|21326146|gb|AF513861.1|[21326146]
Equus caballus N-acetylglucosamine-6-sulfatase (G6S) mRNA, partial cds; gi|21321593|gb|AF510336.1|[21321593]
Equus caballus cullin 4B (CUL4B) mRNA, partial cds; gi|21314575|gb|AF513243.1|[21314575]
Equus caballus glucose-regulated protein (GRP94) mRNA, partial cds and 3'UTR; gi|21070348|gb|AF508791.1|[21070348]
Equus caballus plasminogen activator inhibitor-2 (PAI-2) mRNA, 3'UTR, partial sequence; gi|21070347|gb|AF508790.1|[21070347]
Equus caballus plasminogen activator inhibitor-1 (PAI-1) mRNA, partial cds; gi|21070317|gb|AF508034.1|[21070317]
Equus caballus cullin 4A (CUL4A) mRNA, partial cds; gi|21070315|gb|AF508033.1|[21070315]
Equus caballus AT-rich binding protein-1 (SATB1) mRNA, partial cds; gi|21070313|gb|AF508032.1|[21070313]
Equus caballus capping protein mRNA, 3' UTR'; gi|21070227|gb|AF506976.1|[21070227]
Equus caballus PI-3-kinase-related kinase mRNA, 3' UTR; gi|21070226|gb|AF506975.1|[21070226]
Equus caballus galactocerebrosidase mRNA, partial cds; gi|21070224|gb|AF506974.1|[21070224]
Equus caballus thymosin beta 10 mRNA, complete cds; gi|21070222|gb|AF506973.1|[21070222]
Equus caballus mcp-2 mRNA, complete cds; gi|21070220|gb|AF506972.1|[21070220]
Equus caballus phosphoprotein C8FW mRNA, partial cds; gi|21070218|gb|AF506971.1|[21070218]
Equus caballus small inducible cytokine A5 RANTES mRNA, complete cds; gi|21070216|gb|AF506970.1|[21070216]
Equus caballus ubiquitin mRNA, complete cds; gi|21070214|gb|AF506969.1|[21070214]
Equus caballus LPS-induced TNF-alpha factor (LITAF) mRNA, complete cds; gi|21070124|gb|AF503366.1|[21070124]
Equus caballus granulocyte colony stimulating factor (G-CSF) mRNA, complete cds; gi|21070122|gb|AF503365.1|[21070122]
Equus caballus cDNA fragments (AY246701-AY246855)
Equus caballus cDNA fragments (AY343541-AY343545)

Presentations

18th annual Research Symposium, VA-MD Regional College of Veterinary Medicine, Blacksburg, VA, June 7-9, 2003: Large-scale expression analysis of recombinant equine interleukin-1β treated equine synovium using suppression subtractive hybridization, **VA Takafuji**, KL Seat, LV Sharova, MV, Crisman, RD Howard

18th annual Research Symposium, VA-MD Regional College of Veterinary Medicine, Blacksburg, VA, June 7-9, 2003: Complementary DNA array expression analysis of equine articular cartilage chondrocytes treated with equine interleukin-1, **VA Takafuji**, KL Seat, LV Sharova, MV, Crisman, RD Howard

American College of Veterinary Surgeons (ACVS) annual meeting, September 23rd, 2000, Arlington VA: Effects of recombinant equine IL-1 on equine articular cartilage explants, **V Takafuji** and RD Howard

12th annual Research Symposium, VA-MD Regional College of Veterinary Medicine, Blacksburg, VA, June 7-9, 2000: Effects of recombinant equine IL-1 on proteoglycan metabolism in equine articular cartilage explants, **VA Takafuji** and RD Howard

16th annual research symposium (Graduate student association), Virginia Tech, Blacksburg VA, March 27th, 2000: Effects of recombinant equine IL-1 on proteoglycan metabolism in equine articular cartilage explants, **VA Takafuji** and R Howard

Minority Opportunity Program, Virginia Tech, Blacksburg VA, August 2001: Cloning of an equine extracellular matrix gene, J Rosero, **VA Takafuji**, RD Howard

18th annual Research Symposium, VA-MD Regional College of Veterinary Medicine, Blacksburg, VA, June 7-9, 2003: Large-scale expression analysis of recombinant equine interleukin-1β treated equine synovium using suppression subtractive hybridization, **VA Takafuji**, KL Seat, LV Sharova, MV, Crisman, RD Howard.